

VIBRATORY INSERTION AND EXTRACTION
OF SURGICAL IMPLANTS

By

JEFF E. SCOTT

A thesis submitted in partial fulfillment of
the requirements for the degree of
Master of Science in Mechanical Engineering

WASHINGTON STATE UNIVERSITY
School of Mechanical and Materials Engineering

DECEMBER 2006

© Copyright by Jeff E. Scott, 2006
All Rights Reserved

© Copyright by Jeff E. Scott, 2006
All Rights Reserved

To the Faculty of Washington State University:

The members of the Committee appointed to examine the thesis of JEFF E. SCOTT find it satisfactory and recommend that it be accepted.

Chair

ACKNOWLEDGMENT

I would like to acknowledge the guidance and mentorship that Dr. Bill Kinsel has given to me throughout my educational endeavors at Washington State University. He has demonstrated an outstanding ability to teach and instruct mechanical engineering in every class I have taken from him.

Also, I would like to acknowledge Steve Jordan, the mechanical engineering technician, for his help and support with laboratory equipment and experiment set up. His expertise, knowledge, and time spent in the laboratory is greatly appreciated.

Finally, I would like to give thanks to my wife, Tasha Scott, for her patience, understanding, and unselfishness as I strived to reach this academic goal. She has been supportive in all aspects of my life since the day I met her.

VIBRATORY INSERTION AND EXTRACTION
OF SURGICAL IMPLANTS

Abstract

by Jeff E. Scott, M.S.
Washington State University
December 2006

Chair: William (Bill) C. Kinsel

Intramedullary structural implants, commonly called nails, can be inserted through a patient's fractured bone to align the bone fragments, speed up the healing process, and give it strength while it heals. The procedure for insertion of the nails into the fractured bone requires drilling a small hole at the top of the bone and pushing the nail through the hole. Pushing the nail through the hole in the bone necessitates using a T-handle tool for the orthopaedic surgeon to grip because of the amount of force required. However, even with the T-handle tool, applying the necessary force to get the nail to slide through the bone hole can be strenuous and present difficulties for the surgeon performing the operation.

The concept of using vibratory excitation to reduce the force and time required for insertion of the nail is evaluated. Proof of concept is demonstrated through experimentation and engineering analysis. Correlations are shown between the results of the experimentation and engineering analysis to prove that vibration does reduce insertion and extraction force by as much as 73%. Both transverse and axial vibrations are demonstrated to be effective and the most effective forcing frequencies for each of these vibration types are determined. The effectiveness of a frequency sweep during insertion is also evaluated. The conclusion of the thesis is that a vibratory excitation device can be used to facilitate easy implant insertion during orthopaedic surgeries.

TABLE OF CONTENTS

	Page
ACKNOWLEDGEMENTS	iii
ABSTRACT	iv
TABLE OF CONTENTS	v
LIST OF TABLES	ix
LIST OF FIGURES	xi
NOMENCLATURE	xii
1.0 INTRODUCTION	1
1.1 History of the Nail	1
1.2 Types of Nails	2
1.3 Difficulty with Nail Insertion.....	2
1.4 Purpose of Thesis.....	3
2.0 BACKGROUND	4
2.1 Bone Description	4
2.2 Bone Mechanical Properties	5
3.0 VIBRATION EXPERIMENTS OF SURGICAL IMPLANT INSERTION.....	7
3.1 Purpose of the Vibration Experiments.....	7
3.2 Equipment Used in the Vibration Experiments	7
3.3 Methodology and Procedure of the Vibration Experiments	13
3.4 Equipment Calibration Procedure and Results	15
3.5 Vibration Experiment Results on Biomechanical Test Blocks.....	18
3.6 Vibration Experiment Results on UHMW-PE.....	21

3.7	Vibration Experiment Results on Wet Bovine Bone	26
3.7.1	Difficulties Encountered with Wet Bone Experiments.....	26
3.7.2	Explanation of the Wet Bone Difficulties.....	27
3.7.3	Bovine Wet Bone Experiments.....	31
3.8	Vibration Experiment Conclusions and Discussions.....	36
3.8.1	How the Vibrations Affected the Insertion Force.....	36
3.8.2	Discussion of Proof of Concept	38
3.8.3	Discussion of Transverse and Axial Vibration	38
3.8.4	Discussion of the Most Effective Vibration Frequency.....	40
3.8.5	Testing Materials Affect on Results	41
3.8.6	Frequency Sweep Experiments.....	42
4.0	VIBRATION ANALYSIS OF SURGICAL IMPLANT INSERTION.....	43
4.1	Purpose of the Vibration Analysis	43
4.2	Software Tools Used in the Vibration Analysis	44
4.2.1	Brief Software Description	44
4.2.2	ALGOR Brief Software Methodology.....	44
4.2.3	ALGOR Benchmarking	46
4.2.3.1	Linear Static Stress Module Benchmarking Results.....	47
4.2.3.2	Linear Dynamics Module Benchmarking Results	49
4.2.3.3	Mechanical Event Simulation Module Benchmarking Results	50
4.2.3.4	ALGOR Benchmarking Results and Comparisons.....	52
4.3	Vibration Analysis Methodology and Results	52
4.3.1	Linear Static Stress Analysis of the T-Handle.....	52

4.3.2 Critical Buckling Load Analysis of the T-Handle	54
4.3.3 Natural Frequency Analysis of the Nail.....	56
4.3.4 Natural Frequency Analysis of the Experimental Setup.....	60
4.3.5 Range of Natural Frequencies During Experimental Nail Insertion.....	63
4.3.6 Range of Natural Frequencies During Actual Nail Insertion.....	68
4.3.7 Load Stiffening Affect on the Natural Frequency of the Nail	71
4.4 Vibration Analysis Conclusions and Discussion	74
5.0 THESIS CONCLUSION AND RESULTS	
5.1 Brief Re-statement of Thesis Purpose.....	74
5.2 Thesis Conclusion.....	74
5.2.1 Vibration Frequencies Recommended for Vibratory Device	75
5.2.2 Vibration Frequencies of Common Commercially Available Devices	75
5.3 Further Research Topics for Advancement	76
REFERENCES	79
APPENDIX	
A. SIGN T-Handle Design Drawing.....	81
B. Biomechanical Test Blocks Specification and Properties	82
C. Typical UHMW-PE Specification and Properties	83
D. Transverse Vibration Voltage Data with Biomechanical Test Blocks	84
E. Transverse Vibration Force Data with Biomechanical Test Blocks.....	85
F. Transverse Vibration Maximum Force with Biomechanical Test Blocks.....	86
G. Axial Vibration Voltage Data with Biomechanical Test Blocks.....	87

H. Axial Vibration Force Data with Biomechanical Test Blocks.....	88
I. Axial Vibration Maximum Force with Biomechanical Test Blocks	89
J. Transverse Vibration Voltage Data with UHMW-PE	90
K. Transverse Vibration Force Data with UHMW-PE.....	95
L. Transverse Vibration Maximum Force with UHMW-PE.....	100
M. Axial Vibration Voltage Data with UHMW-PE.....	105
N. Axial Vibration Force Data with UHMW-PE	110
O. Axial Vibration Maximum Force with UHMW-PE	111
P. UHMW-PE Transverse and Axial Vibration Results Comparison.....	112
Q. Material Properties Used in ALGOR Analyses.....	113
R. MathCAD Natural Frequency Analysis.....	114

LIST OF TABLES

1. Mechanical Properties of Cancellous and Cortical Bone	6
2. Load Cell Calibration Data	17
3. Transverse Vibration Average Force Results with Biomechanical Tests Blocks.....	19
4. Axial Vibration Average Force Results with Biomechanical Tests Blocks	20
5. Transverse Vibration Average Force Results with UHMW-PE	22
6. Axial Vibration Average Force Results with UHMW-PE.....	24
7. Bovine Wet Bone Weights.....	33
8. Bone Specimen One Results	34
9. Bone Specimen Two Results	34
10. Bone Specimen Three Results	35
11. Insertion Force Comparison with and without Vibration	37
12. Vibration Type Results Comparison.....	37
13. Vibration Frequency Results Comparison	38
14. Results of ALGOR Benchmarking	52
15. Fundamental Natural Frequency Comparison of the Nail Only	59
16. Fundamental Natural Frequency Comparison of the Nail with End Mass	63
17. Fundamental Natural Frequency Change During Experimental Nail Insertion.....	66
18. Fundamental Natural Frequency Change During Actual Nail Insertion	70
19. Natural Frequency Change During Actual Nail Insertion with Load Stiffening	73
20. Forcing Frequencies of Common Vibratory Devices	77

LIST OF FIGURES

1. Conceptual Representation of a Nail	1
2. Two Main Types of Bone Tissue.....	5
3. Simulated Nail	8
4. Biomechanical Test Blocks.....	9
5. UHMW-PE Test Block.....	10
6. Fresh Bovine Wet Bone	11
7. Vibration Shaker Table and Controllers	12
8. Load Cell and Digital Multi-Meter.....	13
9. Transverse Vibration Experiment Set Up.....	14
10. Axial Vibration Experiment Set Up.....	14
11. Precision Weights Used for Calibration	16
12. Graph of the Load Cell Calibration Data.....	18
13. Transverse Vibration Average Force Graph with Biomechanical Test Blocks	19
14. Axial Vibration Average Force Graph with Biomechanical Test Blocks.....	20
15. Transverse Vibration Average Force Graph with UHMW-PE.....	23
16. Axial Vibration Average Force Graph with UHMW-PE	25
17. Wet Bone Showing Cortical Bone and Marrow	28
18. Free Body Diagram of Bone Specimens on the Nail.....	29
19. Experiment Configuration with Bovine Bone	32
20. Bovine Wet Bone Specimens.....	33
21. Displacement Plot of the Linear Static Stress Module Benchmark Case	48
22. Mode Shape Plot of the Linear Dynamics Module Benchmark Case	50
23. Acceleration Plot of the Mechanical Event Simulation Module Benchmark Case	51

24. T-Handle Finite Element Model	53
25. Von Mises Stress Distribution in the T-Handle	54
26. T-Handle Finite Element Model with Nail	55
27. Fundamental Natural Frequency of the Nail Only	58
28. Fundamental Natural Frequency of the Nail with End Mass	62
29. Fundamental Mode of the Nail with the Mass Down One-Third	64
30. Fundamental Mode of the Nail with the Mass Down Two-Thirds	65
31. Fundamental Mode of the Nail with the Mass at the Bottom	66
32. Graph of Natural Frequency versus Nail Insertion Distance	67
33. Fundamental Mode of the Nail and T-handle at the Beginning of Insertion	69
34. Fundamental Mode of the Nail and T-handle Halfway Though Insertion	69
35. Fundamental Mode of the Nail and T-handle at the End of Insertion	70
36. Fundamental Mode of the Nail/T-handle at the Beginning of Insertion	72
37. Fundamental Mode of the Nail and T-handle Halfway Though Insertion	72
38. Fundamental Mode of the Nail and T-handle at the End of Insertion	73
39. Oscilloscope and Piezo-Accelerometer Used	76

NOMENCLATURE

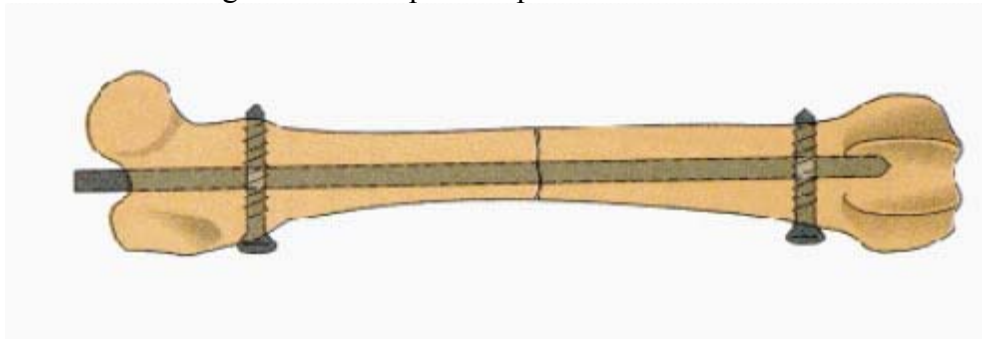
ALGOR	Commercially available finite element analysis software
ASTM	American Society of Testing and Materials
BC	Boundary conditions
CAD	Computer aided design
FEA	Finite element analysis
G	One unit of Earth's gravitational acceleration
Gm	Gram, metric unit of mass
Hz	Hertz (cycles per second)
In	Inch, English unit of length
Lbs	Pounds, English unit of mass
MES	Mechanical event simulation
MSI	Measurement Specialties, Inc.
Nail	Rod used as a surgical implant
PH	Precipitation hardened
SIGN	Surgical Implant Generation Network
UHMW-PE	Ultra-high molecular weight polyethylene
WSU	Washington State University

1.0 INTRODUCTION

1.1 History of the Nail

The first recorded use of intramedullary structural implants, commonly called nails, to fix a fracture site was performed by the Incas and Aztecs in the 16th century. These natives used resinous wooden pegs in the medullary canal of long bones for non-union fractures [3]. The first steel intramedullary nail was invented by Gerhard Kuntscher of Germany. Kuntscher pioneered intramedullary fixation in 1940s during World War II. Kuntscher continued developing and re-designing the intramedullary nail after the war, which led to the first interlocking nail. An interlocking nail is one that is fixed at the ends by screws or some other method to prevent rotation and telescoping of the fracture [2]. Figure 1 shows a conceptual picture to illustrate what a nail is and how it is used.

Figure 1. Conceptual Representation of a Nail.



Since the implementation of Kuntscher's ingenious methods for stabilizing and fixing fracture sites, intramedullary nails have received worldwide acceptance and are the common treatment for lower extremity fractures by today's orthopaedic surgeons. The use of intramedullary nails fixes the fracture site firmly, which has allowed patients increased mobility immediately following the surgical procedure making the recovery and healing process easier on the patient [2]. The increased mobility is attributed to the load bearing capabilities of the nail.

The interlocking nails have remained the preferred method of fracture fixation over Steinmann pins and bone plates because they can resist bending, axial, and torsional loads.

1.2 Types of Nails

There are two main types of intramedullary interlocking nails in use today, defined by their diameter and method of intramedullary insertion. The two types are reamed and unreamed nails. The diameter of reamed nails is approximately the same as the intramedullary canal diameter. This ensures an interference fit between the inner bone and the nail which provides a more rigid fixation at the fracture site. Unreamed nails have a smaller diameter than the intramedullary canal diameter, which makes for easier insertion but also allows more movement at the fracture site that could lead to a non-union [3].

Compared to an intact tibia, reamed (large diameter) nails are 117% as rigid in axial loading while the unreamed (small diameter) nails are 55% as rigid. Also, compared to an intact tibia, reamed nails are 6.5% as stiff in torsion while the unreamed nails are 3.1% as stiff in torsion [3]. Both types of intramedullary interlocking nails require surgical time for insertion, therefore, the ease of insertion is a major consideration for orthopaedic surgeons.

1.3 Difficulty with Nail Insertion

One of the difficulties that have been observed by physicians is that a considerable amount of force is required to insert the nail through the bone. These forces are large enough to be tiring, strenuous, and time-consuming for an orthopaedic surgeon. Many times, the orthopaedic surgeon may elect to use a mallet to help with insertion of the nail; however, this method can lead to splitting of the bone [1].

The use of a nail requires that a hole be drilled through one end of the bone so the nail can be inserted through the hole into the intramedullary canal of the bone. Usually the hole is

drilled to a very tight tolerance fit with the nail, making insertion of the nail very difficult and strenuous [1]. If the nail is the reamed type, it is even more difficult to insert since it is in contact with the intramedullary canal as it is inserted. Some manufacturers of orthopaedic supplies have developed a handle that can be attached to the nail. The handle provides the orthopaedic surgeon a comfortable, ergonomic grip to push the nail through the bone. However, even with the handle, the orthopaedic surgeons may tire and fracture the bone during insertion.

SIGN (Surgical Implant Generation Network) is one such local manufacturer of orthopaedic supplies that has developed a T-shaped handle with a threaded end to that it can screw onto the nail (see Appendix A). SIGN was founded in 1999 by Lewis G Zirkle, MD, the president and chief executive officer. SIGN designs and manufactures stainless steel nails to be donated to surgeons in third world countries. Dr. Zirkle, a practicing orthopaedic surgeon, trains the surgeons in these third world countries on the procedures for insertion of these nails. Dr. Zirkle has attested to the fact that insertion of the nails requires a considerable amount of force that can tire a surgeon and increase surgical time. Dr. Zirkle has acknowledged that a device that would allow easier insertion and extraction of nails would be very beneficial to the field of orthopaedic implants [6].

1.4 Purpose of Thesis

The purpose of this thesis is to investigate the use of vibration to reduce the amount of force and time needed for insertion and extraction of surgical implants such as nails. The concept of applying vibration to surgical implants to help facilitate easier insertion and extraction is novel to the field of orthopaedic implants. The clinical use of vibration as a means of reducing the necessary applied force may go beyond the insertion of typical nails used in large bones such as the tibia and femur as it could be used in total hip implants and smaller pins and fixation devices in long bone.

This thesis will focus on the “proof of concept” that vibration can be used to significantly reduce the force needed for insertion of nails. The hypothesis is that applying vibratory forces at an appropriate frequency or range of frequencies will reduce the amount of force required for nail insertion. Although it is beyond the scope of this thesis, should the concept be proven effective, prototype devices could be designed, manufactured, and tested. Prototype testing in vivo would be the optimum and provide the most conclusive results.

Proof of concept will be demonstrated by two methods, experimentation and engineering analysis. Data will be collected from the laboratory experiments and results will be obtained from the analytical techniques and then compared. From the results comparison, conclusions will be drawn and discussed.

2.0 BACKGROUND

2.1 Bone Description

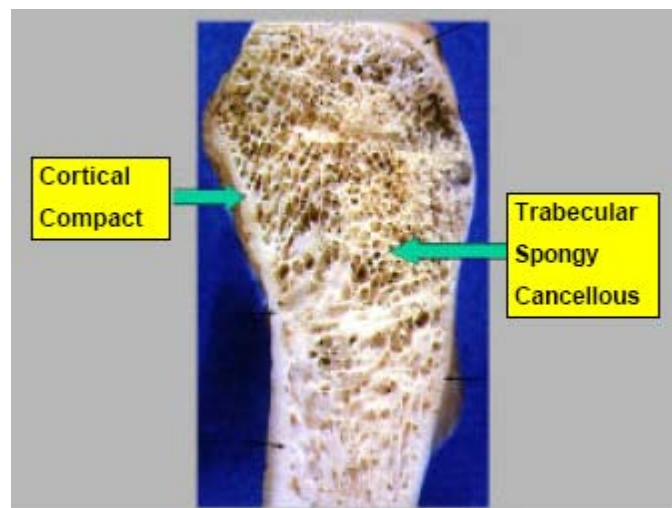
In order to investigate vibratory nail insertion, a thorough understanding of the material in which the nail is inserted is needed. Bone is the material that supports the body against external forces, enables muscles to transfer forces, and provides protection for vital internal organs. The skeletal system, comprised of 206 distinct bones, contains 99% of the total body calcium. Other elements that are stored in bone include phosphorus, sodium, potassium, zinc, and magnesium.

Bone is divided into five main classes based on bone shape. They are long bones, short bones, flat bones, irregular bones, and sesamoid bones. Long bones and short bones provide strength and transmit longitudinal force. Long bones are also used to act as levers for the muscular tissues. Flat bones provide protection and points of attachment for tendons and ligaments. Irregular bones can perform a variety of functions and sesamoid bones give an improved leverage for muscular tissue.

Bone is constructed of an organic matrix, approximately 95% collagen fibers, strengthened by calcium and phosphate salt deposits in the form of hydroxyapatite. It is these deposits that give bone strength, hardness, and rigidity. The collagen fibers allow the bone to be somewhat flexible [5].

Bone can be classified into two main types of hard tissue structures: cortical and cancellous bones. Cortical bone, sometimes referred to as compact bone, is the dense, more rigid outer bone that composes the shaft, otherwise known as the diaphysis, of long bones such as the femur and tibia. This bone type is solid, strong, and has a high bending strength. Cancellous, sometimes referred to as trabecular or spongy bone, is the softer, more porous bone material located on the inside of tubular long bones such as the femur and tibia. Cancellous bone is also found inside the knobby ends, otherwise known as the epiphysis, of long bones. Cancellous bone is usually oriented in the direction of applied forces; therefore, this bone type has a high compressive strength. Figure 2 shows these two main bone types at the knobby end of a long bone.

Figure 2. Two Main Types of Bone Tissue.



2.2 Bone Mechanical Properties

Bone is an anisotropic, non-homogenous, viscoelastic material. Bone mechanical properties are also known to vary widely depending on many factors including genetics, diet, and age. Because the mechanical properties of bone change as a function of the specific location in the bone and the direction in which force is applied, it is extremely difficult to model and analyze. Modeling bone as a linearly elastic, isotropic material can be adequate in certain circumstances but it is more accurate to model it as a linearly elastic anisotropic material at strain rates determined from experimentation. The broad ranges of mechanical properties for cancellous and cortical bone are presented in Table 1 below.

Table 1. Mechanical Properties of Cancellous and Cortical Bone.

Bone	Density (kg/m ³)	Poisson's Ratio	Elastic Modulus (GPa)	Tensile Strength (MPa)	Compressive Strength (MPa)
Cortical	1700-2000	0.28-0.45	5-28	80-150	106-224
Cancellous	100-1000	-	0.1-10	-	1-100

Ref [4]

If modeling the bone as an anisotropic material, the governing equations are presented. The well known constitutive equation for a linearly elastic material is the generalized version of Hooke's Law below:

$$\sigma_i = c_{ij} \cdot \epsilon_j \quad (\text{Eqn. 1})$$

Note that sigma in the above equation represents the principal stresses and the index possesses a range of six. The stress-strain relationship can be similarly expressed in terms of the compliance matrix, S_{ij} . This equation is shown below.

$$\varepsilon_i = S_{ij} \cdot \sigma_j \quad (\text{Eqn. 2})$$

This compliance matrix of an orthotropic material in terms of the material constants, Young's modulus, E_i , and Poisson's ratio, ν_{ij} , and the shear modulus, G_{ij} , becomes:

$$S_{ij} = \begin{bmatrix} 1/E_1 & -\nu_{21}/E_2 & -\nu_{31}/E_3 & 0 & 0 & 0 \\ -\nu_{12}/E_1 & 1/E_2 & -\nu_{32}/E_3 & 0 & 0 & 0 \\ -\nu_{13}/E_1 & -\nu_{23}/E_2 & 1/E_3 & 0 & 0 & 0 \\ 0 & 0 & 0 & 1/G_{23} & 0 & 0 \\ 0 & 0 & 0 & 0 & 1/G_{31} & 0 \\ 0 & 0 & 0 & 0 & 0 & 1/G_{12} \end{bmatrix} \quad (\text{Eqn. 3})$$

These twelve material constants can be determined by mechanical and/or ultrasonic testing. Of course, mechanical testing must be performed in all directions to determine all the independent elastic constants of the anisotropic bone. With ultrasound, all the independent elastic constants can be measured on a single specimen.

3.0 VIBRATION EXPERIMENTS OF SURGICAL IMPLANT INSERTION

3.1 Purpose of the Vibration Experiments

The purpose of the vibration experiments is to provide "proof of concept" that vibration can be used to decrease the amount of force required for insertion of surgical implants. The experiments involve applying vibrational excitations directly to the surgical implant at different frequencies and in different directions while measuring the force required for insertion. This will show whether the applied vibration reduces the insertion force for the implant.

3.2 Equipment Used in the Vibration Experiments

The simulated nail used for the experiments is a carbon steel rod, 13 inches in length and 0.312 inches in diameter. The actual dimensions of commercially available nails varies depending on the manufacturer, however, this diameter and length is within the dimension range of nails typically used for long bones such as the tibia. SIGN is one manufacturer of nails designed to be used on tibia fractures. SIGN's nails are approximately 0.315 inches in diameter and 13 3/8 inches in length. Figure 3 shows the simulated nail used in the experiments.

Figure 3. Simulated Nail.



The vibration experiments are conducted on three types of materials. The materials are ultra-high molecular weight polyethylene (UHMW-PE), biomechanical test blocks, and fresh wet bone from bovine. The biomechanical test blocks and fresh wet bone provide a testing material with properties similar to human bone. Therefore, experimentation with these materials is more realistic and the results of the experiments are more representative of the actual surgical procedure. However, the biomechanical test blocks and wet bovine bone do not provide a good

material for trial testing. Under repetitive trial experimentation, the biomechanical test blocks and wet bovine bone were found to wear down giving inconsistent results. To illustrate “proof of concept”, experimentation with multiple trials must be performed in order to infer a definite conclusion about the effects of vibration on surgical implant insertion. For this reason, testing is also performed on UHMW-PE. UHMW is a tough, wear resistant material that can withstand many trials without wearing enough to affect results.

The biomechanical test blocks are obtained from Sawbones Worldwide, a division of Pacific Research Laboratories, Inc. Sawbones specializes in medical models for orthopedic and medical education. Biomechanical test materials are used as an alternative testing medium to human cadaver bone. The biomechanical test blocks offer uniform and consistent physical properties that eliminate the variability encountered when testing with human cadaver bone. They are primarily used for testing orthopaedic implants, instruments and instrumentation [7]. The biomechanical test blocks are solid, rigid polyurethane foam with mechanical properties in the range of human cancellous bone. These test blocks meet ASTM F-1839 “Standard Specification for Rigid Polyurethane Foam for Use as a Standard Material for Testing Orthopaedic Devices and Instruments” [7]. The biomechanical test block specification and mechanical properties are contained in Appendix B. Figure 4 shows the biomechanical test blocks.

Figure 4. Biomechanical Test Blocks.



The UHMW-PE is obtained from the Washington State University Tri-Cities mechanical engineering laboratory. The UHMW-PE is a very wear resistant material typically used for applications such as wear strips, guide rails, chutes and hoppers, star wheels and sprockets, bushings, bearings, and rollers. The wear resistant properties of UHMW-PE are desired for vibration experiments involving multiple trials. This prevents the material wear from affecting the results. Multiple trial experimentation is needed to collect enough data so that statistics can be calculated and reliable conclusions can be drawn. Typical UHMW-PE mechanical properties are shown in Appendix C. Figure 5 shows the cylindrical block of UHMW-PE used.

Figure 5. UHMW-PE Test Block.



The fresh, wet bovine bones are obtained from a local butcher shop, Knutzen's Meats in Pasco, Washington. The bones were collected from a fresh bovine slaughter and frozen in the store meat freezer. The bovine bones were set out to thaw for over 36 hours before experimentation was conducted. This allowed the wet bone to become soft and the biological fluids to melt. The wet bone is the most realistic material used in the vibration experiments. Figure 6 shows the fresh bovine bone.

Figure 6. Fresh Bovine Wet Bone.



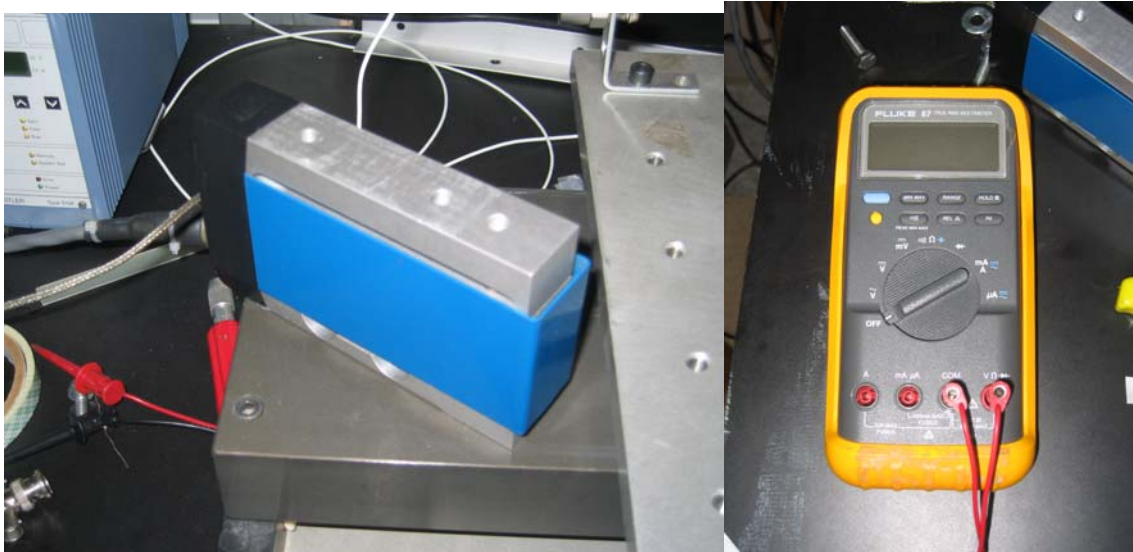
The vibration is applied by a vibratory shaker table provided by the (WSU) Washington State University Tri-Cities mechanical engineering department. The shaker table is powered by compressed air from a compressor and controlled by a vibration monitor and sweep generator. The vibration signal is also run through a signal amplifier. The sweep generator allowed the frequency of the shaker table to be varied over a wide range. The shaker table is approximately two feet by two feet square. Figure 7 shows the vibration equipment that was used.

Figure 7. Vibration Shaker Table and Controllers.



The force measurement device used in the experiments is an S-type load cell also provided by the mechanical engineering department. The S-type load cell utilizes a strain gage and is capable of reading compression or tension with a voltage output. This voltage output is then read using a digital multi-meter. The digital multi-meter, also provided by the engineering department, had recording and averaging capabilities that were very helpful in getting an accurate reading during the experiments. Figure 8 shows the S-type load cell and digital multi-meter used to measure and record force.

Figure 8. Load Cell and Digital Multi-Meter.



3.3 Methodology and Procedure of the Vibration Experiments

The vibration was applied to the nail in two directions, transverse and longitudinal to the long axis of the nail. Torsional vibration was not considered. Although torsional vibration may allow for easier insertion of nails, there is an increased difficulty in designing a device that will apply torsional vibration to the rod without rotating the T-handle and interfering with the orthopaedic surgeon's grip. A device designed to apply transverse or axial vibration can be easily designed and the attached to the T-handle without interfering with the orthopaedic surgeon's grip. Figures 9 and 10 show the experimental set up for the transverse and axial vibration experiments, respectively.

Figure 9. Transverse Vibration Experiment Set Up.

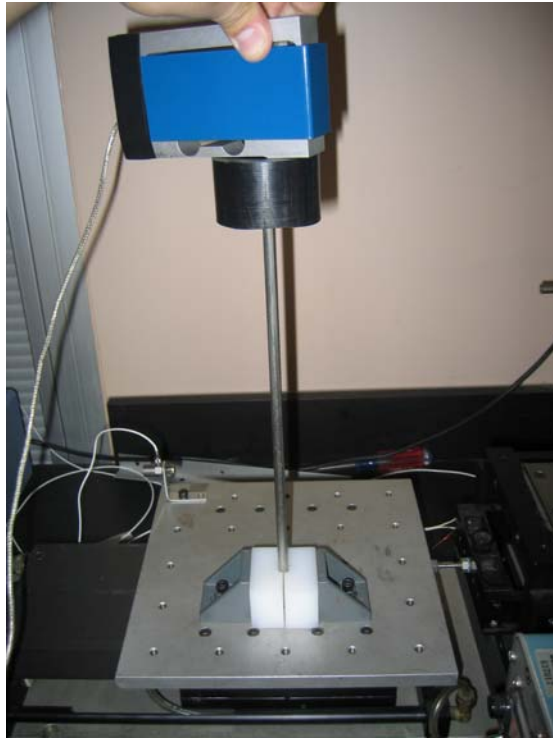
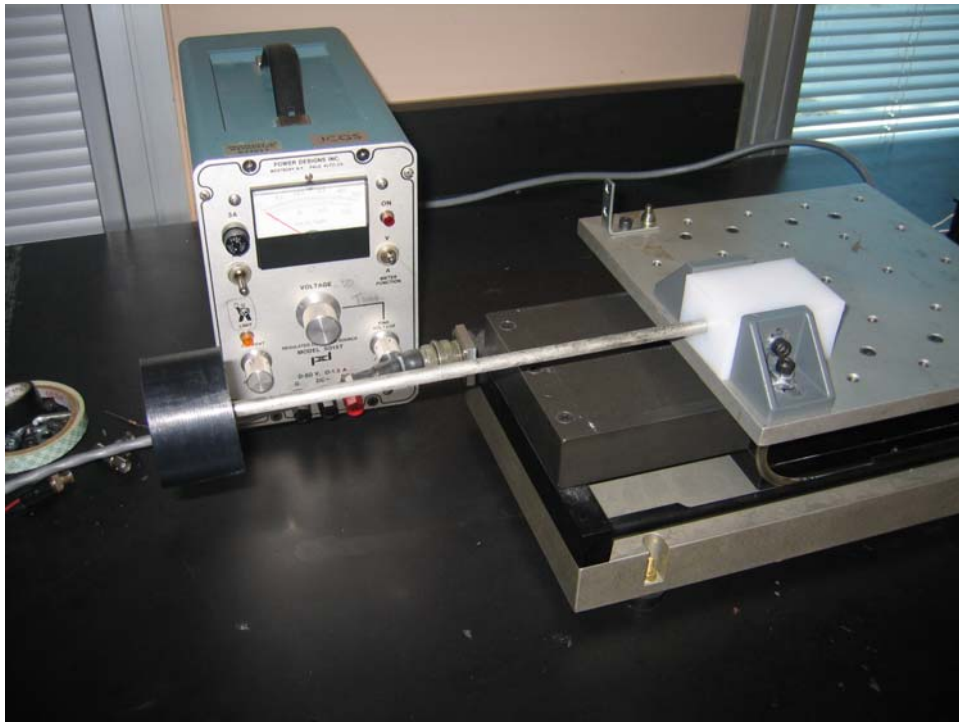


Figure 10. Axial Vibration Experiment Set Up.



As shown in the Figures, the simulated nail is mounted to the vibratory shaker table by means of brackets that are fastened to the table with socket head cap screws. A nylon block with a hole drilled through it and cut in half is used in between these mounting brackets to secure the simulated nail. Once the simulated nail has been firmly mounted to the shaker table, the vibration experiments are performed.

The procedure for one trial of the vibration experiments is outlined below:

1. The shaker table and controllers are turned on and set to the desired vibration frequency and the amplifier turned up to the maximum.
2. The testing material is then placed on the end of the simulated nail without application of force.
3. The load cell is placed directly on top of the testing material. At the same time, the digital multi-meter begins recording and a person performing the experiment begins to push down on the load cell with their hand.
4. As the person pushes the load cell, the load cell pushes on the test material forcing it down the vibrating nail. All the voltage output during this time is captured and recorded by the digital multi-meter.
5. At the same time that the testing material has been pushed all the way down to the bottom of the simulated nail, the digital multi-meter recording feature is stopped.
6. Then the maximum, minimum, and average voltage output can be read off the digital multi-meter recording memory. The voltage output can be converted to force using the conversion factor for the load cell.

3.4 Equipment Calibration Procedure and Results

Before any experiments were performed, the load cell was calibrated so that the voltage output could be converted into force correctly. Calibration of the load cell involved placing precision weight with very low uncertainties on the load cell and recording the voltage output.

This calibration procedure was performed with no weight for a baseline reading and an additional eight different precision weights. Figure 11 shows the precision weights used to calibrate the S-type load cell.

Figure 11. Precision Weights Used for Calibration.



Using no weight and the eight precision weights and gives a total of nine data points, which are used to calibrate the load cell and determine the correct conversion factor for converting voltage to force. In addition, the uncertainty of the force conversion factor was also determined. Table 2 shows the calibration data for the load cell.

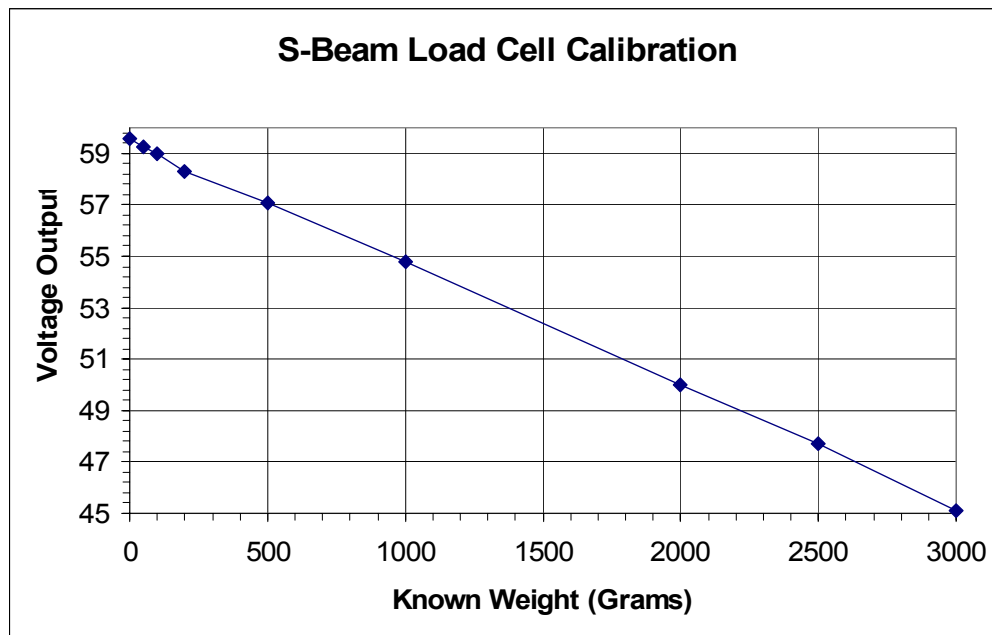
Table 2. Load Cell Calibration Data.

Precision Weights (grams)	Weight (lbs)	Voltage Output (mV)	Conversion Factor (lbs/mV)
0	0.00	59.6	NA
50	0.11	59.25	0.31
100	0.22	59	0.44
200	0.44	58.3	0.31
500	1.10	57.1	0.55
1000	2.21	54.8	0.48
2000	4.41	50.0	0.46
2500	5.51	47.7	0.48
3000	6.62	45.1	0.42

Average Conversion Factor (lbs/mV)	0.43
Standard Deviation (lbs/mV)	0.082

The conversion factor in Table 2 appears to be linear; however, the standard deviation of the conversion factor is a little bit higher than expected. If funds were available, a higher precision load cell with lower uncertainty could be used, however, some of the error can be attributed to the digital multi-meter error in reading the voltage. A market study was performed and concluded that at least \$300.00 would be needed for a new S-type load cell. Purchasing a new load cell was determined to be not economically feasible. Figure 12 shows the Table 2 data in graph format where is easier to see the linear behavior of the load cell.

Figure 12. Graph of the Load Cell Calibration Data.



The S-type load cell is determined to be adequate for use in the vibration experiments. The average conversion factor from Table 2 is used to convert all experimental data.

3.5 Vibration Experiment Results on Biomechanical Test Blocks

The first material used in the vibration experiments was the biomechanical test blocks. First, baseline data was collected by measuring the amount of force required for full insertion of the nail with no vibration applied. Three trials were conducted with no vibration. For each of these trials, the data collected is the maximum, minimum, and average force. Then the vibration experiments are carried out at the desired vibrational frequencies. Again, for each vibration frequency, three trials were conducted and again for each trial, the maximum, minimum, and average force is recorded. Statistical analysis is performed on the data to determine the standard deviation. The amplifier was turned up to the maximum for all frequencies. This resulted in an average acceleration of 0.75 Gs; however, the acceleration did fluctuate anywhere from 1.25 Gs

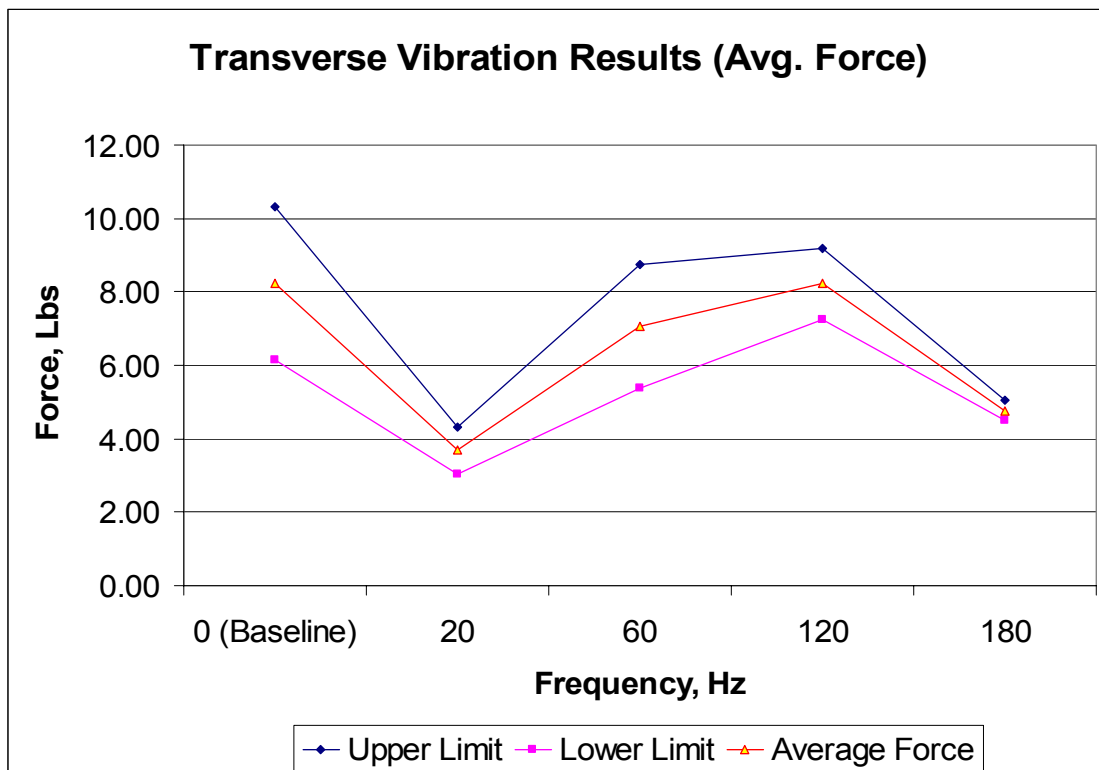
to 0.5 Gs with change in frequency. The higher accelerations occurred at the lower frequencies. Table 3 shows the transverse vibration average force results of the biomechanical test block experiments.

Table 3. Transverse Vibration Average Force Results with Biomechanical Tests Blocks.

Frequency	Average Force	Standard Deviation	Upper Limit Standard Deviation	Lower Limit Standard Deviation
0 (Baseline)	8.24	2.09	10.33	6.16
20	3.68	0.64	4.32	3.04
60	7.04	1.68	8.73	5.36
120	8.21	0.96	9.18	7.25
180	4.76	0.27	5.03	4.49

Figure 13 shows a graph of the transverse vibration average force data in Table 3.

Figure 13. Transverse Vibration Average Force Graph with Biomechanical Test Blocks.



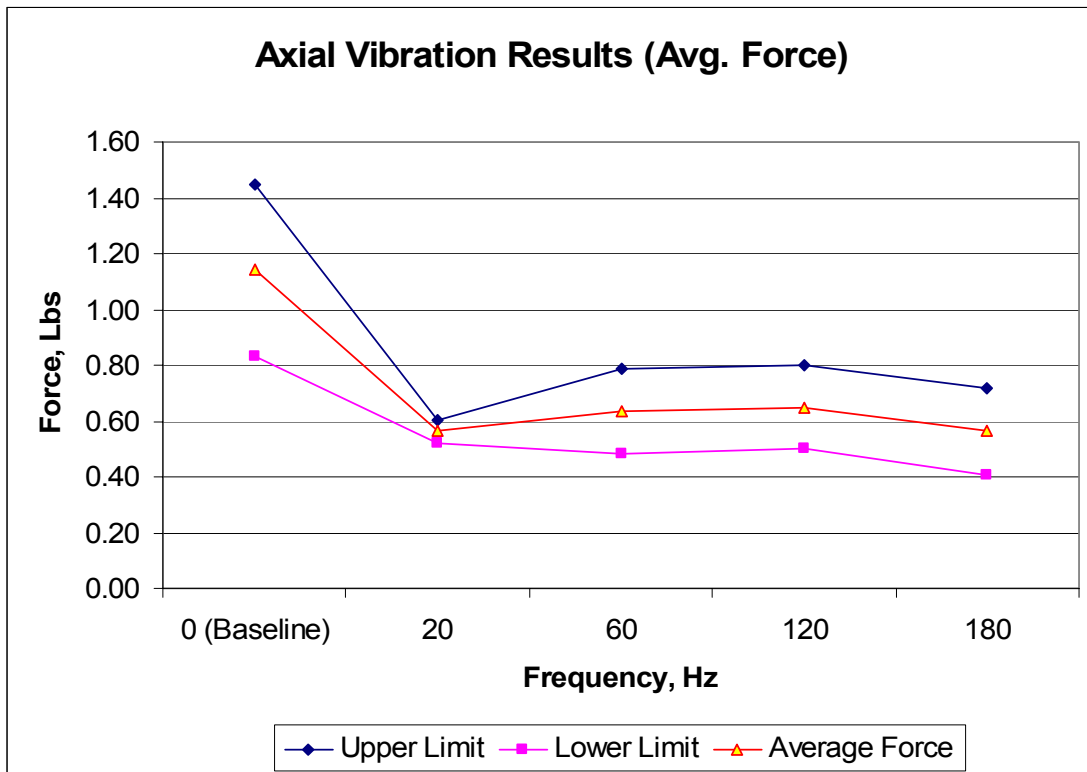
The same experiment on biomechanical test blocks was performed with axial vibration applied as opposed to transverse vibration. Table 4 shows the axial vibration average force results of the biomechanical test block experiments.

Table 4. Axial Vibration Average Force Results with Biomechanical Tests Blocks.

Frequency	Average Force	Standard Deviation	Upper Limit Standard Deviation	Lower Limit Standard Deviation
0 (Baseline)	1.14	0.31	1.45	0.83
20	0.56	0.04	0.61	0.52
60	0.64	0.15	0.79	0.48
120	0.65	0.15	0.80	0.50
180	0.56	0.16	0.72	0.41

Figure 14 shows a graph of the axial vibration average force data in Table 4.

Figure 14. Axial Vibration Average Force Graph with Biomechanical Test Blocks.



The transverse and axial vibration data in terms of voltage output before conversion into force is shown in Appendices D through I. Also the average and maximum force data and associated maximum force graphs are all contained in Appendices D through I. In almost all of the cases, the maximum force data follows the average force data trends. Therefore, the maximum force data is redundant in nature to the average force data. Maximum force data is shown in Appendices D through I.

The transverse and axial vibration minimum force data is also contained in Appendices D through I. In almost all of the cases, the minimum force data tended to be zero or near zero. The minimum force of zero or near zero occurs on the multi-meter recording at the beginning when the force is just starting to be applied or at the end when the applied force is being removed completely. Therefore, the minimum force data is trivial and only provides evidence that the multi-meter recording was started just after the applied force and ended prematurely before the applied force was removed.

3.6 Vibration Experiment Results on UHMW-PE

The second material used in the vibration experiments was the wear resistant UHMW-PE. First, baseline data was collected by measuring the amount of force required for full insertion of the nail with no vibration applied. Ten trials are conducted with no vibration. For each of these trials, the maximum, minimum, and average force is the collected data. Then the vibration experiments are carried out at the desired vibrational frequencies. The vibration experiment was also performed with a frequency sweep between 10 Hz up to 260 Hz. For each vibration frequency and the frequency sweep, five trials are conducted and for each trial, the maximum, minimum, and average force is recorded. There were more trials performed with the UHMW-PE because of its wear resistant properties. Statistical analysis is performed on the data to determine the standard deviation. Again, the amplifier was turned up to the maximum for all frequencies. This resulted in an average acceleration of 0.75 Gs; however, the acceleration did

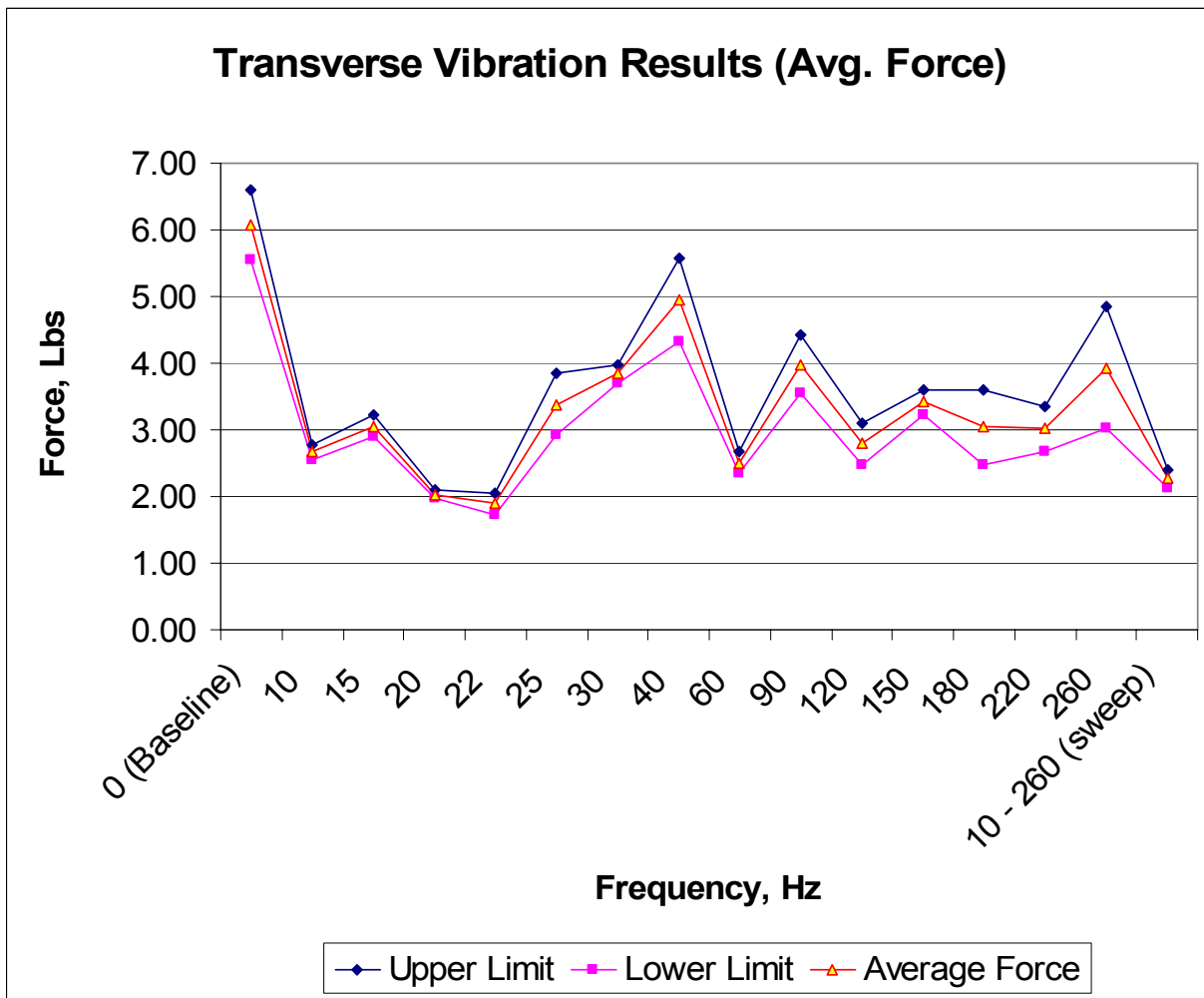
fluctuate anywhere from 1.25 Gs to 0.5 Gs with change in frequency. The higher accelerations occurred at the lower frequencies. Table 5 shows the transverse vibration average force results of the UHMW-PE experiments.

Table 5. Transverse Vibration Average Force Results with UHMW-PE.

Frequency (Hz)	Average Force (lbs)	Standard Deviation	Upper Limit Standard Deviation	Lower Limit Standard Deviation
0 (Baseline)	6.08	0.52	6.60	5.56
10	2.67	0.12	2.78	2.55
15	3.06	0.16	3.22	2.90
20	2.04	0.05	2.09	1.98
22	1.89	0.16	2.05	1.73
25	3.38	0.46	3.84	2.91
30	3.85	0.13	3.98	3.71
40	4.95	0.63	5.58	4.31
60	2.51	0.17	2.68	2.34
90	3.98	0.43	4.42	3.55
120	2.79	0.32	3.11	2.47
150	3.42	0.19	3.61	3.23
180	3.04	0.57	3.61	2.47
220	3.01	0.33	3.34	2.69
260	3.93	0.91	4.84	3.02
10 - 260 (sweep)	2.27	0.14	2.40	2.13

Figure 15 shows a graph of the transverse vibration average force data in Table 5.

Figure 15. Transverse Vibration Average Force Graph with UHMW-PE.



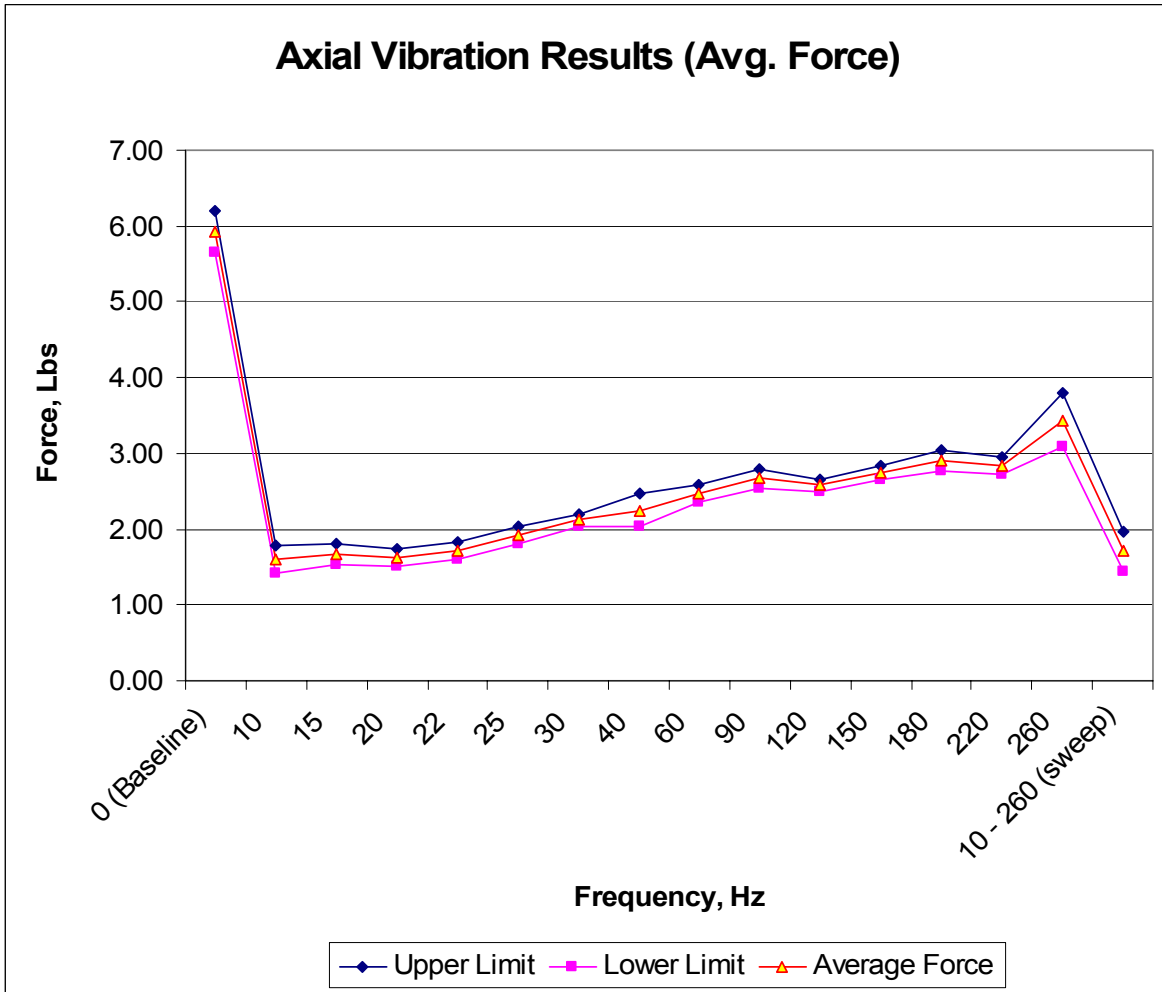
The same experiment on UHMW-PE was performed with axial vibration applied as opposed to transverse vibration. Table 6 shows the axial vibration average force results of the UHMW-PE.

Table 6. Axial Vibration Average Force Results with UHMW-PE.

Frequency (Hz)	Average Force (lbs)	Standard Deviation	Upper Limit Standard Deviation	Lower Limit Standard Deviation
0 (Baseline)	5.93	0.27	6.20	5.66
10	1.60	0.19	1.79	1.41
15	1.67	0.14	1.81	1.52
20	1.62	0.11	1.74	1.51
22	1.72	0.11	1.83	1.61
25	1.93	0.12	2.05	1.81
30	2.12	0.07	2.19	2.05
40	2.25	0.22	2.47	2.03
60	2.47	0.12	2.59	2.36
90	2.67	0.13	2.80	2.54
120	2.58	0.08	2.65	2.50
150	2.74	0.09	2.84	2.65
180	2.91	0.13	3.03	2.78
220	2.85	0.11	2.96	2.73
260	3.44	0.36	3.81	3.08
10 - 260 (sweep)	1.71	0.27	1.98	1.44

Figure 16 shows a graph of the axial vibration average force data in Table 6.

Figure 16. Axial Vibration Average Force Graph with UHMW-PE.



The transverse and axial vibration data in terms of voltage output before conversion into force data is shown in Appendices J through O. Also the average and maximum force data and associated maximum force graphs are contained in Appendices J through O. In almost all of the cases, the maximum force data follows the average force data trends. Therefore, the maximum force data is redundant in nature to the average force data. Appendix P shows a graphical comparison between the transverse and axial vibration average force results.

The transverse and axial vibration minimum force data is also contained in Appendices J through O. In almost all of the cases, the minimum force data tended to be zero or near zero. The minimum force of zero or near zero occurs on the multi-meter recording at the beginning

when the force is just starting to be applied or at the end when the applied force is being removed completely. Therefore, the minimum force data is trivial and only provides evidence that the multi-meter recording was started after the applied force and ended prematurely before the applied force was removed.

3.7 Vibration Experiment Results on Wet Bovine Bone

The third and last material used in the vibration experiments was the wet bovine bone. Before experimentation, the wet bovine bones had been frozen; therefore, the bones were placed into a cooler with no ice and allowed to thaw for over 36 hours. The bones were examined and verified to be completely thawed before experimentation. The bones were prepared for experimentation but they were not wiped dry in an effort to preserve the natural bio-fluids on the bone. Preparation included cutting the bone into two inch long sections and drilling the holes transverse to the longitudinal axis of the bone. Refer to Figure 19 for to see the configuration.

The wet bovine bone experiments were first set up to be conducted in the same fashion as the previous experiments with the other two materials. The intention was to follow the same procedure; however, several unexpected difficulties presented themselves during the wet bovine bone experiments. This prevented the experiments from being carried out in the same manner as the other two materials.

3.7.1 Difficulties Encountered with Wet Bovine Bone Experiments

Several observations were made about the difficulties with performing the vibration experiments. The most notable and important observations are described in detail below:

- The wet bones were of an irregular shape and were covered with bio-fluids such as bone marrow, blood, mucus, etc. The irregular shape and bio-fluids made the bone slippery

and therefore, made it difficult to apply a load to the bone with the load cell without it slipping off the bone.

- The same hole size was drilled in each of the 4 specimens, but it was observed during baseline experiments (no vibration) that each specimen required a different amount of insertion force. With the same hole size, some specimens required almost no insertion force (sliding down the nail under its own weight) while others required significant force for insertion.
- It was also observed that using the same specimen, the insertion force required varied. In one baseline trial the specimen would require a large insertion force and the same specimen in another baseline trial would require very little insertion force. The insertion force was not consistent even with the same specimen.
- Another observation was that if the bone specimen required some insertion force to move it down the nail, once the specimen began moving it required significantly less or no force. In other words, the bone specimen took significantly more force to get it moving, than it took to keep it moving down the nail. Static friction was greater than dynamic friction.
- The last observation is that the bone specimens tended to wear out after a number of trials. Eventually, after completing a number of trials with the same bone specimen, the bone hole would be reamed or worn such that considerably less insertion force was needed.

3.7.2 Explanation of the Wet Bone Difficulties

After conducting the wet bovine bone experiments and making the aforementioned observations, the bone specimens were examined more closely and some experiments were performed to try to explain the behavior of the bone. The conclusions and the speculative explanations of the observations are listed below:

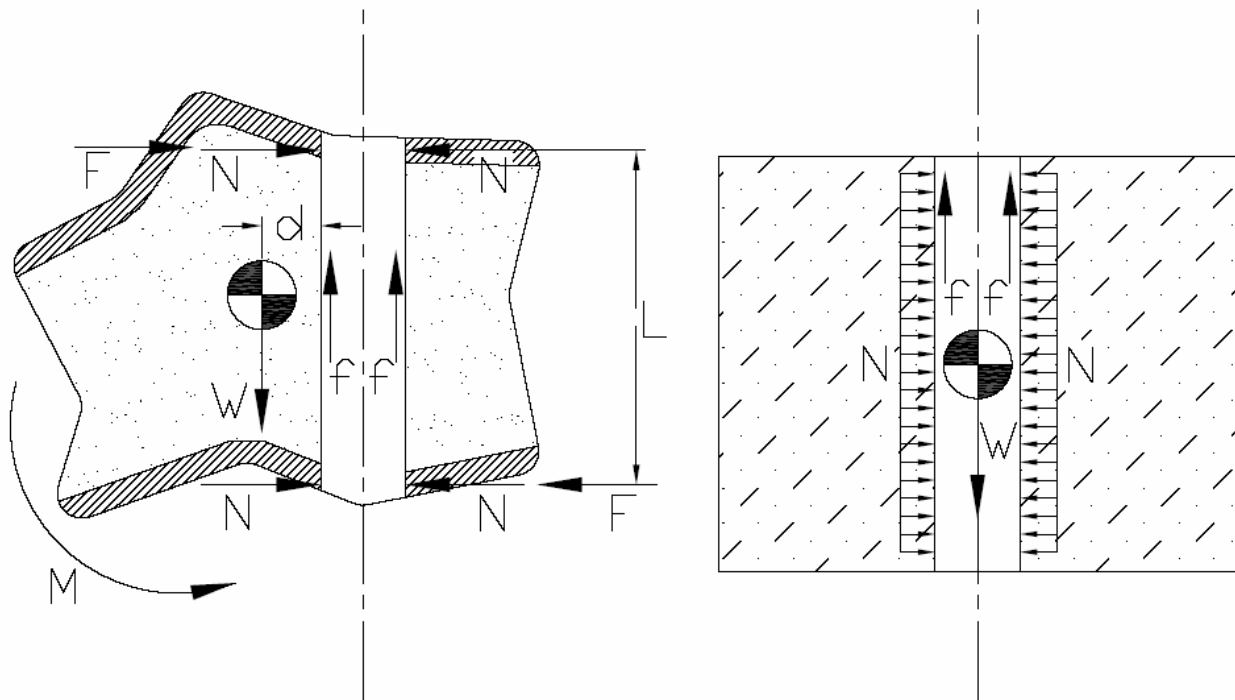
- Based on the first observation, it was concluded that the experiments could not be carried out in the same manner as they were with the first two materials. The irregular shape and bio-fluids make using the load cell too difficult.
- The second observation may likely be due to the non-uniformity of the bone specimens both in shape and cortical bone thickness. The cortical bone thickness on the specimens was seen to vary widely between specimens and also on each specimen going around the perimeter. The cortical bone thicknesses were measured on the 4 specimens and found to range from about 1/8 inch thick to 3/4 inch thick. In the middle of the cortical bone is the bone marrow, which is soft and gives almost no resistance to nail insertion. So the cortical bone provides the primary resistance to nail insertion and its thickness variance would affect insertion force. Figure 17 shows a picture of a couple of the specimens so that the cortical bone thickness and bone marrow can be seen.

Figure 17. Wet Bone Showing Cortical Bone and Marrow.



- The non-uniformity of the bone specimens shape also may contribute to the third observation. Having an irregular shape makes the center of gravity of the specimen be offset from the location where the drilled hole is. The offset center of gravity causes a moment to be placed on the specimen from its own weight. This moment must be counteracted by lateral forces on the steel nail. These lateral forces introduce a couple that increases the frictional resistance to insertion. This concept is better understood by an illustrated free body diagram. Figure 18 shows a free body diagram of a bone specimen with an offset center of gravity and a block of material such as UHMW-PE with no offset center of gravity.

Figure 18. Free Body Diagram of Bone Specimens on the Nail.



From Figure 18, it is clear how the center of gravity offset puts a moment on the specimen. The lateral force of the nail to counteract this moment is shown in Figure 18 as force, F . Force, F , is in addition to normal force, N , and increases the total lateral

force considerably. The force, F , can be determined by a simple moment equation shown in equation 4.

$$\sum M = 0 = W \cdot d - F \cdot L \quad (\text{Eqn. 4})$$

The increase in the total normal force is the existing normal force, N , due to the hole tightness and the added force, F , due to the moment. This increases the overall frictional resistance, f , as shown in equation 5 below.

$$f = \mu \cdot (F + N) \quad (\text{Eqn. 5})$$

For the specimen on the right of Figure 18, the hole is drilled through the center of gravity, therefore, the extra force, F , does not exist and does not add to the normal force, N . This same concept with respect to the location of the applied force was also observed. If the applied downward force was located right where the hole in the bone is, then the bone would move down the nail more easily. If the applied downward force was placed away from the hole, then the bone would not move. When the force was applied with a greater moment arm, an extremely large downward force could be applied and the bone would not move. The moment created by the applied downward force at some distance away from the hole affected the wet bone results considerably more than it affected experiments with the other materials. This is most likely due to the fact that the wet bone center is bone marrow, which can not support any load. Therefore, the cortical bone which is relatively thin (small cross sectional area) takes the entire load due to the moment. Refer to Figure 18.

- With respect to the fourth observation, that the bone requires noticeably more force to start moving down the nail than it takes to keep moving down the nail, this seems to be related to the frictional resistance between the nail and the bone specimen. It appears that

cortical bone has a substantially higher static coefficient of friction than the dynamic or sliding coefficient of friction. This would explain why the bone moves easier once it is moving. A literature search did not find data on the difference between the static and dynamic coefficients of friction of cortical bone, although the cortical bone average static coefficient of friction has been reported as 0.74 on porous metal [8]. The coefficient of friction on smooth stainless steel would likely be lower.

- The last observation of the bone hole wearing after repeated use correlates well with the observed behavior of the biomechanical test blocks that were designed to simulate bone. Both materials exhibited a tendency to wear easily under a frictional load. A literature search produced some evidence that bone does have poor wear resistance against some materials such as titanium [9].

3.7.3 Bovine Wet Bone Experiments

Although the wet bone experiments were difficult to conduct in the same manner as the other materials, some bone experiments were conducted that provided valuable data.

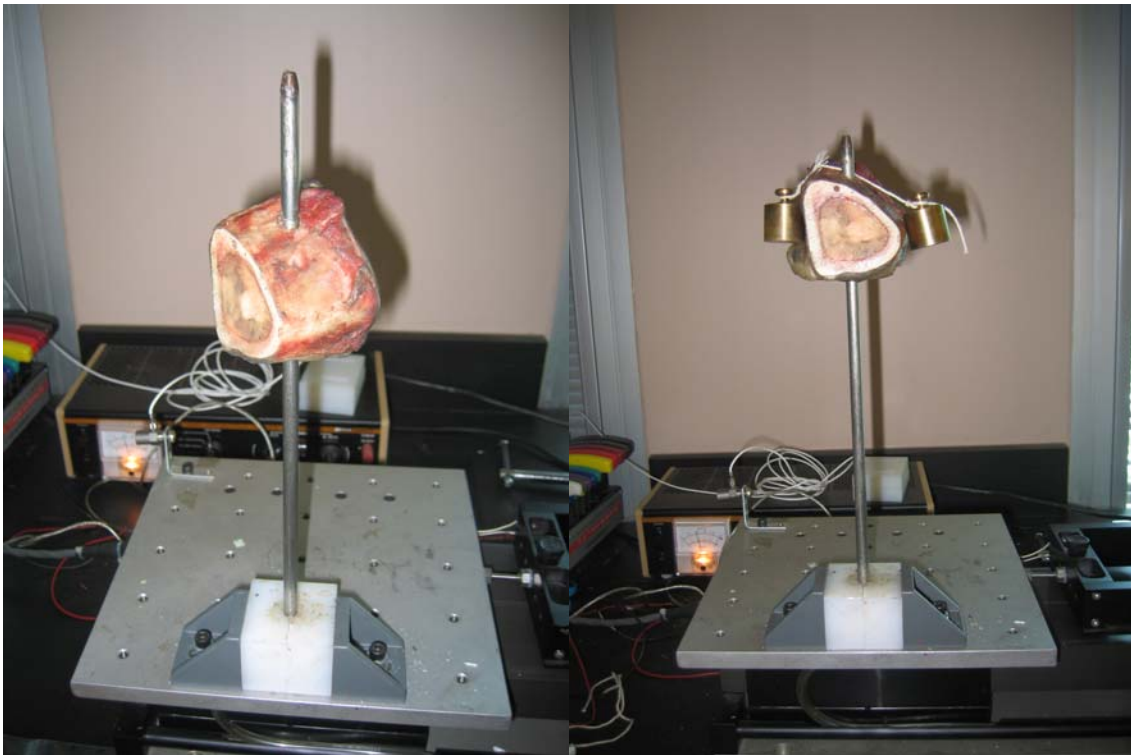
It was observed that some bone specimens would not move down the nail without vibration because the frictional resistance of the hole was enough to prevent sliding down the nail. However, for some specimens, very little applied force was needed to move the bone specimen down the nail.

When the nail is mounted to the vibration table vertically, the bone specimen can be placed on top of the nail. The nail can undergo transverse vibration with the bone on top and the vibration frequency can be swept to determine if the vibration causes the bone specimen to move down the nail under its own weight. This is the experiment that was performed.

The experiment was also conducted with calibrated weights hanging on the bone to increase the total mass. The experiment was conducted with the bone weight only and then with 200 grams added to the bone weight and finally with 400 grams added to the bone weight. The

weights added are calibrated weights hanging off the bone with string. The experiment configuration and setup is shown in Figure 19.

Figure 19. Experiment Configuration with Bovine Bone.



In all the bone experiments, the amplifier was turned up to the maximum for all frequencies. As before, this resulted in an average acceleration of 0.75 Gs; however, the acceleration did fluctuate anywhere from 1.25 Gs to 0.5 Gs with change in frequency. The higher accelerations occurred at the lower frequencies.

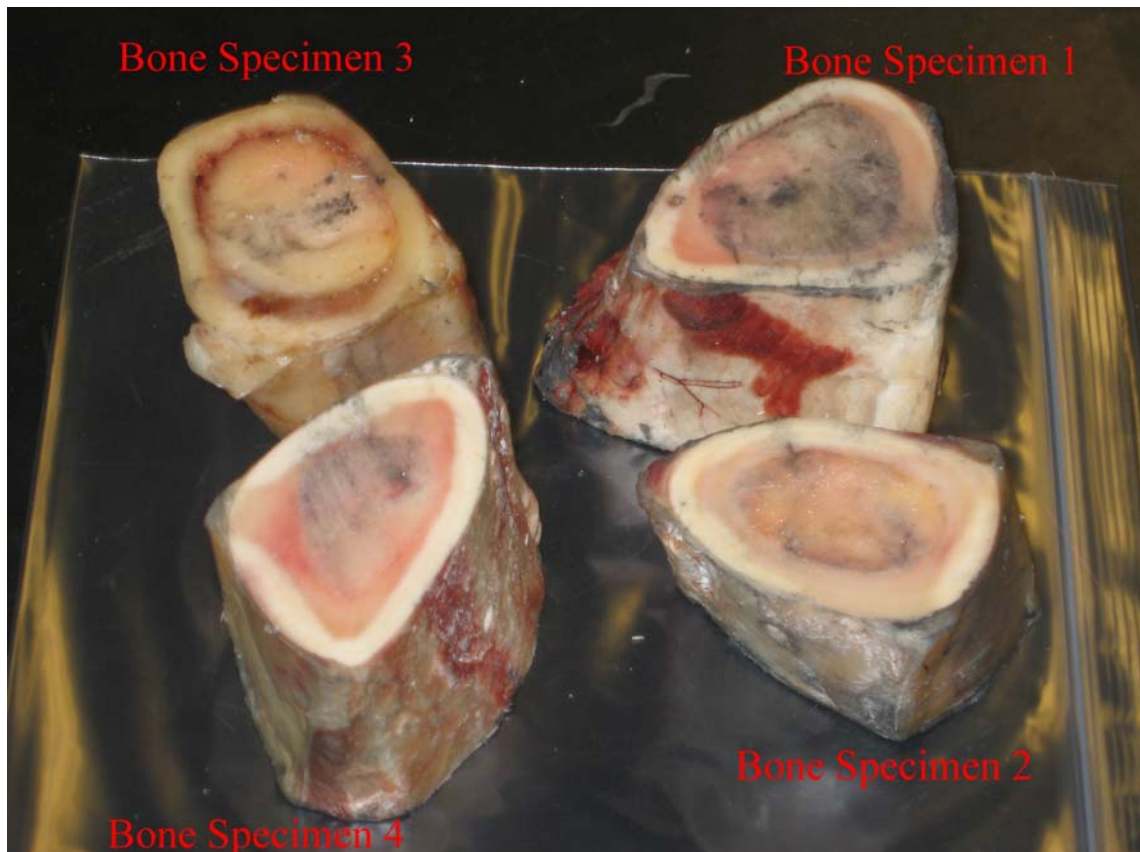
Gravity is the mechanism by which the insertion force is provided. The insertion force is equal to the bone specimen weight. The four bone specimens were weighed to determine the amount of insertion force the bone itself applies to the nail. This is shown in Table 7.

Table 7. Wet Bovine Bone Weights.

Specimen	Weight (grams)	Weight (lbs)
Bone 1	220.12	0.49
Bone 2	152.66	0.34
Bone 3	146.53	0.32
Bone 4	171.00	0.38

The four bone specimens used in the experiments are shown in Figure 20 below.

Figure 20. Bovine Wet Bone Specimens.



The experiment was performed with bone specimen 1 first. Bone specimen 1 provided the most reliable results. When the bone completed a full drop, the time was recorded to determine how fast the drop occurred. The results of the experiments are shown in Table 8.

Table 8. Bone Specimen One Results.

Bone Weight Only		
	Frequency, (Hz)	Movement Down Nail (inches)
	Baseline (No vibration)	0
	20 Hz	0
	23.5 Hz	12.5 in. (Full Drop in 85 sec.)
	30 - 260 Hz	0
Bone Weight with 200 Grams Added		
	Baseline (No vibration)	0
	20 Hz	6.25 in.
	23.5 Hz	9.25 in.
	30 Hz	3.25 in.
	45 Hz	0.25 in.
	60 - 260 Hz	0
Bone Weight with 400 Grams Added		
	Baseline (No vibration)	0
	20 Hz	12.5 (Full Drop in 5 sec.)
	23.5 Hz	12.5 (Full Drop in 4 sec.)
	30 - 260 Hz	0

The same experiment was also conducted with bone specimens 2 through 4; however, the results more were inconsistent and unreliable. This may have been because the holes on these specimens became worn or reamed enough to affect the results. Table 9 and 10 shows the results of these experiments.

Table 9. Bone Specimen Two Results.

Bone Weight Only		
	Frequency, (Hz)	Movement Down Nail (inches)
	Baseline (No vibration)	0
	20 Hz	12.5 in. (Full Drop in 19 sec.)
	23.5 Hz	12.5 in. (Full Drop in 7 sec.)
Bone Weight with 200 Grams Added		
	Baseline (No vibration)	0
	20 Hz	1.5 in.
	23.5 Hz	4.75 in.
	30 Hz	12.5 in. (Full Drop in 100 sec.)

Table 10. Bone Specimen Three Results.

Bone Weight Only		
	Frequency, (Hz)	Movement Down Nail (inches)
	Baseline (No vibration)	0
	20 Hz	12.5 in. (Full Drop in 30 sec.)
Bone Weight with 200 Grams Added		
	Baseline (No vibration)	0
	20 Hz	12.5 in. (Full Drop in 5 sec.)

Bone specimen four results are not shown because the hole of bone specimen four had worn enough that it would fall down the nail without any vibration at all. No results were recorded with bone four.

In the bone two experiments, the “bone weight with the added 200 grams” experiment was performed first before the “bone weight only” experiment. The first experiment may have worn the hole enough so that the second experiment had less resistance. The second experiment shows more movement down the nail than the first experiment even though the second experiment had less weight. In both experiments after the last full drop was completed, the bone specimen began to drop down the nail without any vibration at all.

In the bone three experiments, after the full drop, the bone specimen began to drop down the nail without any vibration at all, similar to what occurred with bone four. It is most likely that the bone holes in bones two and three began to wear and enlarge, which caused the bone hole fit on the nail to be too loose.

Bone specimen one provided the most meaningful results that indicate that the applied vibration does reduce the necessary insertion force and the most effective applied vibration appears to be at the lower frequencies between 20 and 30 Hz. The most effective frequency of vibration was 23.5 Hz. From Table 8, no frequencies greater than 30 Hz caused the bone specimen to start moving down the nail.

A frequency sweep experiment conducted on bone specimen one also yielded an interesting result. With the bone specimen in place on the top of the nail, the vibration was applied at a high enough frequency that would not cause the bone specimen to move. Then the

vibration frequency was lowered slowly in order to determine just how low the frequency would have to be before the bone specimen would begin to move down the nail slightly. At 27.5 Hz, the bone specimen began to move down the nail just slightly and stopped about 1/4 of the way down the nail. Then the frequency of vibration was increased slowly until the bone specimen began moving again. This occurred at 30 Hz, where the bone specimen moved about halfway down the nail and stopped. Then the frequency of vibration was increased slowly until the bone specimen began moving again. This occurred at 45 Hz, where the bone specimen moved about 3/4 of the way down the nail and stopped. Once again, the frequency of vibration was increased slowly until the bone specimen began moving. At 50 Hz the bone specimen moved the remaining distance down to the bottom of the nail.

This is an interesting result because at any of these higher frequencies the bone specimen would not move down the nail from the top and at only 27.5 Hz the bone specimen would not move down the nail more than a 1/4 of the way. However, starting out slowly at 27.5 Hz and raising the frequency slowly to 50 Hz enabled the bone specimen to travel the entire distance down the nail.

3.8 Vibration Experiment Conclusions and Discussions

3.8.1 How the Vibrations Affected the Insertion Force

From the experiments, several conclusions can be drawn. It is clear that the vibrations applied to the simulated nail did reduce the force required for nail insertion for all three materials tested. All of the data collected from the experiments are in agreement in supporting the theory that vibration reduces the insertion force. Table 11 illustrates this conclusion by using average force values and the most effective vibration frequency, and comparing the insertion forces with and without vibration.

Table 11. Insertion Force Comparison with and without Vibration.

	Experiment Material	Baseline Force	Vibration Force	Percent Difference
<i>Transverse Vibration</i>				
	Biomechanical Blocks	8.24 lbs	3.68 lbs	55.3%
	UHMW-PE	6.08 lbs	1.89 lbs	68.9%
	Bovine Wet Bone	1.37 lbs (No Drop)	1.37 lbs (Full Drop)	NA
<i>Axial Vibration</i>				
	Biomechanical Blocks	1.14 lbs	0.56 lbs	50.60%
	UHMW-PE	5.93 lbs	1.60 lbs	73.00%

There were two types of vibration that were tested in the experiments; transverse and axial vibration of the nail. For the bovine bone material, only transverse vibration was tested. Both types of vibration were tested for the UHMW-PE and the biomechanical test blocks and shown to decrease the necessary insertion force. On a percentage basis, using the average values, the two types of vibration are compared to determine which type of vibration decreases the insertion force the most. The results of this comparison are shown below in Table 12.

Table 12. Vibration Type Results Comparison.

Test Material	Transverse Vibration	Axial Vibration
Biomechanical Blocks	55.3% reduction	50.6% reduction
UHMW-PE	68.9% reduction	73.0% reduction
Average for Both Materials	62.1% reduction	61.8% reduction

Many vibration frequencies were tested, but not all the vibration frequencies reduced the insertion force by the same amount. The experiments conducted with each of the three materials shows that the lower frequencies between 20 Hz and 30 Hz reduced the frequencies the most in both the axial and transverse vibration. Table 13 shows the most effective vibration frequency for each of the materials tested and for both axial and transverse vibration.

Table 13. Vibration Frequency Results Comparison.

Test Material	Transverse Vibration	Axial Vibration
Biomechanical Blocks	20 Hz	20 and 180 Hz
UHMW-PE	22 Hz	10 Hz
Bovine Wet Bone	23.5 Hz	-

3.8.2 Discussion of Proof of Concept

The experiments are in complete agreement and confirm that applied vibration does reduce the amount of the insertion force, as it was hypothesized. The notion of using vibration to overcome friction is not a new concept as examples of this concept can be found in some industries. Nevertheless it must be proven for each specific application in an industry. In this specific application, insertion force for driving the nail through bone is needed to overcome frictional resistance at the hole through which it being inserted.

The objective is to prove the concept that applied vibration can be used as a method to overcome friction in a tight tolerance hole fit. The experimental results of this thesis confirm the theory and demonstrate that applied vibration reduces the necessary insertion and extraction force in tight tolerance hole fit. The experiments carried out closely simulate the surgical procedure of inserting a stainless steel implant into human bone, therefore, it is concluded the “proof of concept” is established and applied vibration will reduce the insertion and extraction force of surgical implants.

3.8.3 Discussion of Transverse and Axial Vibration

Both transverse and axial vibration can reduce insertion force by approximately the same margin. However, from the experimental data, it is seen that the transverse vibration must be optimized for the system in order to be effective. The transverse vibration results indicate that effectiveness is highly dependent on vibrational frequency. In the case where the vibration

frequency is optimized for the mechanical system being vibrated, it can be very effective. There are some results from the transverse vibration data that indicate other frequencies may not be as effective.

The vibrational energy applied to the mechanical system in the transverse direction is orthogonal or perpendicular to the insertion force. Therefore, the energy applied to the mechanical system from transverse vibrations would not directly cause a large reduction in insertion force. However, the transverse vibrational energy indirectly causes a large reduction in insertion force by exciting the natural mode shapes of the mechanical system. The transverse vibrations can be the most efficient at exciting the natural mode shapes of the system because the transverse modes of the system have lower natural frequencies compared to axial modes. The mode is excited when the forcing frequency of the transverse vibrations is in resonance with the natural frequency of the system. This resonance would explain why the transverse vibration effectiveness is highly dependent on frequency.

On the other hand, the axial vibration results appear to be very consistent and linear. Like the transverse vibration, axial vibration reduces the insertion force more at the lower frequencies, but this may be attributed to the slight range of acceleration. The amplifier was set to the maximum for all frequencies; however, the acceleration still fluctuated, with slightly higher accelerations occurring at the lower frequencies. If it is assumed that lower frequencies were more effective for axial vibration due to the slightly higher accelerations, then the conclusion could be made that axial vibration reduces insertion force and is not dependent upon frequency. From the experimental data, it can be seen that axial vibration effectiveness is not highly dependent on frequency. In the case of axial vibration, the vibrational energy applied to the system is in line with the axis of the nail and the line of action of the insertion force. Therefore, the energy applied to the mechanical system from axial vibrations directly causes a large reduction in insertion force. Consequently, the reduction of insertion force is more directly proportional to the vibrational energy added to the system. If the energy applied to the system is the same for all forcing frequencies, then the reduction in insertion force should be nearly the

same for all forcing frequencies. The experimental data shows that the reduction in insertion force was comparable at different frequencies.

Although insertion force reduction might be greater for axial vibration at resonance with the nail, the steel nail possesses an extremely high stiffness in the axial direction. Therefore, since the nail stiffness is so large in the axial direction, all natural modes in the axial direction will have very high natural frequencies. Consequently, it is not probable that axial vibration could be applied with a high enough forcing frequency to activate or excite the natural modes in the axial direction. The first three natural modes in the axial direction are calculated and shown in Appendix R. The axial natural frequencies are much higher than the transverse natural frequencies.

3.8.4 Discussion of the Most Effective Vibration Frequency

The transverse vibration experiments correlated very well for all materials showing that the lower frequencies, around 23 Hz, were the most effective at reducing insertion force. Several possible explanations exist for this result. The most probable explanation is that the forcing frequency around 23 Hz may be in resonance with the natural frequency of the system. In the transverse vibration experiment configuration, the nail is essentially a cantilevered beam fixed at the bottom end where the transverse vibration is being applied. The top end is the cantilevered part free to move and vibrate. Furthermore, the test material at the top of the nail adds extra mass to the cantilevered end that is free to vibrate. With this configuration, it is reasonable to assume that the system might have a low natural frequency such as 23 Hz. This is investigated further in analytical chapter of this thesis in section 4.3.4.

From the data, it can be observed that for all materials in both the transverse and axial vibration experiments, the lower frequencies were the most effective at reducing the insertion force.

In the transverse vibration experiments, the data is non-linear suggesting that certain frequencies are much more effective than an adjacent high or low frequencies. This would also suggest that the effectiveness of transverse vibration is very sensitive to frequency. Low frequencies of 20 and 22 Hz were the most effective while 40 Hz was the least effective frequency tested. The rest of the frequencies were somewhat effective. However, even within the statistical variance, all tested frequencies were more effective than the baseline which used no vibration. The frequency sweep tested on the UHMW-PE proved to be in the same effectiveness range as the lower frequencies of 20 and 22 Hz.

In the axial vibration experiments, the data is very linear suggesting the change in effectiveness is not highly dependent on frequency. All of the frequencies tested reduced the amount of insertion force significantly with minimal variation at different frequencies. The data was also very precise meaning statistically, there was minimal error. For the UHMW-PE, the most effective frequency was 10 Hz, the lowest frequency tested, while the least effective frequency was 260 Hz, the highest frequency tested. The frequencies in between 10 and 260 Hz decreased linearly in effectiveness from 10 to 260 Hz. The frequency sweep experiment proved to be almost as effective as the lower frequencies.

3.8.5 Testing Material's Effect on Results

Most of the vibration experiments were performed with the UHMW-PE because of its excellent wear resistance properties. Although this material does not simulate cortical or cancellous bone, this material allowed more trial testing at more frequencies without wearing excessively. Consequently, it is an excellent material to illustrate the “proof of concept” that applied vibration reduces the force needed to push a nail through a material.

The wet bone and biomechanical test blocks both simulate human bone accurately; however, during the experiments it became apparent that both materials have a tendency to wear easily from multiple uses and trials. As experimentation was being conducted and results were being

recorded, this material characteristic was discovered. Thus, fewer results were acquired with these testing materials.

From the data, it is apparent that the UHMW-PE experiments were more precise, meaning there was less statistical variance in the data.

3.8.6 Frequency Sweep Experiments

In the UHMW-PE experiments, testing was conducted with frequency sweeps between 10 Hz and 260 Hz. The results of this particular test are important because it is hypothesized that applied vibration at a frequency near or exactly at the natural frequency of the simulated nail would reduce the nail insertion force the most. If this hypothesis is correct, then the most effective applied vibration frequency should be the natural frequency of the nail. From the transverse vibration results presented in Section 3.6, the frequency sweep between 10 Hz and 260 Hz was almost as effective as the forcing frequency of 22 Hz. If the forcing frequency of 22 Hz was the most effective because it was in resonance with the natural frequency of the experimental setup, then what is the reason that the frequency sweep of frequencies was almost as effective?

The likely explanation for these results is that the natural frequency of the experimental configuration changes as the UHMW-PE slides down the nail. At each instant in time, the UHMW-PE moved down the nail further, therefore, the mass distribution in the experimental configuration is different at each instant, causing the natural frequency to be different at each instant. Consequently, the natural frequency of the experimental configuration is really a function of how far the bone simulating mass has slid down the nail. This would explain why the frequency sweep was effective since the forcing frequency is changing along with the natural frequency of the experimental configuration, staying in resonance with the system. However, it is unlikely that the rate of change of the forcing frequency was the same as the rate of change of the natural frequency. But if the rates of change had been equal, then the frequency sweep

would be expected to be more effective than any single forcing frequency. This change in natural frequency can also be used to explain the results presented in section 3.7.3 in which the bovine bone began sliding down the nail and stopped incrementally several times. Each time it stopped it did not began sliding until the forcing frequency was raised slightly.

In the case of the actual nail, the mass distribution of the nail and T-handle does not change, but the constraint or boundary condition on that nail and T-handle does. At first, the tip of the nail is constrained where it enters the bone. Midway through, the constraint is at the middle of the nail. At the end, the constraint is near the T-Handle and the orthopaedic surgeon's hand. Consequently, as the constraint moves up the nail, the natural frequency of the nail/T-handle assembly is also changing. Therefore, if the natural frequency of nail changes as it is being inserted, an applied vibration in which the forcing frequency changes over time would reduce the insertion force the greatest. This theory is tested by the frequency sweep experiments.

Observing the data from the frequency sweep suggests that a varying forcing frequency reduces the force required for nail insertion significantly. Even though the frequency sweep experiments reduce the force more than most of the experiments involving a single forcing frequency, it was not the most effective at reducing insertion force in either the transverse vibration or axial vibration tests. However, the frequency sweep might be the most effective if the rate of forcing frequency change was matched with the rate of natural frequency change.

4.0 VIBRATION ANALYSIS OF SURGICAL IMPLANT INSERTION

4.1 Purpose of the Vibration Analysis

The purpose of the vibration analysis is to provide supporting evidence that vibration can be used to decrease the amount of force required for insertion of surgical implants. The analyses utilize multiple software tools and analytical techniques to demonstrate how vibration might be

used to reduce insertion force. The analysis is performed in support of the vibration experiments and to help explain and justify the results of the experiments.

4.2 Software Tools Used in the Vibration Analysis

4.2.1 Brief Software Description

The two main software tools used in the vibration analysis are ALGOR¹ and MathCAD². Autodesk Inventor³ was also used to create 3-D solid models. Once the 3-D solid CAD models are constructed, the geometry is exported to ALGOR.

MathCAD is an industry standard calculation software that combines the live document interface of a spreadsheet with the WYSIWYG interface of a word processor. MathCAD's on-screen interface is a blank worksheet on which you enter equations, graph data or functions, and annotate with text and the calculations are updated instantly.

4.2.2 ALGOR Brief Software Methodology

ALGOR is a multi-physics finite element analysis code able to perform static stress and mechanical event simulation with linear and nonlinear material models, linear dynamics, steady-state and transient heat transfer, steady and unsteady fluid flow, and electrostatics. ALGOR utilizes InCAD technology for direct computer-aided design/computer-aided engineering data exchange with three-dimensional solid modeling software such as Inventor.

The specific modules of ALGOR used were the linear static stress analysis module, the linear dynamics module, and the mechanical event simulation (MES) module. In all three modules, first the geometry is imported and meshed with appropriate element type and size, then

¹ALGOR is a registered trademark of Algor, Inc., Pittsburgh, Pennsylvania.

²MathCAD is a registered trademark of MathSoft Engineering & Education, Inc.,

³Inventor is a registered trademark of Autodesk, Inc.,

the boundary conditions and applied loadings are placed on the meshed geometry, and finally the material properties are selected for the geometry. For each of these modules, the analytical methodology is briefly described.

In the linear static stress analysis module, the solver sets up and solves the linear matrix equation 6 below.

$$\{F\} = [K]^{-1} \{x\} \quad (\text{Eqn. 6})$$

This matrix equation states that force is a linear function of displacement, where F is the applied force vector, K is the stiffness matrix, and x is the displacement vector. Once the solver has calculated the displacements, the displacement vector is normalized to get the strain vector ϵ . Using the strain vector, ϵ , and the modulus of elasticity of the material, E, the stresses, σ , can be calculated from Hooke's Law below in equation 7.

$$\{\sigma\} = E \cdot \{\epsilon\} \quad (\text{Eqn. 7})$$

In the linear dynamics module, the natural frequencies of an object can be calculated. In this case, the software sets up the governing equation of motion without considering damping shown below in equation 8.

$$[m] \{\ddot{x}\} + [K] \{x\} = 0 \quad (\text{Eqn. 8})$$

The governing equation includes the mass matrix, m, the acceleration vector, \ddot{x} , the stiffness matrix, K, and the displacement vector, x. Applied forces are not considered during the natural frequency analysis so this equation is set to zero. Then the solver performs a linear generalized eigenvalue analysis solving for the eigenvalues, which are the natural frequencies of the object. For each eigenvalue, the eigenvector is determined, which defines the mode shape of

the object at that natural frequency. No excitation is applied so the actual values of displacement only serve to define the mode shape and are not the magnitude of motion.

In the mechanical event simulation (MES) module, the entire equation of motion including dissipative forces such as friction is used. MES enables the user to model motion, damping, and mechanical deformation all at once for a complete dynamic analysis. The full equation of motion is shown below in equation 9.

$$[m]\{\ddot{x}\} + [c]\{\dot{x}\} + [K]\{x\} = \{f\} \quad (\text{Eqn. 9})$$

This equation is the same as eqn. 8 with the addition of the damping matrix, c , multiplied by the velocity vector, \dot{x} , and the applied force vector, f . The solver uses numerical method techniques such as the Newton method to solve eqn. 9 for a certain time increment. Once the solver converges on a solution for that time increment, eqn. 9 is then re-formulated and the solver begins converging on another solution for the next time increment. The displacement results are calculated for each time increment in the whole time duration of the dynamic analysis. The stresses at each time increment are calculated using eqn. 7, Hookes Law, in the same fashion as a static stress analysis. All of the displacement and stress results for every time increment can be viewed and presented to show the entire dynamic analysis. MES allows the user to model geometric non-linearity, non-linear materials, inertial effects, load stiffening, multiple body motion and contact, etc.

4.2.3 ALGOR Benchmarking

In an effort to validate ALGOR for use in this thesis, benchmarking is performed for some chosen example problems that have known theoretical solutions. These benchmarking cases serve to validate and show that the finite element results obtained from ALGOR are in reasonable agreement with results obtained by classical analytical techniques.

One example case is chosen for each module of ALGOR discussed in section 4.2.2.

Therefore, there are a total of three benchmarking cases. A brief discussion of each benchmarking case is listed below:

- Linear Static Stress Module – A 1 inch by 1 inch square cross-section cantilever beam is fixed at one end and free at the other. The 16 inch long beam is analyzed for deflection under a 100 lb downward load applied at the center of the beam. The ALGOR model uses beam elements.
- Linear Dynamics Module – A flat circular plate with uniform thickness of 0.01 inches and a radius of 10 inches has its outer edge fully fixed. There is a uniform load per unit area equal to its own weight. A linear mode shapes and natural frequencies analysis was performed to obtain the first natural frequency of the plate for comparison to the theoretical solution. The ALGOR model uses plate elements.
- Mechanical Event Simulation Module – A 100 kg brick is dragged across a surface by a 500 N force. The force is oriented at a 30 degree angle from the surface. The kinematic coefficient of friction between the block and the surface is 0.15. A MES simulation is used to determine the maximum sustained acceleration of the block. The ALGOR model used 2-D elements.

4.2.3.1 Linear Static Stress Module Benchmarking Results

The theoretical solution for this benchmark problem is taken from Ref [10]. The equation for the deflection of the beam at the free end of the beam is given as:

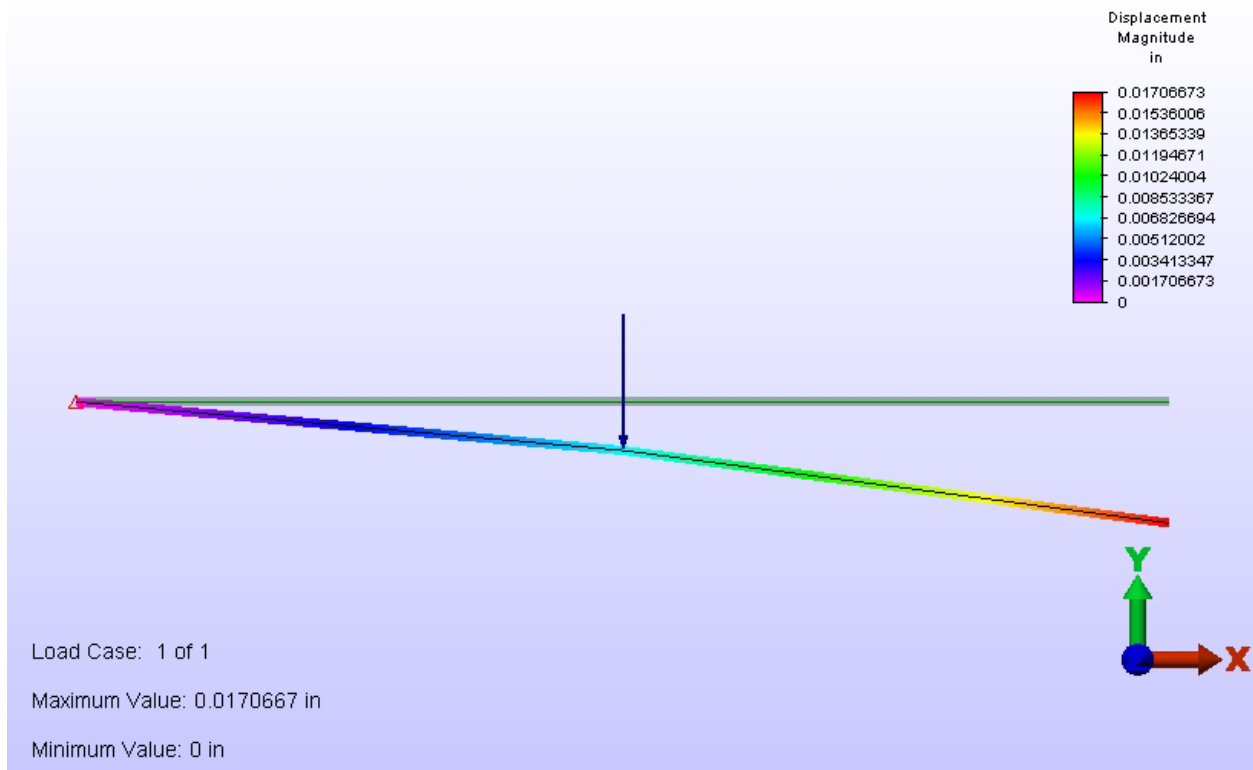
$$y = \frac{-W}{6EI} \cdot (2l^3 - 3l^2a + a^3) \quad (\text{Eqn. 10})$$

Where:

- $W = 100$ lbs, applied force
- $E = 30E6$ psi, modulus of elasticity
- $I = 1/12$ in⁴, moment of inertia
- $l = 16$ inches, length of beam
- $a = 8$ inches, distance from free end of beam to applied load

Figure 21 below shows the displacement results of the ALGOR model. The un-displaced and exaggerated displaced views of the cantilever beam are shown in the plot.

Figure 21. Displacement Plot of the Linear Static Stress Module Benchmark Case.



4.2.3.2 Linear Dynamics Module Benchmarking Results

The theoretical solution for this benchmark problem is taken from Ref [10]. The equation for the natural frequency of the circular plate is given as:

$$f = \frac{K_n}{2\pi} \cdot \sqrt{\frac{Dg}{wr^4}} \quad (\text{Eqn. 11})$$

Where:

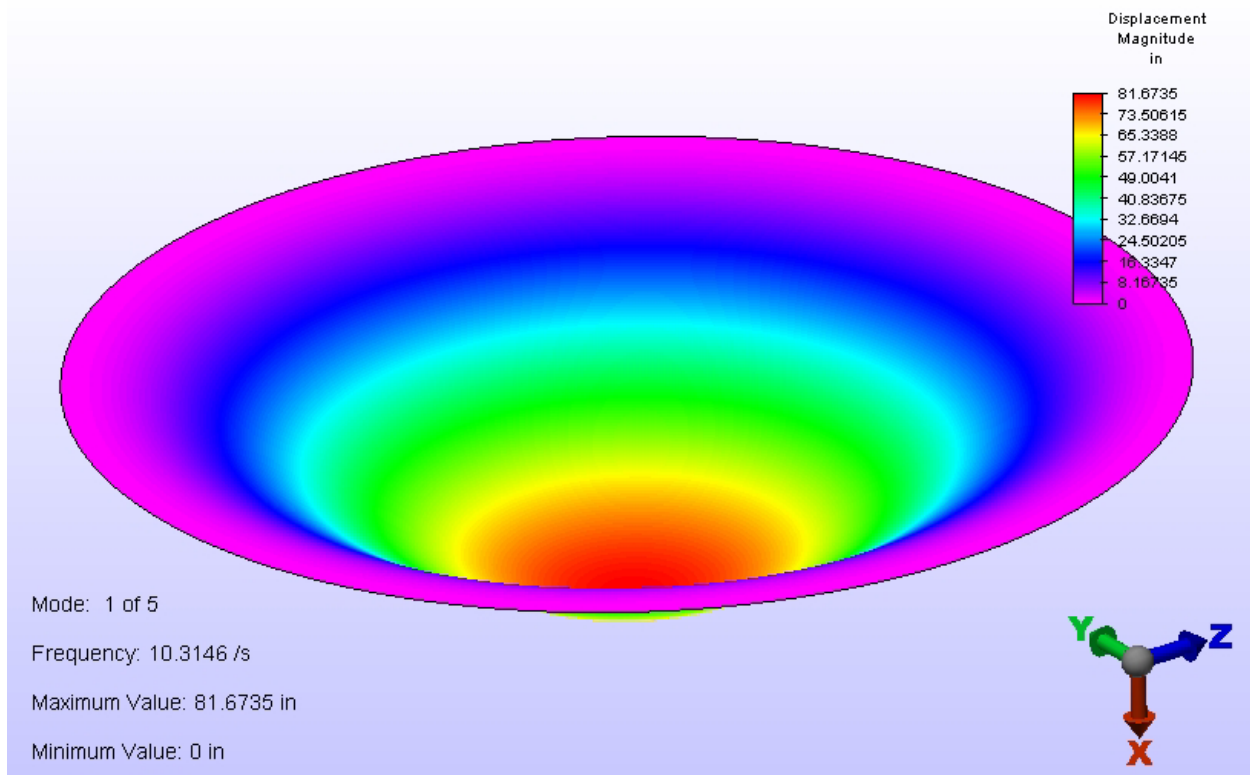
- $r = 10$ inches, radius of the plate
- $g = 386.4$ in/s², gravitational constant
- $K_n = 10.2$, fundamental natural frequency constant
- $D = \frac{E \cdot t^3}{12(1 - \nu^2)}$, flexural stiffness constant for plates

Where:

- $E = 10E6$ psi, modulus of elasticity
- $t = 0.01$ inches, plate thickness
- $\nu = 0.397$, Poisson's ratio

Figure 22 below shows a mode shape plot of the fundamental natural frequency of the ALGOR model. The displaced view is exaggerated to better illustrate the mode shape. The displacements are only relative values, meaning they are not actual displacements since no load has been applied.

Figure 22. Mode Shape Plot of the Linear Dynamics Module Benchmark Case.



4.2.3.3 Mechanical Event Simulation Module Benchmarking Results

The theoretical solution for this benchmark problem is not taken directly from a reference but rather it is an application of the well known Newton's 2nd law. The equation for Newton's 2nd law is shown below in equation 12.

$$\sum F = ma = F \cdot \cos(\theta) - \mu \cdot (mg - 500 \cdot \sin(\theta)) \quad (\text{Eqn. 12})$$

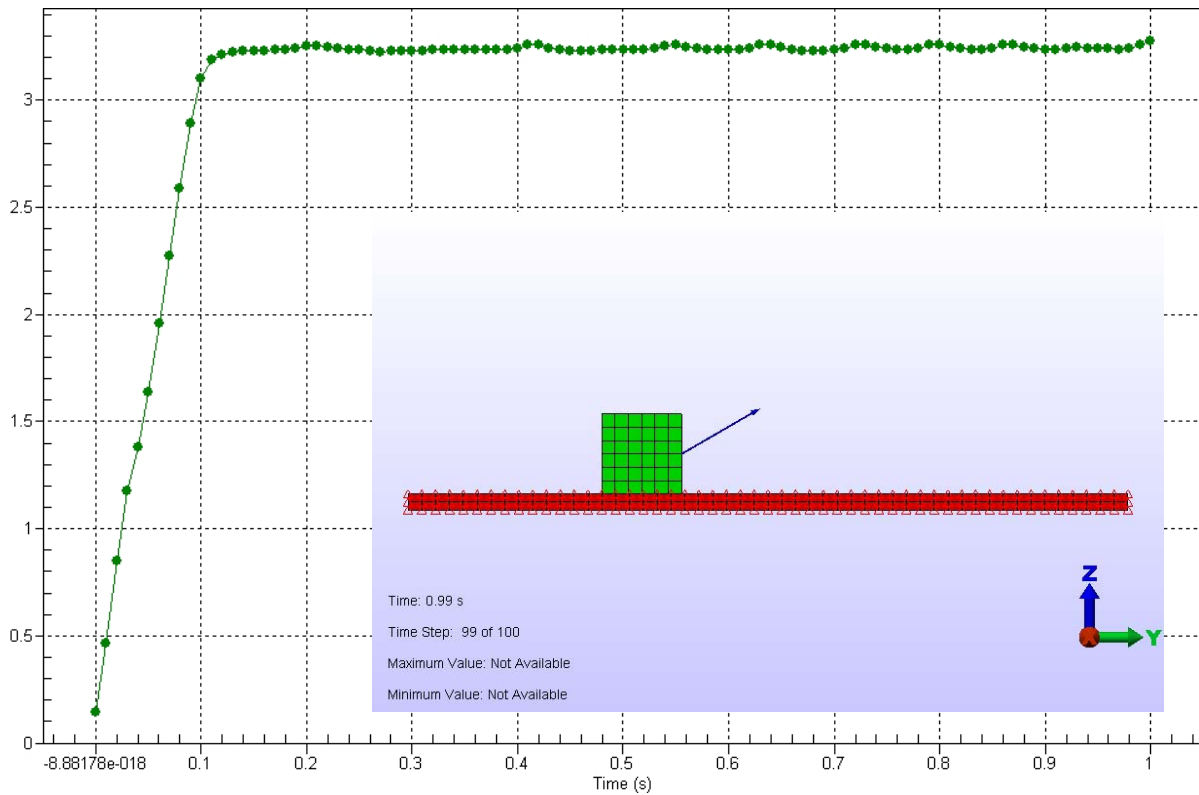
Where:

- $m = 100$ kg, mass of the block
- $g = 9.8$ m/s², gravitational constant
- $F = 500$ N, applied force pulling block

- $\Theta = 30$ degrees, angle of applied force
- $\mu = 0.15$, dynamic coefficient of friction

Figure 23 below shows an acceleration versus time plot during the event simulation. The node that is plotted is the node at the center of gravity of the green block. The arrow shows the applied force of 500 N at the 30 degree angle from the Y axis of the model. From Figure 23, at time 0.1 seconds the block reaches constant acceleration.

Figure 23. Acceleration Plot of the Mechanical Event Simulation Module Benchmark Case.



4.2.3.4 ALGOR Benchmarking Results and Comparisons

Classical analytical techniques are used to verify and validate each of the three benchmarking cases. The results of the classical techniques are compared to the ALGOR results and are shown in Table 14.

Table 14. Results of ALGOR Benchmarking.

<i>Linear Static Module</i>	ALGOR Result	Theoretical Result	Percent Difference
Displacement, inches	-0.017067	-0.017067	0.0
<i>Linear Dynamics Module</i>			
Frequency, hertz	10.29	10.31	0.239
<i>Mechanical Event Simulation</i>			
Acceleration, m/s ²	3.233	3.235	0.1

From Table 14, the ALGOR results match very closely with the theoretical results indicating that ALGOR is an accurate finite element code that yields acceptable results. The percent difference is very small when compared to classical analytical techniques.

4.3 Vibration Analysis Methodology and Results

The analyses presented in this section were performed to support the experimental results from section 3.0 and provide confirmatory analysis for the insertion and extraction of surgical implants.

4.3.1 Linear Static Stress Analysis of the T-Handle

The T-handle, developed by SIGN and discussed in section 1.3, is analyzed to determine the stress in the T-handle during use. The T-handle screws onto the surgical implant (nail) and allows the orthopaedic surgeon to grip and push the nail into place. Orthopaedic surgeons

typically have to exert a considerable amount of force on the T-handle in order to insert the nail. The force placed on the T-handle produces a bending stress in the handle. Reducing the amount of required insertion force would also reduce the amount of stress induced in the nail and T-handle. This analysis is performed to understand how much stress the T-handles undergoes during nail insertion.

The T-handle is analyzed with a static load of 200 lbs, 100 lbs on each side of the T-handle where the orthopaedic surgeon's hands would be pushing. The applied downward force is indicated in Figure 24 by the red arrows pointing in the negative Y direction. The end of the T-handle that screws into the nail has a fixed boundary condition placed on it that simulates the resistance of insertion force. This is indicated by the red triangles in Figure 24. The T-handle solid model is created and then meshed with brick elements with an average size of 0.13 inches. The material properties are specified to simulate 17-4 precipitation hardened (PH) stainless steel and are shown in Appendix Q. This is the material listed on the T-Handle drawing in Appendix A. Figure 24 shows the finite element model completely meshed with the fixed boundary condition at the bottom and the applied loadings on the handle.

Figure 24. T-Handle Finite Element Model.

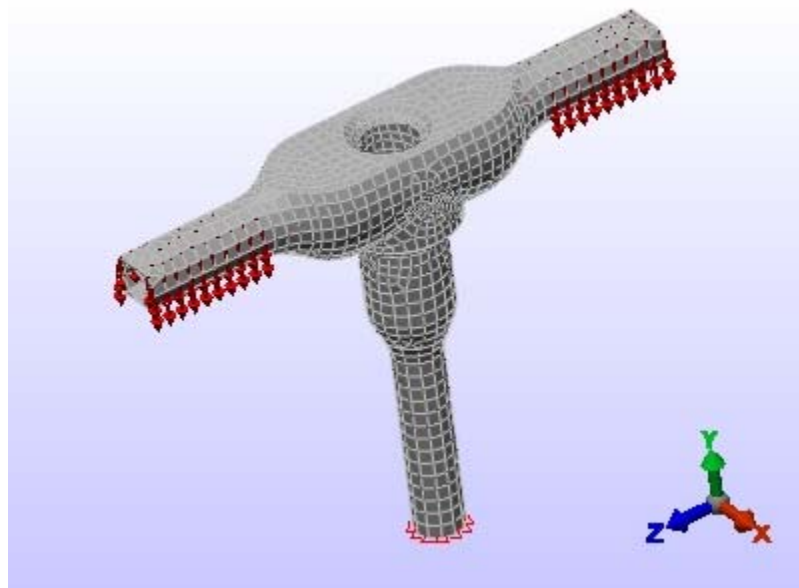
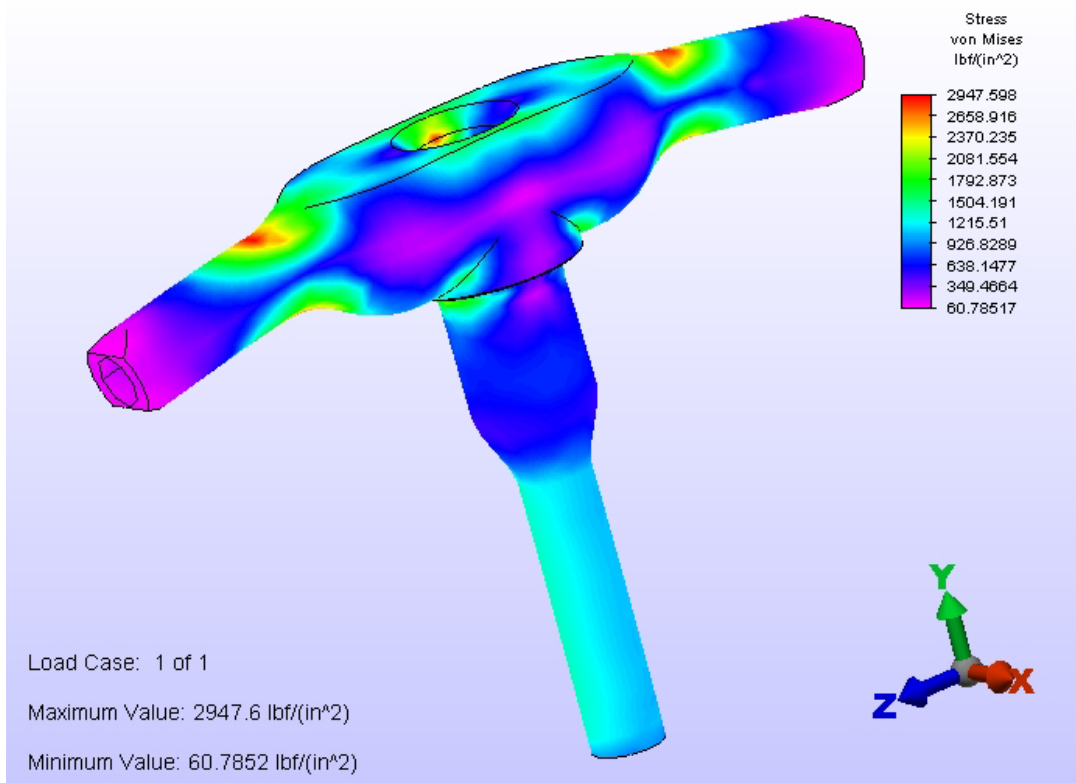


Figure 25 shows the von mises stress results of the analysis. The exaggerated deformation is set to illustrate how the T-Handle deflects under load.

Figure 25. Von Mises Stress Distribution in the T-Handle.



From the results presented in Figure 25, the stresses induced in the T-Handle from the 200 lb applied load are relatively small. The highest von mises stress reported is 2,947.6 psi and the 17-4 PH stainless steel material is known to have a yield strength of approximately 183,000 psi. Therefore, the T-handle has a very significant safety margin before it begins to yield.

4.3.2 Critical Buckling Load Analysis of the T-Handle

Once the T-handle is screwed on the nail, the T-handle/nail assembly becomes very long. As the Orthopaedic surgeon grips the T-handle and begins to push the nail into place, the nail

will resist insertion at the bottom and a load will be applied by the surgeon at the top. This causes the long nail to be in compression much like a column. The elastic stability of the assembly is analyzed to determine the critical buckling load.

Like the static stress analysis, the T-handle is analyzed with a static load of 200 lbs, 100 lbs on each side of the T-handle indicated by the yellow arrows pointing in the negative Y direction. Again, the end of the nail that goes into the bone has a fixed boundary condition placed on it that simulates the resistance of insertion force, indicated by the small red triangles at the end of the nail. The T-handle/nail assembly is meshed with brick elements with an average size of 0.13 inches. The material properties are specified to simulate 17-4 precipitation hardened (PH) stainless steel and are in shown in Appendix Q. Figure 26 shows the finite element model with the fixed boundary condition at the bottom and the applied loadings on the handle.

Figure 26. T-Handle Finite Element Model with Nail.

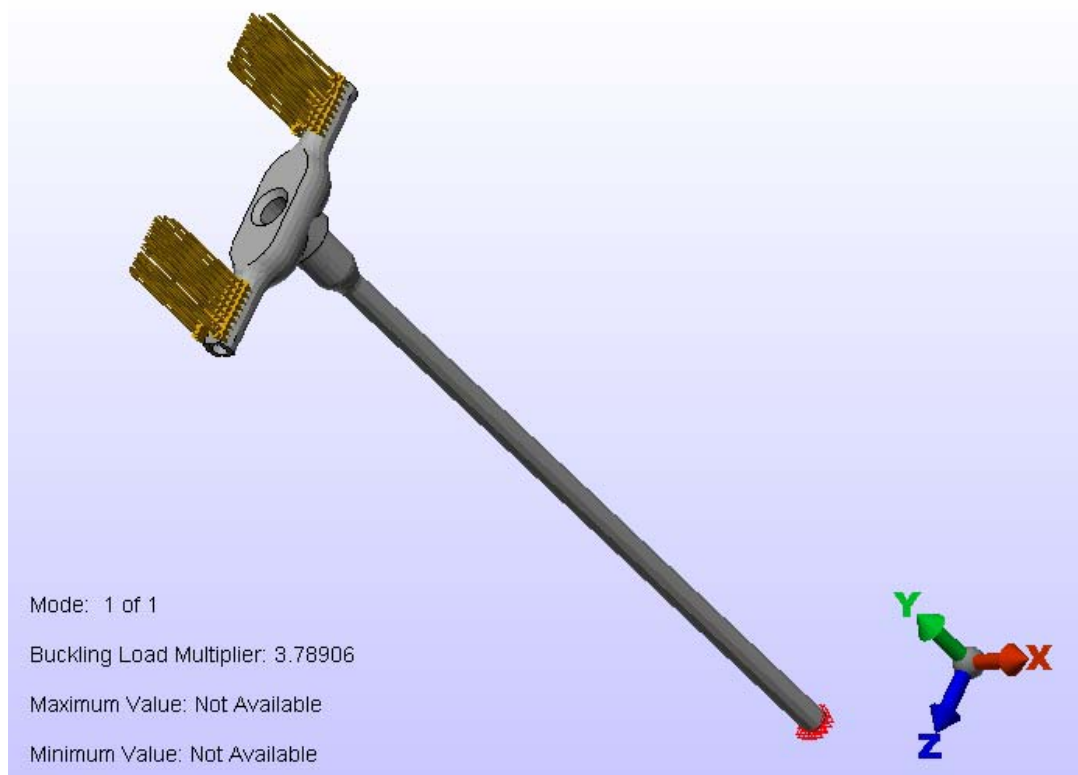


Figure 26 also shows the critical buckling load multiplier for the analysis. From the figure, the critical buckling load multiplier is 3.79; therefore, the critical buckling load is 758 lbs of force. It is unlikely that an Orthopaedic surgeon could apply this much force, consequently, the T-handle/nail assembly is not in danger of buckling.

4.3.3 Natural Frequency Analysis of the Nail

In section 3.8.4 “Discussion of the Most Effective Vibration Frequency” the notion discussed is that transverse vibrations are most effective when the forcing frequency is in resonance with the natural frequency of the nail. This theory was developed because during the transverse vibration experiments, certain forcing frequencies were observed to be more effective than others. If this notion has merit, than knowing the natural frequency of the nail is extremely important for transverse vibrations.

This analysis determines the natural frequency of the nail by three different methods and compares the results. The three independent methods are used to confirm the results and show correlation between experimental and analytical techniques.

The first method is experimental, whereby the nail is affixed to the vibration platform and a piezo-accelerometer from Measurement Specialties, Inc. (MSI), shown in Figure 39 in section 5.2.2, is placed at the base of the nail. The nail is then excited by hitting it with another steel rod and left to vibrate at its fundamental natural frequency. Since the nail is constrained at the bottom, the fundamental mode shape is that of a cantilevered beam fixed one end and free on the other. As the nail vibrates at its fundamental frequency, the frequency is read off the oscilloscope shown in Figure 39 in section 5.2.2. The oscilloscope reading revealed a fundamental natural frequency of 52.5 Hz for the nail.

The second method is an analytical technique derived from Ref. [11]. The equations and variables were set up and solved with MathCAD. The methodology is to analyze the nail as a continuous medium with infinite degrees of freedom. This approach can be taken for simple

geometries such as bars and beams. The approach involves determining dynamic equilibrium equations, sometimes in both the x and y direction. In addition, a moment equilibrium equation is also introduced. These dynamic equilibrium and moment equilibrium equations are combined into a governing equation of motion for the model. In the case of transverse free vibrations of a beam, the governing equation is:

$$\frac{\partial^4 v}{\partial x^4} = \frac{1}{a^2} \cdot \frac{\partial^2 v}{\partial t^2} \quad (\text{Eqn. 13})$$

Where:

$$a = \sqrt{\frac{EI}{\rho A}} \quad (\text{Eqn. 14})$$

The general form of the solution to this fourth-order differential equation is shown in equation 15.

$$X = C_1 \cdot \sin(kx) + C_2 \cdot \cos(kx) + C_3 \cdot \sinh(kx) + C_4 \cdot \cosh(kx) \quad (\text{Eqn. 15})$$

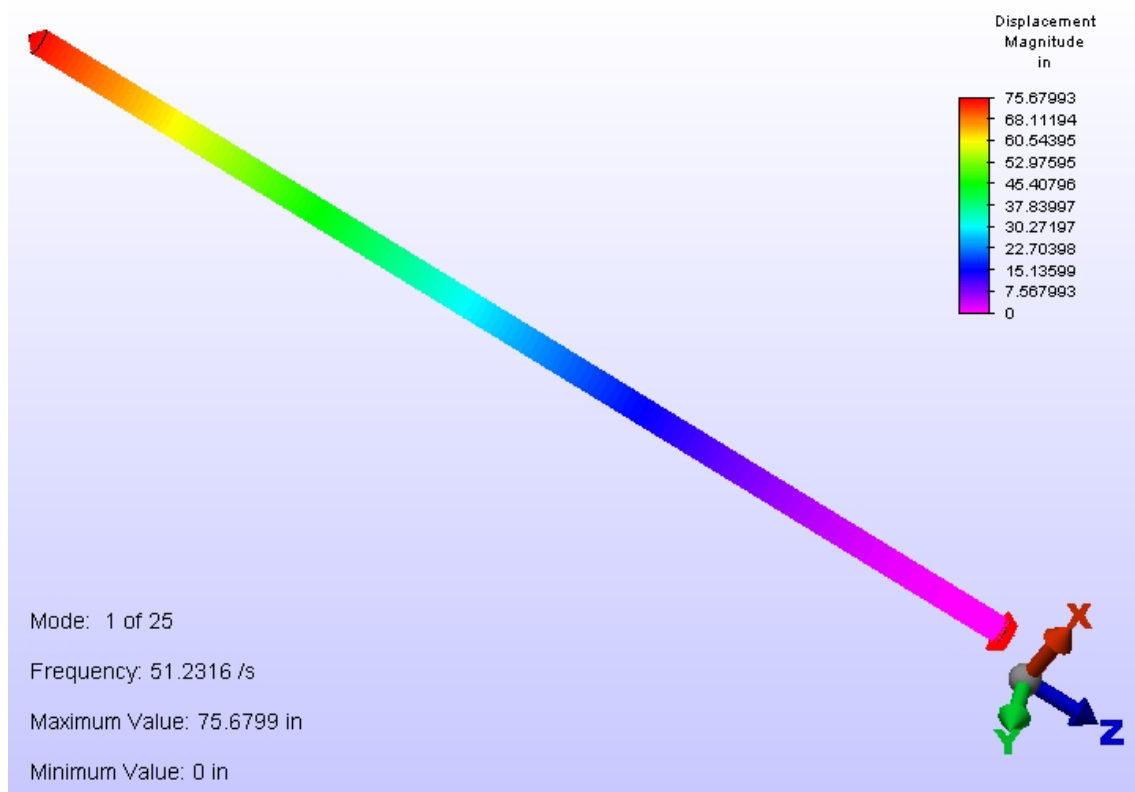
The constants C1, C2, C3, and C4 are determined by the boundary conditions placed on the beam undergoing transverse vibration. In this case, one end of the beam is fixed and the other end is free. These boundary conditions are used to simplify the general solution into a frequency equation. Then the consecutive roots of the equation can be determined and used to find the frequency of vibration of any mode using equation 16.

$$f_1 = \frac{\omega_1}{2\pi} = \frac{ak_1^2}{2\pi} = \frac{a}{2\pi} \cdot \left(\frac{1.875}{l} \right)^2 \quad (\text{Eqn. 16})$$

The value in the parenthesis is the first root the frequency equation obtained from the general solution. Using equation 16, the fundamental frequency of the nail is calculated to be 51 Hz.

The third methodology is an analytical technique using ALGOR as the finite element solver. The nail model was created and meshed with brick elements averaging 0.05 inches in size. Then the fixed boundary condition was placed at one end while the other end remained free to move. The material properties are specified to simulate 17-4 precipitation hardened (PH) stainless steel. The natural frequency (modal) analysis was performed and the first fundamental mode is shown to be 51.2 Hz in Figure 27. Since no load is applied in a modal analysis, the displacements reported are only relative values.

Figure 27. Fundamental Natural Frequency of the Nail Only.



The fundamental natural frequency of the nail determined by three different methodologies compares very favorably. All three methods result in a fundamental natural frequency of approximately 52 Hz. Table 15 shows highest percent difference between the results.

Table 15. Fundamental Natural Frequency Comparison of the Nail Only.

Result Methodology	Frequency Result
Experimental Test	52.5 Hz
Elastic Continuum Analysis	51.0 Hz
Finite Element Analysis	51.2 Hz
Largest Percent Difference	2.9%

The theory is that the most effective forcing frequency is the natural frequency of the nail. However, the natural frequency result of approximately 52 Hz was not the most effective forcing frequency in the transverse vibration experiments as seen in the data presented in sections 3.0. The most effective forcing frequency from the experimental results is approximately 23 Hz. These analytical results do not support the theory.

The likely explanation for this is that the natural frequency calculated was for the nail alone, not for the experimental setup with the end mass. Without considering the end mass, the nail would be the most excited at the natural frequency of the nail alone, calculated above to be approximately 52 Hz. These results do not correlate with the theory, but the natural frequency of the nail alone may be an important result for designing a vibratory device.

The vibration experiments performed and presented in section 3.0 had a slightly different configuration in which the block of bone simulating material was already mounted to the top of the nail. Even though the natural frequency of the nail alone is 52 Hz, the natural frequency of the experimental setup with the bone simulating material mounted to the top of the nail was lower. Consequently, the natural frequency of the masses acting together is the natural frequency of the system and should be the most effective forcing frequency for the experiments.

4.3.4 Natural Frequency Analysis of the Experimental Setup

In the preceding section, the notion that the natural frequency of the experimental setup is lower than the natural frequency of the nail alone is suggested. This is the reason that the most effective forcing frequency of the experimental results do not match the calculated natural frequency of the nail alone. It is expected that the natural frequency of the experimental setup is lower since it is essentially a mass attached to the end of a cantilevered beam. To verify and confirm the theory, the natural frequency of the experimental setup is analyzed in this section.

This analysis determines the natural frequency of the experimental setup by the same three methods used in the preceding section and compares the results. The three independent methods are used to confirm the results and show correlation between experimental and analytical techniques.

The first method is experimental, whereby the nail is affixed to the vibration platform with the UHMW-PE mass mounted to the top. The same piezo-accelerometer from Measurement Specialties, Inc. (MSI), shown in Figure 39 in section 5.2.2, is placed at the base of the nail. The nail with the UHMW-PE mass at the top is then excited by hitting it with a steel rod and left to vibrate at the fundamental natural frequency of the system. Since the nail is constrained at the bottom, the fundamental mode shape is that of a cantilevered beam fixed at one end and free at the other end. As the nail vibrates at the fundamental frequency, the frequency is read off the oscilloscope shown in Figure 39 in section 5.2.2. The oscilloscope reading revealed a fundamental natural frequency of 25 Hz for the mechanical system.

The second method is an analytical technique derived from Ref. [10]. The equations and variables were set up and solved with MathCAD. The methodology is to analyze the nail as a mass-less with the correct beam stiffness and a concentrated mass at the end. This is only a simple approximation since the beam does have continuous mass along its length. For the purposes of using this analytical technique, the beam mass is lumped together with the bone simulating material mass at the end of the beam. Note that this conservative mass lumping at the

end of the nail will result in a lower natural frequency than it would be in reality. In the case of transverse free vibrations, the governing natural frequency equation for this analytical model is:

$$f_1 = \frac{1.732}{2\pi} \cdot \sqrt{\frac{EIg}{Wl^3}} \quad (\text{Eqn. 17})$$

Where:

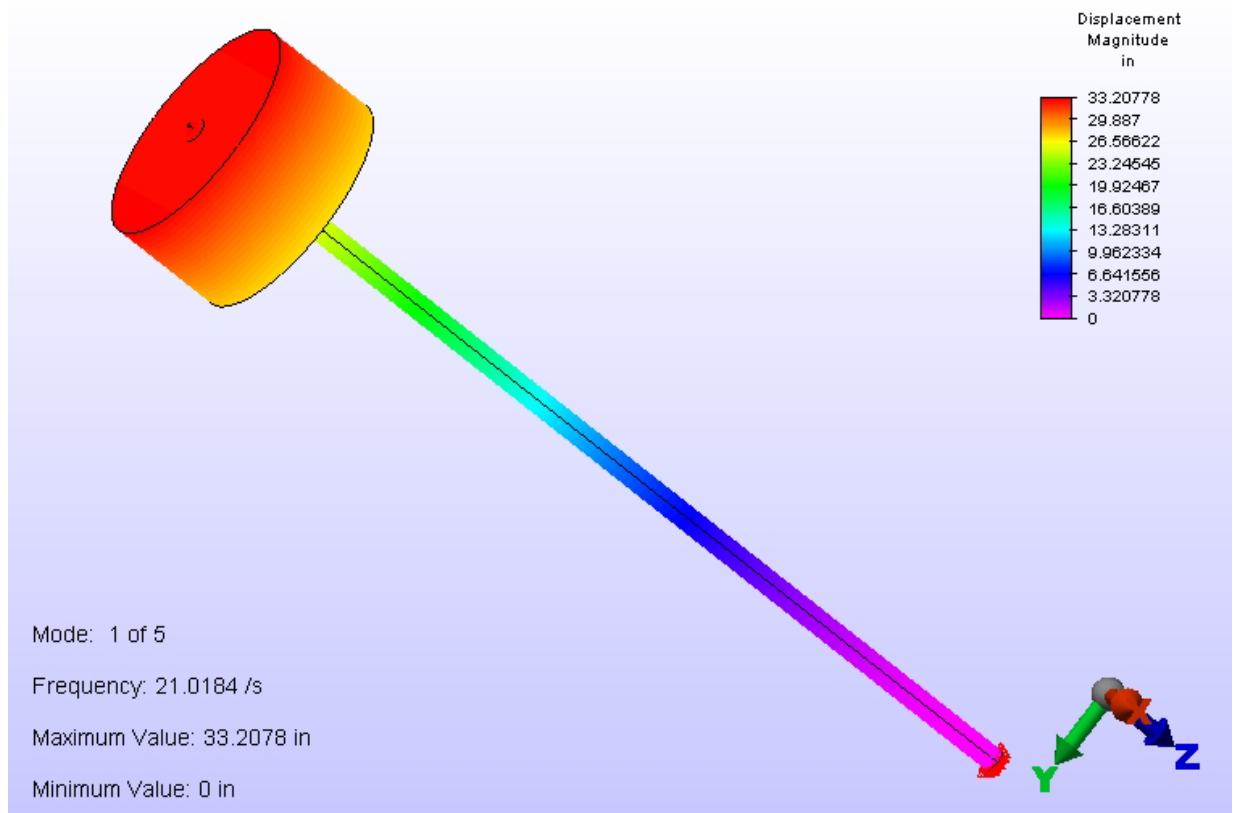
- E = 28,500,000 psi, modulus of elasticity
- I = 0.000465 in⁴, moment of inertia
- g = 386.4 in/s², gravitational constant
- W = 0.63 lbf, total weight of nail and average end mass in experiments
- l = 13 in, length of the nail

The analytical technique results in a fundamental natural frequency of 16.8 Hz. Because the beam mass is lumped with the end mass, this result is expected to be a lower frequency than would be expected in reality. Therefore, the result of 16.8 Hz is in the expected range for the analytical model used and is encouraging in supporting the proposed theory that the most effective transverse vibration frequency occurs at the mechanical system fundamental natural frequency.

The third methodology is an analytical technique using ALGOR as the finite element solver. The nail with end mass model was created and meshed with brick elements averaging 0.1 inches in size. Then the fixed boundary condition was placed at the end without the mass while the other end with the mass remained free to move. The material properties are specified to simulate 17-4 precipitation hardened (PH) stainless steel for the rod and a customized material representative of the average end mass used in the experiments. The material properties are shown in Appendix Q. Since many end masses were used in the experiments with slightly different weights, the average end mass was used. The natural frequency (modal) analysis was

performed and the first fundamental mode is shown to be 21.0 Hz in Figure 28. Since no load is applied in a modal analysis, the displacements reported are only relative values.

Figure 28. Fundamental Natural Frequency of the Nail with End Mass.



The fundamental natural frequency of the nail determined by three different methodologies compares very favorably. All three methods result in a fundamental natural frequency between 21 and 25 Hz with the exception of the lumped mass method, which resulted in a fundamental natural frequency of 16.8 Hz. However, the lumped mass method result is expected to be lower than the other two results because of the mass distribution in that analytical model. Therefore, the results of all three methods are in agreement with expected results. Table 16 shows highest percent difference between the results.

Table 16. Fundamental Natural Frequency Comparison of the Nail with End Mass.

Result Methodology	Frequency Result
Experimental Test	25 Hz
Lumped Mass Analysis	16.8 Hz
Finite Element Analysis	21.0 Hz
Largest Percent Difference	32.8%

The theory is that the most effective forcing frequency in the transverse vibration experiments is the natural frequency of the entire experimental configuration is supported by these analytical results. The experimental results in section 3.0 indicate the a forcing frequency of approximately 22 Hz is the most effective and the results of this section show that the fundamental natural frequency of the experimental configuration is in the range of 21 to 25 Hz. This is an important confirmation that transverse vibration effectiveness is dependent on the natural frequency of the system.

4.3.5 Range of Natural Frequencies During Experimental Nail Insertion

From the transverse vibration results presented in Section 3.6, the frequency sweep between 10 Hz and 260 Hz was almost as effective as the forcing frequency of 22 Hz. From the discussion in section 3.8.6, the natural frequency of the experimental configuration is a function of how far the bone simulating mass slid down the nail. An important factor is knowing how significant the change in natural frequency is.

This analysis is performed to determine how the natural frequency of the experimental configuration changed as the mass slid down the nail. Three natural frequency analyses are performed with ALGOR to calculate the natural frequency of the experimental configuration at three different instants in time. This will result in a range of natural frequencies from the start of nail insertion to complete nail insertion. The first natural frequency at the start of nail insertion has already been calculated in section 4.3.4 and was reported to be 21.0 Hz.

In all three ALGOR modal analyses, the solid model was created first and then meshed with brick elements with an average size of 0.1 inches. Then the fixed boundary condition was placed at the end without the mass while the other end with the mass remained free to move. The material properties are specified to simulate 17-4 precipitation hardened (PH) stainless steel for the nail and a customized material representative of the average end mass used in the experiments. The material properties are shown in Appendix Q. Since many end masses were used in the experiments with slightly different weights, the average end mass was used. For each ALGOR modal analysis, the fundamental natural frequency is reported. Figure 29 shows the fundamental natural frequency when the mass has moved a third of the way down the nail. Since no load is applied in a modal analysis, the displacements reported are only relative values.

Figure 29. Fundamental Mode of the Nail with the Mass Down One-Third.

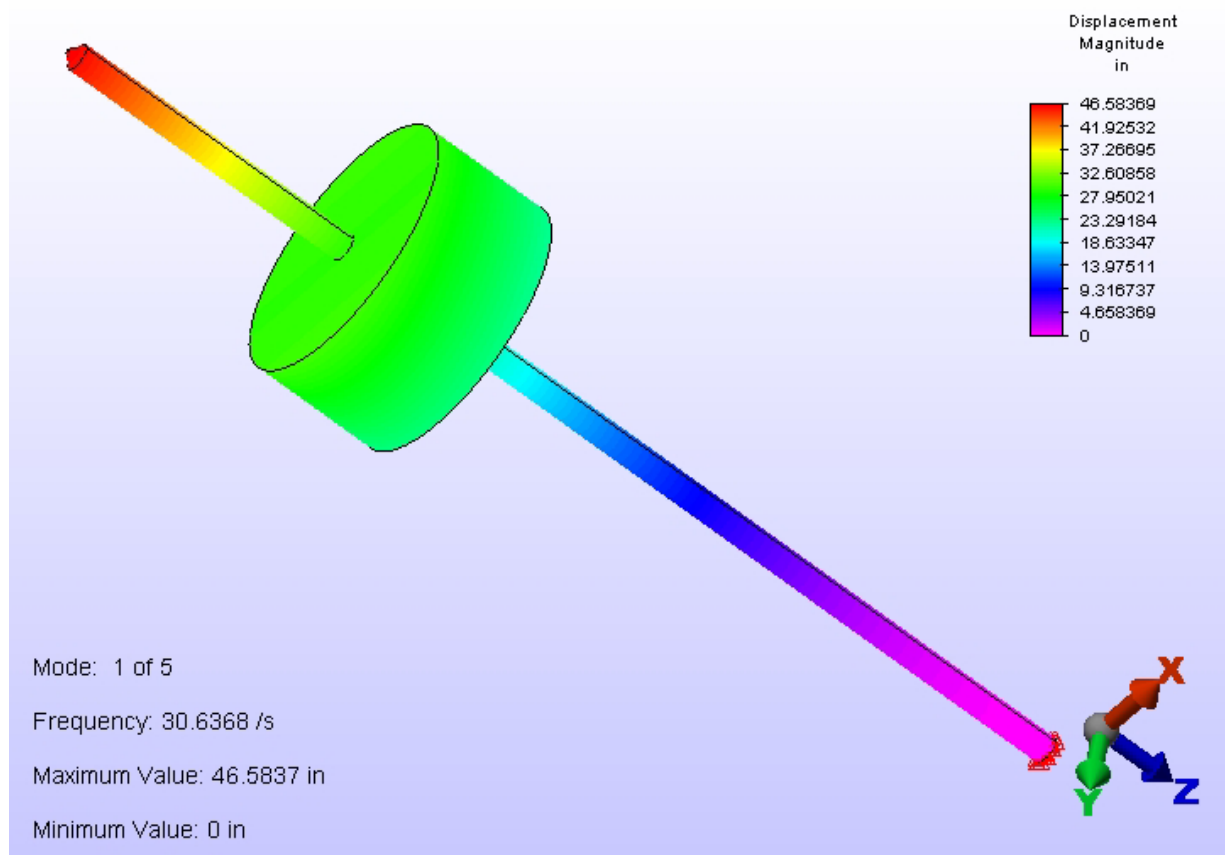


Figure 30 shows the fundamental natural frequency when the mass has moved two-thirds of the way down the nail. Again, since no load is applied in a modal analysis, the displacements reported are only relative values.

Figure 30. Fundamental Mode of the Nail with the Mass Down Two-Thirds.

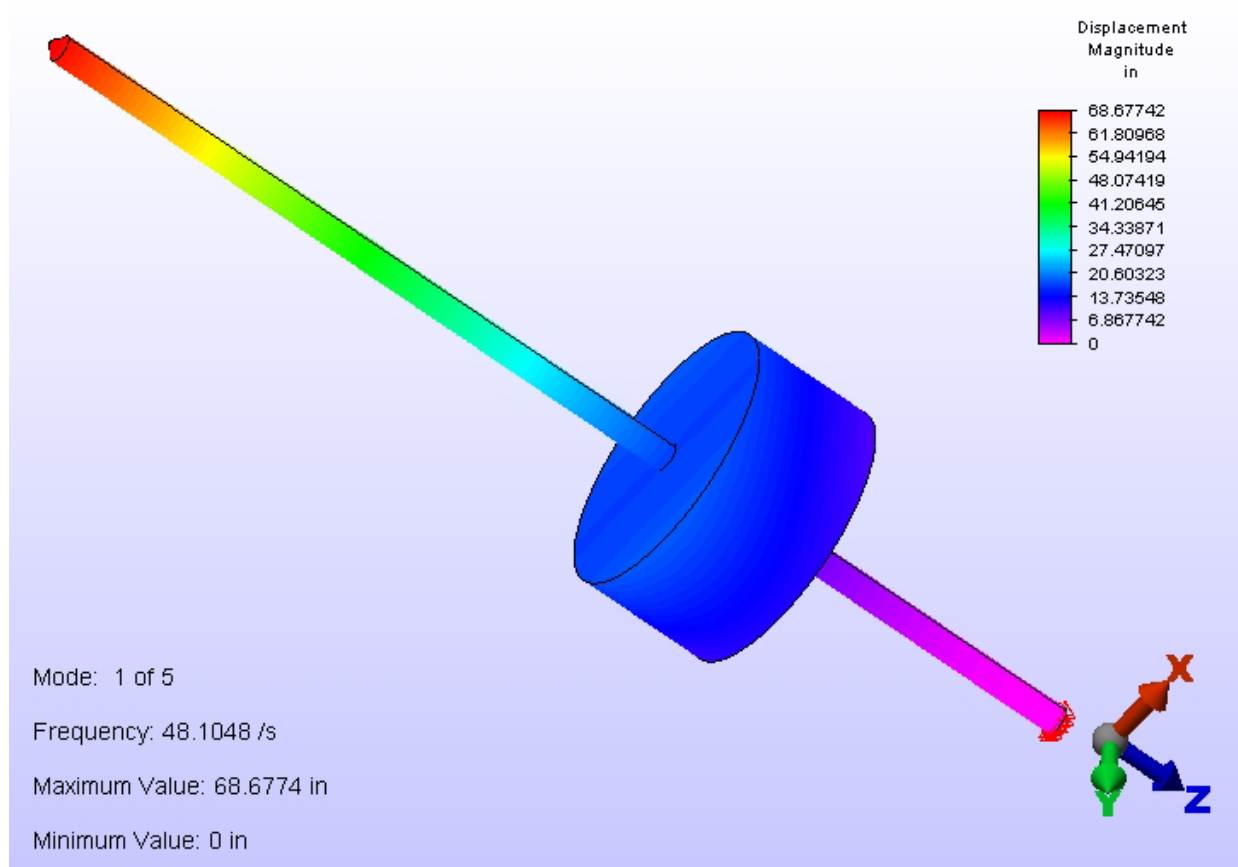
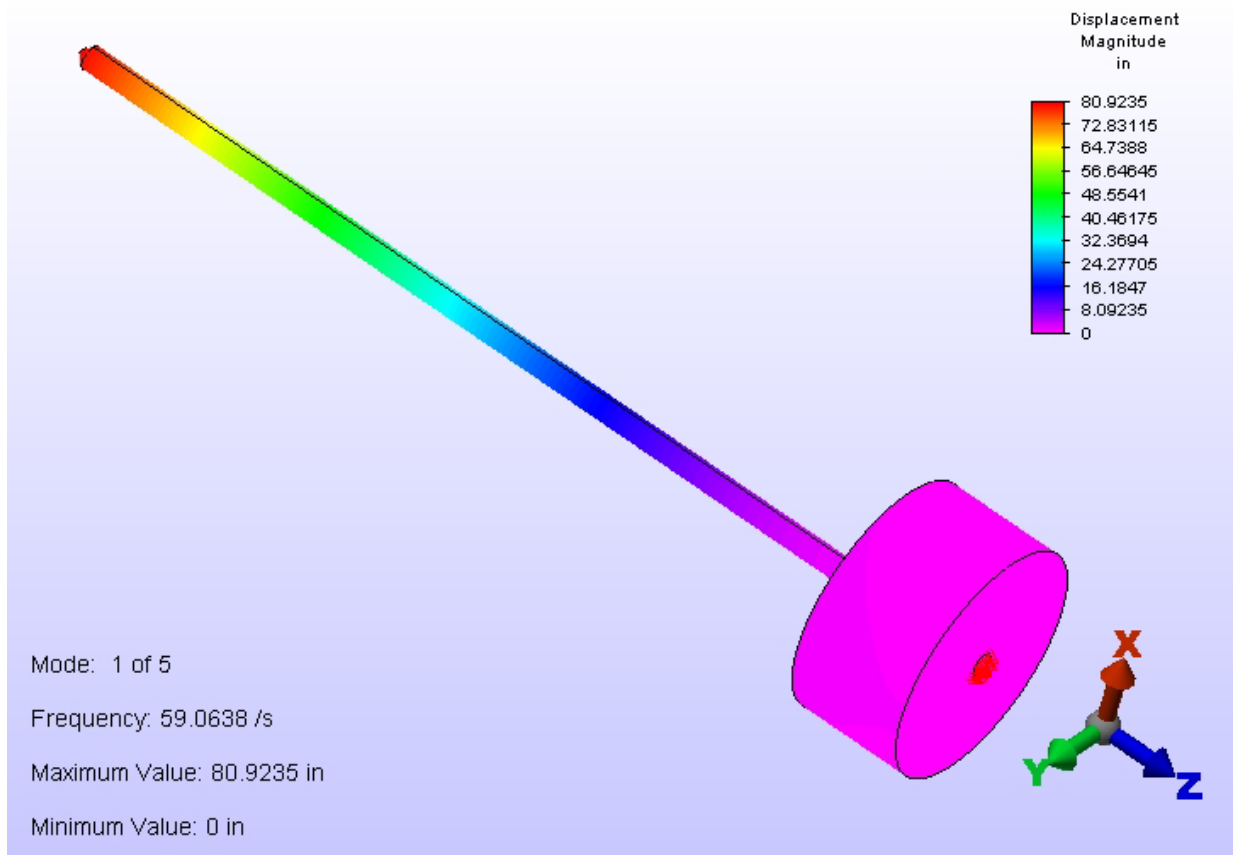


Figure 31 shows the fundamental natural frequency when the mass has moved all of the way down to the bottom of the nail. Again, since no load is applied in a modal analysis, the displacements reported are only relative values.

Figure 31. Fundamental Mode of the Nail with the Mass at the Bottom.



The results of these modal analyses are summarized in Table 17. As expected, the fundamental natural frequency of experimental setup changes as the bone simulating material moves down the nail.

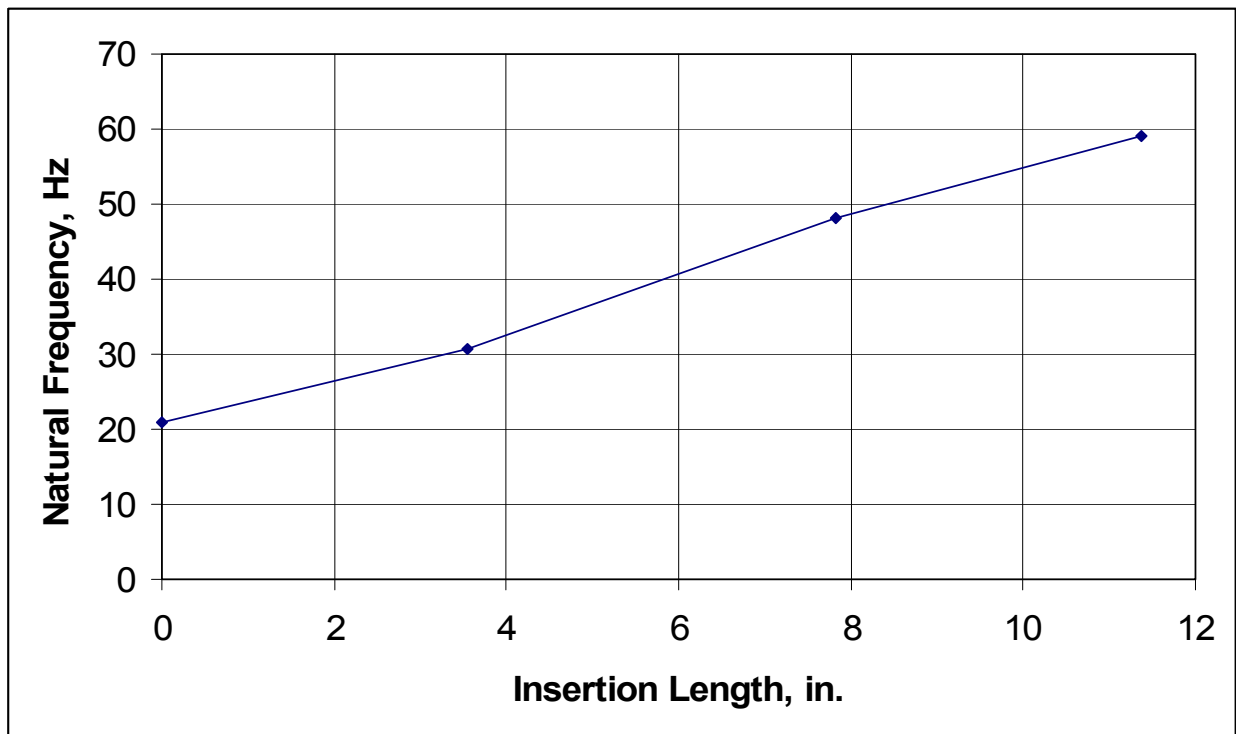
Table 17. Fundamental Natural Frequency Change During Experimental Nail Insertion.

Amount of Nail Insertion	Fundamental Natural Frequency
No Nail Insertion	21.0 Hz
1/3 Nail Insertion	30.6 Hz
2/3 Nail Insertion	48.1 Hz
Full Nail Insertion	59.1 Hz

For the experimental configuration, the natural frequency ranges from 21.0 Hz at the start of nail insertion to 59.1 Hz when the nail has been fully inserted. This natural frequency change would explain why the frequency sweep experiments were almost as effective as a single forcing frequency of 22 Hz. In fact, if the frequency sweep was configured to sweep between 20 Hz and 60 Hz at the same rate that the bone simulating material moved down the nail, one could expect the frequency sweep to be more effective than the single forcing frequency of 22 Hz. Knowing the natural frequency range would be very important information needed in designing a vibratory device with an optimum frequency sweep.

From the results above, the fundamental natural frequency of the experimental configuration has been shown to be proportional to nail insertion distance. The following Figure 32 is a graph of Table 17 and it is included to show that the relationship between natural frequency and nail insertion distance appears to be linear.

Figure 32. Graph of Natural Frequency Versus Nail Insertion Distance.



4.3.6 Range of Natural Frequencies During Actual Nail Insertion

The natural frequency range above is for the experimental configuration; however, the actual configuration during surgery is slightly different. The T-handle or similar device will be attached to the nail and instead of the bone simulating material sliding on the nail; the nail will be sliding through the bone. These differences make the natural frequency range during orthopaedic surgery different. Therefore, the actual configuration during orthopaedic surgery is analyzed to determine the natural frequency range during insertion. This natural frequency range would be necessary information for developing or designing an efficient and effective vibratory device for orthopaedic surgeons.

Three different modal analyses are performed in ALGOR. The first one is at the beginning of nail insertion, the second is halfway through nail insertion, and the last is when the nail is fully inserted. In all three ALGOR modal analyses, the solid model was created first and then meshed with brick elements with an average size of 0.15 inches. Then the fixed boundary condition was placed at the location of the bone hole for each modal analysis. The material properties are specified to simulate 17-4 precipitation hardened (PH) stainless steel for the nail and T-handle. These material properties are shown in Appendix Q. For each of the three ALGOR modal analyses, the fundamental natural frequency is reported. Figure 33 through 35 show the fundamental natural frequencies of all three points in time during insertion. As before, since no load is applied in a modal analysis, the displacements reported are only relative values.

It must be noted that the surgeon's hands will be placed on the T-handle during the surgery and this will affect the natural frequency of the T-handle and nail assembly. The surgeon's hands will add mass to the assembly and also add a resistance to vibration due to the surgeon's clamping. The effect of the extra mass and vibration resistance due to clamping is not modeled in this analysis. These unknowns are difficult to quantify and will vary with each surgeon.

Figure 33. Fundamental Mode of the Nail and T-handle at the Beginning of Insertion.

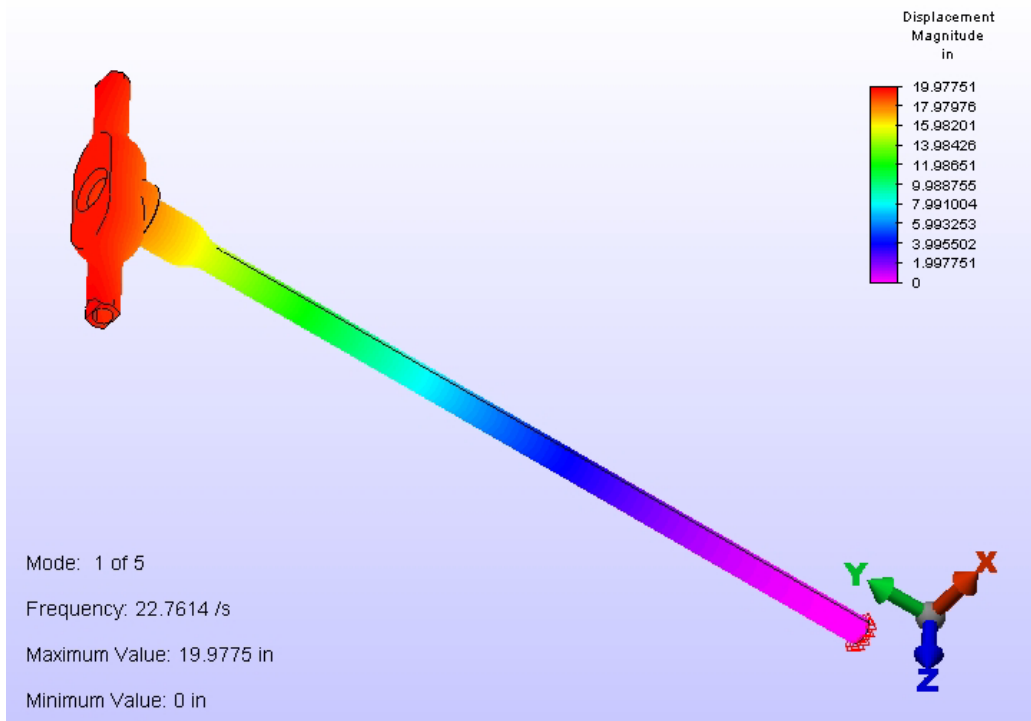


Figure 34. Fundamental Mode of the Nail and T-handle Halfway Through Insertion.

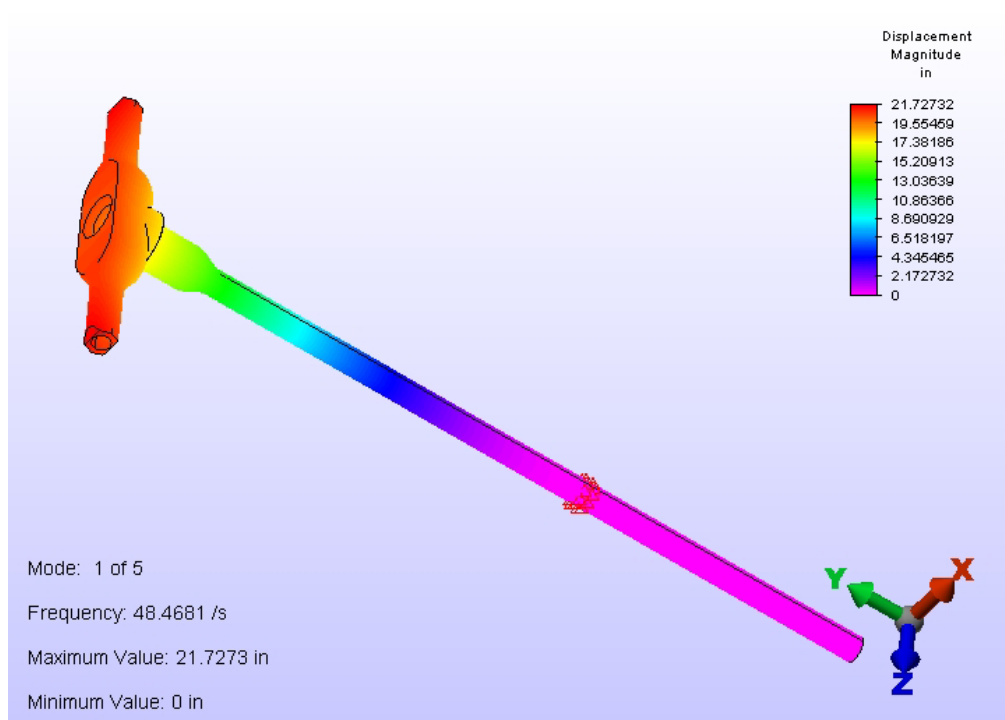
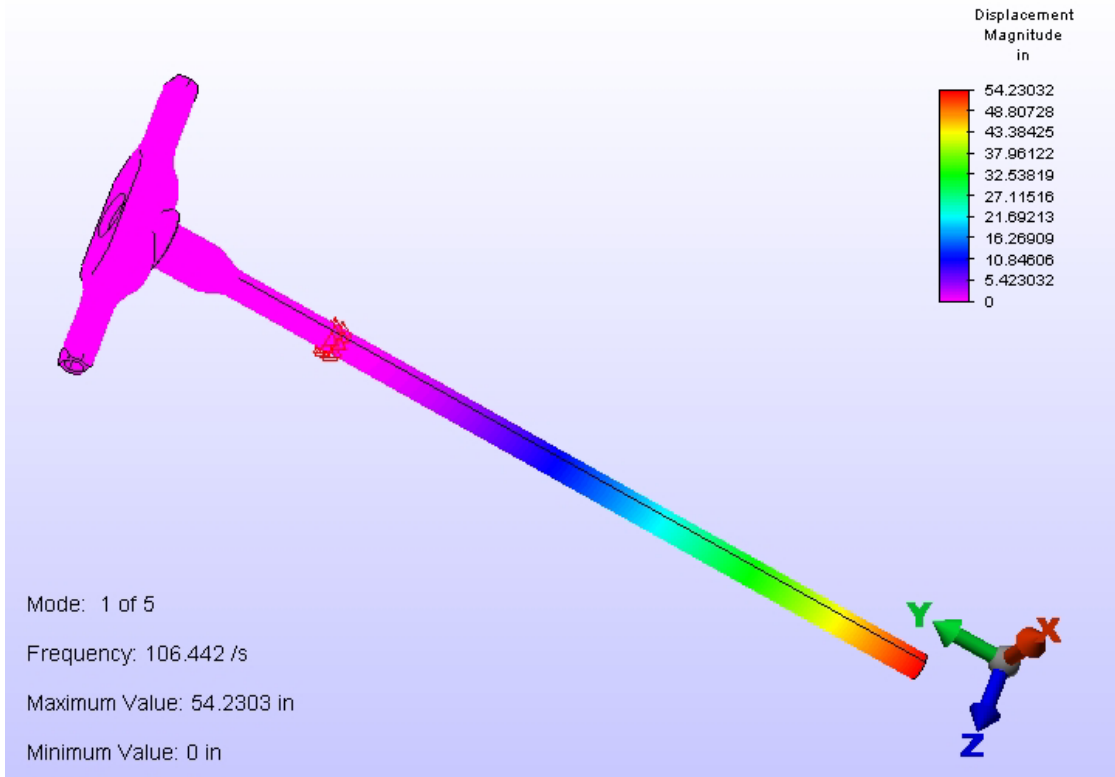


Figure 35. Fundamental Mode of the Nail and T-handle at the End of Insertion.



The results of these modal analyses are summarized in Table 18.

Table 18. Fundamental Natural Frequency Change During Actual Nail Insertion.

Amount of Nail Insertion	Fundamental Natural Frequency
No Nail Insertion	22.8 Hz
1/2 Nail Insertion	48.5 Hz
Full Nail Insertion	106.4 Hz

The results show the fundamental natural frequency ranges between 22.8 Hz and 106.4 Hz during nail insertion. This natural frequency range is for a realistic orthopaedic surgical implant scenario. These results could be used in the design and development of a vibratory device because the results could be used to determine the optimum frequency sweep and rate for a vibratory device.

4.3.7 Load Stiffening Effect on the Natural Frequency of the Nail

In the section 4.3.6 above, the fundamental natural frequency range is determined by analysis. While the nail is being inserted into the bone, the orthopaedic surgeon will be applying a load to the T-handle/nail assembly. This section ascertains whether the effect of the surgeon's applied load will significantly change the natural frequencies reported in the previous section 4.3.6. The effect of an applied load causing a change in natural frequency is known as load stiffening. The most obvious example of this phenomenon is how tightening or loosening a guitar string changes its natural frequency, thus changing its sound.

Three different modal analyses are performed in ALGOR. The first being at the beginning of nail insertion, the second is halfway through nail insertion, and the final is when the nail is fully inserted. In all three ALGOR modal analyses, the solid model was created first and then meshed with brick elements with an average size of 0.15 inches. Then the fixed boundary condition was placed at the location of the bone hole for each modal analysis. The material properties are specified to simulate 17-4 precipitation hardened (PH) stainless steel for the nail and T-handle. These material properties are shown in Appendix Q. For each of the three ALGOR modal analyses, the fundamental natural frequency is reported. Figure 36 through 38 show the fundamental natural frequencies of all three points in time during insertion. As before, since no load is applied in a modal analysis, the displacements reported are only relative values.

Figure 36. Fundamental Mode of the Nail/T-handle at the Beginning of Insertion.

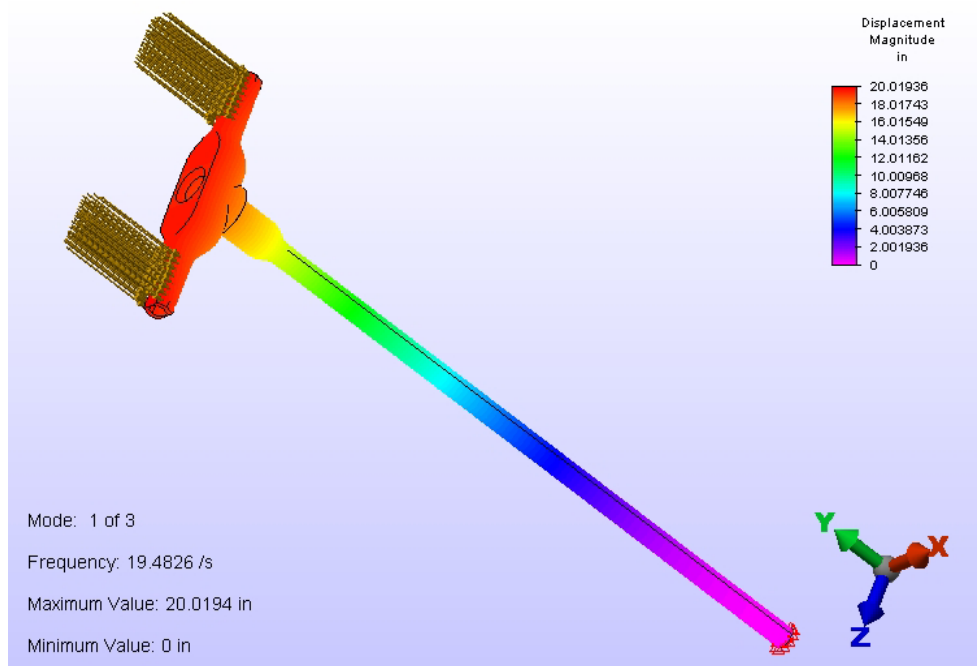


Figure 37. Fundamental Mode of the Nail and T-handle Halfway Through Insertion.

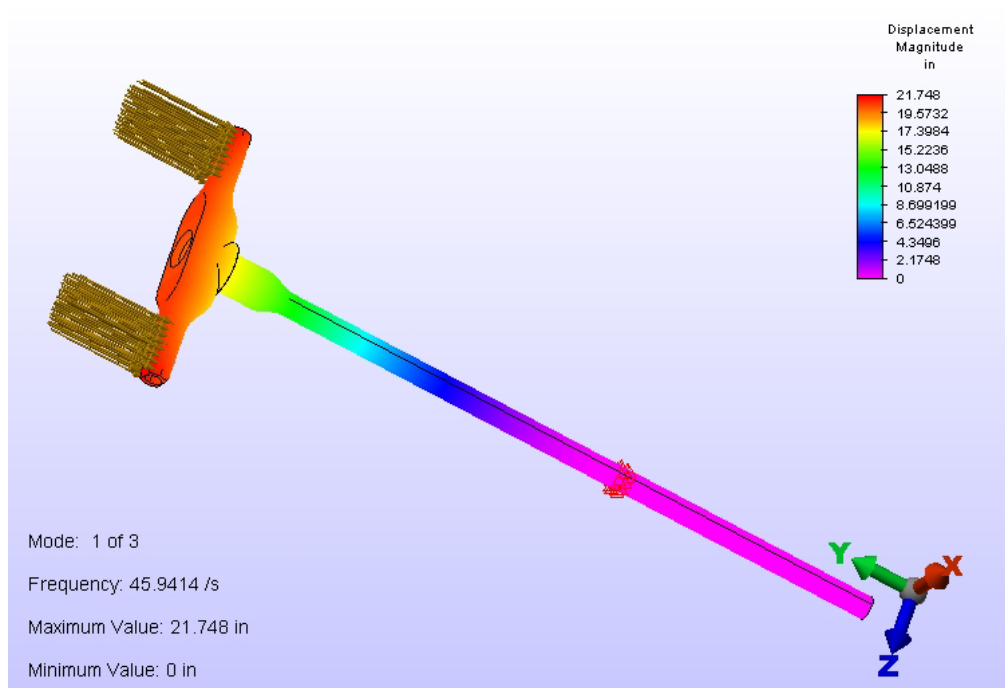


Figure 38. Fundamental Mode of the Nail and T-handle at the End of Insertion.

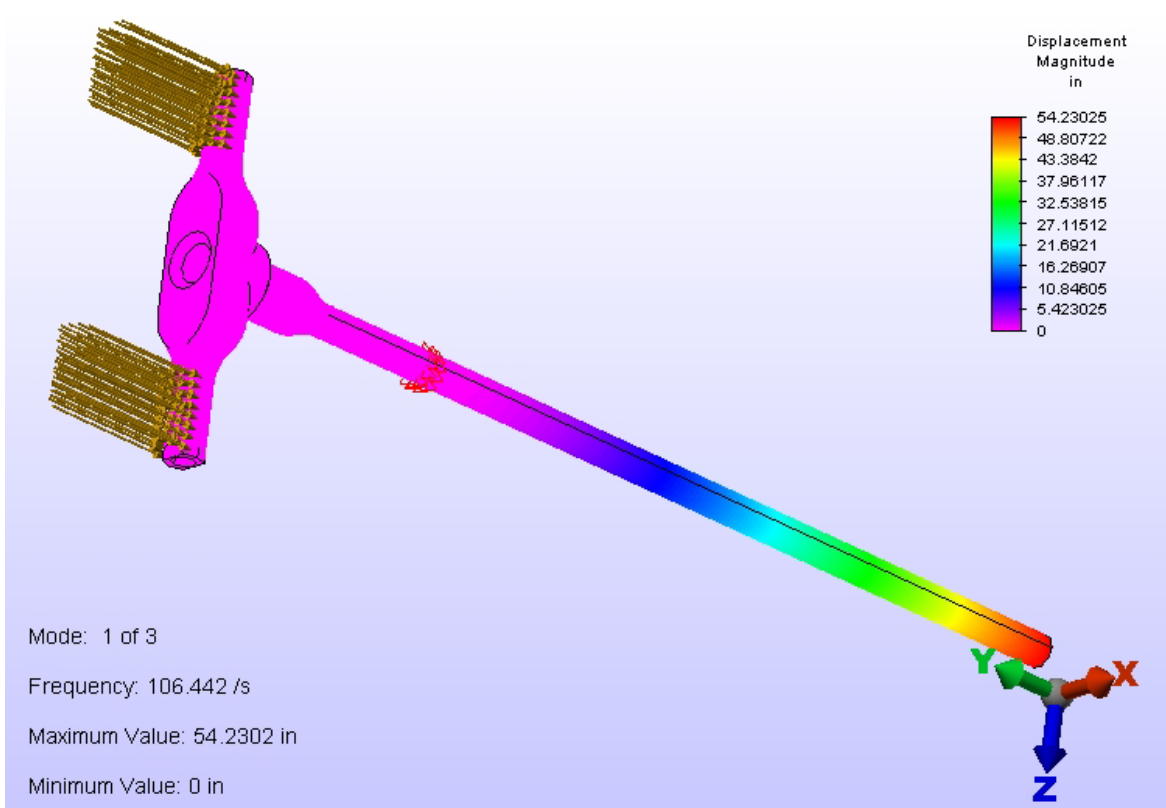


Table 19 summarizes the results of these modal analyses and compares them with the results obtained in section 4.3.6.

Table 19. Natural Frequency Change During Actual Nail Insertion with Load Stiffening.

Amount of Nail Insertion	Natural Frequency (No Load Stiffening)	Natural Frequency (Load Stiffening)	Percent Difference
No Nail Insertion	22.8 Hz	19.5 Hz	14.5%
1/2 Nail Insertion	48.5 Hz	45.9 Hz	5.3%
Full Nail Insertion	106.4 Hz	106.4 Hz	0.0%

From Figure 19, the effect of load stiffening is demonstrated to be more significant at the beginning of nail insertion. The natural frequency of the nail at the beginning of nail insertion changed 14.5 percent from an applied load of 200 lbs. The natural frequency of the nail when

inserted halfway into the bone changes 5.3 percent due to load stiffening. In the last case during full nail insertion, the natural frequency is observed to have no change. Upon further observation of the mode shape, the reason is because the section of the nail that is vibrating is not between the load and the fixed constraint. Therefore, the part of the nail that is vibrating in the mode shape is not loaded, thus it does not experience load stiffening. Only the section above the fixed constraint is loaded and this section of the nail does not move during the fundamental mode. In conclusion, load stiffening can have some effect on the natural frequency of the nail and should be taken into account when designing a vibratory device optimized to help nail insertion.

4.4 Vibration Analysis Conclusions

The supporting vibration analyses performed in this section help demonstrate and verify the conclusions and observations derived from the experimental results. The experimental results in conjunction with the analytical results provide a solid basis for the conclusions drawn in this thesis.

5.0 THESIS CONCLUSION AND RESULTS

5.1 Brief Re-statement of Thesis Purpose

The objective of this thesis is to provide “proof of concept” that vibration can be applied to orthopaedic surgical implants for the purpose of significantly reducing the force needed for insertion of these implants.

5.2 Thesis Conclusion

The results are conclusive in demonstrating that applied vibration can be used to reduce the force required for insertion of orthopaedic surgical implants. The experimental results show that both transverse and axial vibrations are effective in reducing insertion force for the three materials tested; biomechanical test blocks, UHMW-PE, and bovine wet bone. Even considering the statistical variance in the multi-trial data, the results are conclusive.

5.2.1 Vibration Frequencies Recommended for Vibratory Insertion/Extraction Device

One of the most important parameters needed for the development of a prototype vibratory insertion and extraction device is the forcing frequency of the applied vibration. The results of this thesis provide valuable data to determine the most efficient and effective forcing frequency for the prototype vibratory device.

Although all forcing frequencies of the vibration that was tested in the laboratory did reduce the insertion force, some forcing frequencies were more effective than others. Using the average force data for all the experiments conducted, the most effective forcing frequency tested for transverse vibrations was between 20 and 22 Hz. Also using the average force data for all experiments conducted, the most effective forcing frequency tested for axial vibrations was between 10 and 20 Hz. However, in both types of vibration tested, the frequency sweep experiments proved to be quite effective as well. Variation and adjustment of parameters in the frequency sweep such as the sweep rate and the sweep range could increase effectiveness making it the most effective at reducing insertion and extraction force.

The results of the analytical work in this thesis suggest that for the actual T-handle and nail configuration used in surgery, the most effective frequency range for a transverse vibration sweep is 19.5 Hz to 106.4 Hz. However, for a single transverse forcing frequency instead of a frequency sweep, the most effective forcing frequency is 19.5 Hz. A single transverse forcing

frequency would be easier to apply but the data suggests that a transverse frequency sweep would also be effective. For a single axial forcing frequency, the most effective frequencies would be between 10 and 20 Hz with a high acceleration. The high acceleration is important for axial vibration because the data suggests the effectiveness is proportional to the vibration energy put into the system. Frequency sweeps in the axial direction were shown to be almost as effective as a single axial forcing frequency.

5.2.2 Vibration Frequencies of Common Commercially Available Devices

There are many vibratory devices used everyday for common purposes, some of which might potentially be modified for use as the applied excitation device for surgical implant insertion and extraction. Laboratory experiments were conducted with a few common commercially available vibratory devices to determine the forcing frequencies of the devices. The purpose of the experiments is to determine a sample range of forcing frequencies used in commercially available devices.




The forcing frequencies of the devices were found by using the oscilloscope and a piezo-accelerometer from Measurement Specialties, Inc. (MSI) shown in Figure 39.

Figure 39. Oscilloscope and Piezo-Accelerometer Used.



The MSI piezo-accelerometer is placed directly onto the vibratory device and the output is read on the oscilloscope. The results of this experiment for the devices tested are shown below in Table 20.

Table 20. Forcing Frequencies of Common Vibratory Devices.

Picture	Description	Frequency
	Sonicare vibrating toothbrush, (battery operated, rechargeable)	260 Hz
	Conair handheld massager, (powered by 120 volt AC plug in)	120 Hz
	Black & Decker Mouse Sander (powered by 120 volt AC plug in)	180 Hz

5.3 Recommendations for Further Research

There are a couple worthwhile experiments related to the work presented in this thesis that would be beneficial and provide valuable results. One would be to determine the actual insertion force of a nail in bone by having surgeons conduct in-vivo experiments. Another would be to perform nail insertion experiments in-vitro on long bones from smaller animals such as pigs or sheep.

Also, based on the conclusions in this thesis, there are several suggested major research topics that would be worth exploring.

One research topic would be the design and development of a prototype vibratory device. This would require a more in depth research of commercially available vibratory devices, the frequencies at which they operate, how the vibration is induced and applied, and how the device is powered. If no commercially available vibratory device is suitable for modification, then a prototype device would be designed and constructed. There are several design requirements for such a device that would make designing it challenging. Experimentation with a prototype vibratory device would yield some interesting and conclusive results.

Another research topic would be to do extensive research on the tribology of the problem. Experimentation could be conducted to determine the static and dynamic coefficient of friction between surgical implants and bone. This useful information could be used to determine whether lubrication could enhance the effects of applied vibration, thus making surgical implant insertion and extraction require less force than using vibration alone. The topic of lubrication would require an immense amount of research on what types of lubrication are available, what types would be compatible and not detrimental to the human body, how effective the lubricants can be, and how much each type reduces the friction coefficients.

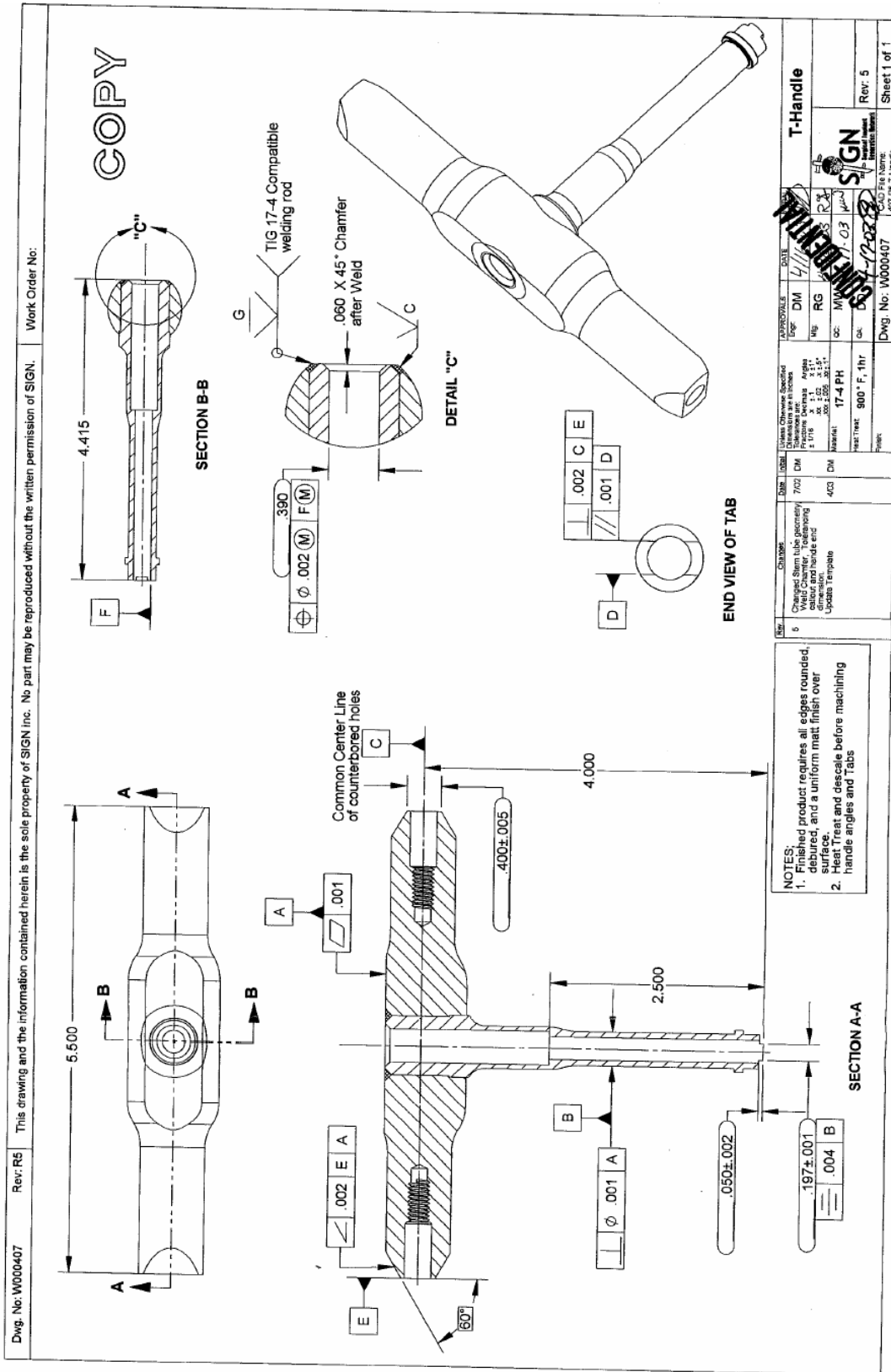
This thesis and the two suggested research topics discussed above are based on the surgical implants in use today. However, it is conceivable that another method could be developed to fix the fracture site, give support to the fracture area, and speed up the healing process. This is yet another suggested research topic that would require researching other methods or techniques to achieve the same purposes as an intramedullary nail.

REFERENCES

- [1] SIGN, Surgical Implant Generation Network, Dr. Lewis G. Zirkle, M.D.
- [2] Witzigreuter, Timothy, 2005, "The Origin, History, and Use of the Intermedullary Nail," National Association of Orthopaedic Technologists, <http://www.naot.org/onlineceusdec2005.html>
- [3] Funk, Lennard, 2001, "Physiological Mechanical Testing of Tibial Intramedullary Nails," Technical Report, Orthoteers Orthopaedic Educational Resource, <http://www.lenfunk.co.uk/>
- [4] Kreith, Frank, 1998, "The CRC Handbook of Mechanical Engineering," CRC Press, Boca Raton, Florida.
- [5] Nigg, Benno M. and Herzog, Walter, 1999, "Biomechanics of the Musculo-Skeletal System, 2nd edition, John Wiley and Sons, Inc., Chichester, England.
- [6] Kinsel, William C. and Zirkle, Lewis G, 2001, "Entrepreneur's Proposal for Vibratory Insertion and Extraction of Surgical Implants," Technical Proposal, Richland, Washington.
- [7] Sawbones Worldwide, A Division of Pacific Research Laboratories, Inc.,
- [8] Fitzpatrick, D., Ahn, P., Brown, T., Poggie R., 1997, "Friction Coefficients of Porous Tantalum and Cancellous & Cortical Bone," American Society of Biomechanics, Clemson University, South Carolina
- [9] Strzepa, P., Klawitter, JJ., 2005, "Ascension Pyrocarbon Hemisphere Wear Testing Against Bone," 51st Annual Meeting of the Orthopaedic Research Society, Ascension Orthopedics, Inc., Austin, TX.
- [10] Roark, R. J. and Young, W.C., 2002, "Roark's Formula for Stress and Strain", Seventh Edition, McGraw-Hill. New York, New York.
- [11] Timoshenko, S.P., Weaver, W. Jr., Young, D.H., 1990, "Vibration Problems in Engineering", Fifth Edition, John Wiley & Sons. New York, New York.
- [12] ALGOR version 19.2 SP1, 2006, ALGOR Inc., Pittsburgh, PA.
- [13] Inventor 8, 2006, Autodesk Inc., San Rafael, CA.
- [14] AutoCAD 2006, 2006, Autodesk Inc., San Rafael, CA.
- [15] MathCAD 12, 2006, Mathsoft, Inc., Cambridge, MA

APPENDIXES

Appendix A – SIGN T-Handle Design Drawing



Appendix B – Biomechanical Test Blocks Specification and Properties

Solid Rigid Polyurethane Foam



[Solid rigid polyurethane foam products list](#)

Primary Use

Solid rigid polyurethane foam is primarily used as an alternative test medium for human cancellous bone. These products aren't intended to replicate the mechanical properties of human bone; however, it does provide consistent and uniform material with properties in the range of human cancellous bone. Relevant mechanical properties for comparison to human cancellous bone may depend on the particular test method that is being developed.

The [ASTM F-1839 "Standard Specification for Rigid Polyurethane Foam for Use as a Standard Material for Testing Orthopaedic Devices and Instruments"](#) states that; "The uniformity and consistent properties of rigid polyurethane foam make it an ideal material for comparative testing of bones screws and other medical devices and instruments."

Description

Solid rigid polyurethane foam has a closed cell content ranging from 96.0 to 99.9%. Foam is available in a range of sizes and densities, from 0.16 to 0.80 grams per cubic centimeter (5 to 50 pounds per cubic foot).

Standard block size: 13cm x 18cm x 4cm

Standard sheet size: 13cm x 18cm x 3mm

Typical Properties

Density (pcf) (g/cc)	Compressive		Tensile		Shear		
	Strength (MPa)	Modulus (MPa)	Strength (MPa)	Modulus (MPa)	Strength (MPa)	Modulus (MPa)	
10*	0.16*	2.2	77	2.2	57	1.4	23
15*	0.24*	4.9	153	3.9	143	2.8	44
20*	0.32*	8.8	260	5.9	267	4.5	67
30	0.48	20	553	11	640	8.9	122
40*	0.64*	37	943	16	1,190	14	187
50	0.80	58	1,400	32	2,000	20	262

Coefficient of Thermal Expansion (CTE) = 6.3×10^{-5} K⁻¹ (from -46 to +93 °C)

Water absorption ranges from 0.301 to 0.0 kg/m²

Material property data parallel to rise of foam using test methods ASTM D-1621, D-1623, D-273. ASTM F-1839 is currently being revised and will match the improved property values given above.

*Foam densities designate "graded" foams per ASTM standard specification F-1839.

Copyright ©2006 Pacific Research Laboratories. All rights reserved.

Appendix C – Typical UHMW-PE Specification and Properties

Polystone® M (UHMW-PE)

A tough, wear resistant plastic that combines an incredibly low coefficient of friction with outstanding impact strength. This self-lubricating polymer has excellent chemical resistance and a broad temperature range making it the perfect choice for engineers in a variety of industries such as conveyor and bulk material handling.



Range

Sheets, rods, tubes, standard and custom profiles, cut-to-size strips and blocks

Polystone® Applications:

- Chute, hopper and truck bed liners
- Wear strips and guide rails
- Star wheels, sprockets and conveyor tracks
- Bumpers and dock fenders
- Bushings, bearings and rollers

Physical Properties			Polystone® M (UHMW-PE)			
Property	Units	ASTM Test	Natural	XL Cross linked	MPG Glass filled	Reprocessed
Density	gm/cm ³	D792	.930	.932	.96	.935
Tensile strength at yield 73°F	psi	D638	3100	2900	2700	3000
Elongation 73°F	%	D638	350	330	265	290
* Relative volumetric abrasion loss	*	*	100	85	75	90
Coefficient of friction 73°F on steel	-	-	Static .15-.20 Dynamic .10-.20	.15-.20 .08-.18	.15-.20 .10-.20	.17-.20 .10-.20
IZOD impact strength 73°F	KJ/m ²	D4020-96	125	120	110	96
Hardness 73°F	-	D785	Shore D 62-66	D 62-66	D 63-67	D 63-69
Melting point	°F	D789	275°-280°	275°-280°	275°-280°	275°-280°
Coefficient of linear thermal expansion	1/K	D696	2.0 x 10 ⁻⁴	1.0 x 10 ⁻⁴	1.0 x 10 ⁻⁴	1.9 x 10 ⁻⁴
Continuous service temperature in air (max)	°F	-	180	180	180	180
Volume resistivity	Ohm/cm	D257	>10 ¹⁵	>10 ¹⁵	>10 ¹⁵	>10 ¹⁵
Dielectric constant (10 ³ Hz)	-	D150	2.3	2.3	2.3	-
Dielectric strength	KV/mm	D149	900	900	900	900

Appendix D – Transverse Vibration Voltage Data With Biomechanical Test Blocks

Biomechanical Material Vibration Experiments Transverse Vibration of the Rod at Varying Frequencies

Frequency (Hz)	20		
Trial	Maximum Reading (mV)	Minimum Reading (mV)	Average Reading (mV)
1	64	42	52.9
2	64.4	40.4	55.3
3	64.8	48.4	55.6
Trial Average	64.4	43.6	54.6
Standard Deviation	0.40	4.23	1.48

Frequency (Hz)	60		
Trial	Maximum Reading (mV)	Minimum Reading (mV)	Average Reading (mV)
1	64.8	21.6	42.5
2	64.8	24.8	50
3	64	27.2	48
Trial Average	64.53	24.53	46.83
Standard Deviation	0.46	2.81	3.88

Frequency (Hz)	120		
Trial	Maximum Reading (mV)	Minimum Reading (mV)	Average Reading (mV)
1	62.8	21.6	42.7
2	63.6	20.8	46.7
3	63.2	24.4	43
Trial Average	63.2	22.27	44.13
Standard Deviation	0.40	1.89	2.23

Frequency (Hz)	180		
Trial	Maximum Reading (mV)	Minimum Reading (mV)	Average Reading (mV)
1	64	36	51.4
2	63.6	42.4	52.6
3	64	39.2	52.3
Trial Average	63.86666667	39.2	52.1
Standard Deviation	0.23	3.20	0.62

Frequency (Hz)	0 (Baseline)		
Trial	Maximum Reading (mV)	Minimum Reading (mV)	Average Reading (mV)
1	63.6	20	38.6
2	63.6	22	45.9
3	61.2	32.4	47.7
Trial Average	62.80	24.80	44.07
Standard Deviation	1.39	6.66	4.82

Appendix E - Transverse Vibration Force Data With Biomechanical Test Blocks

Frequency (Hz)	20		
Trial	Maximum Force (lbs)	Minimum Force (lbs)	Average Force (lbs)
1	9.14	0.00	4.42
2	9.83	0.00	3.38
3	6.37	0.00	3.25
Trial Average	8.44	0.00	3.68
Standard Deviation	1.83	0.00	0.64

Frequency (Hz)	60		
Trial	Maximum Force (lbs)	Minimum Force (lbs)	Average Force (lbs)
1	17.97	0.00	8.92
2	16.59	0.00	5.67
3	15.55	0.00	6.54
Trial Average	16.70	0.00	7.04
Standard Deviation	1.22	0.00	1.68

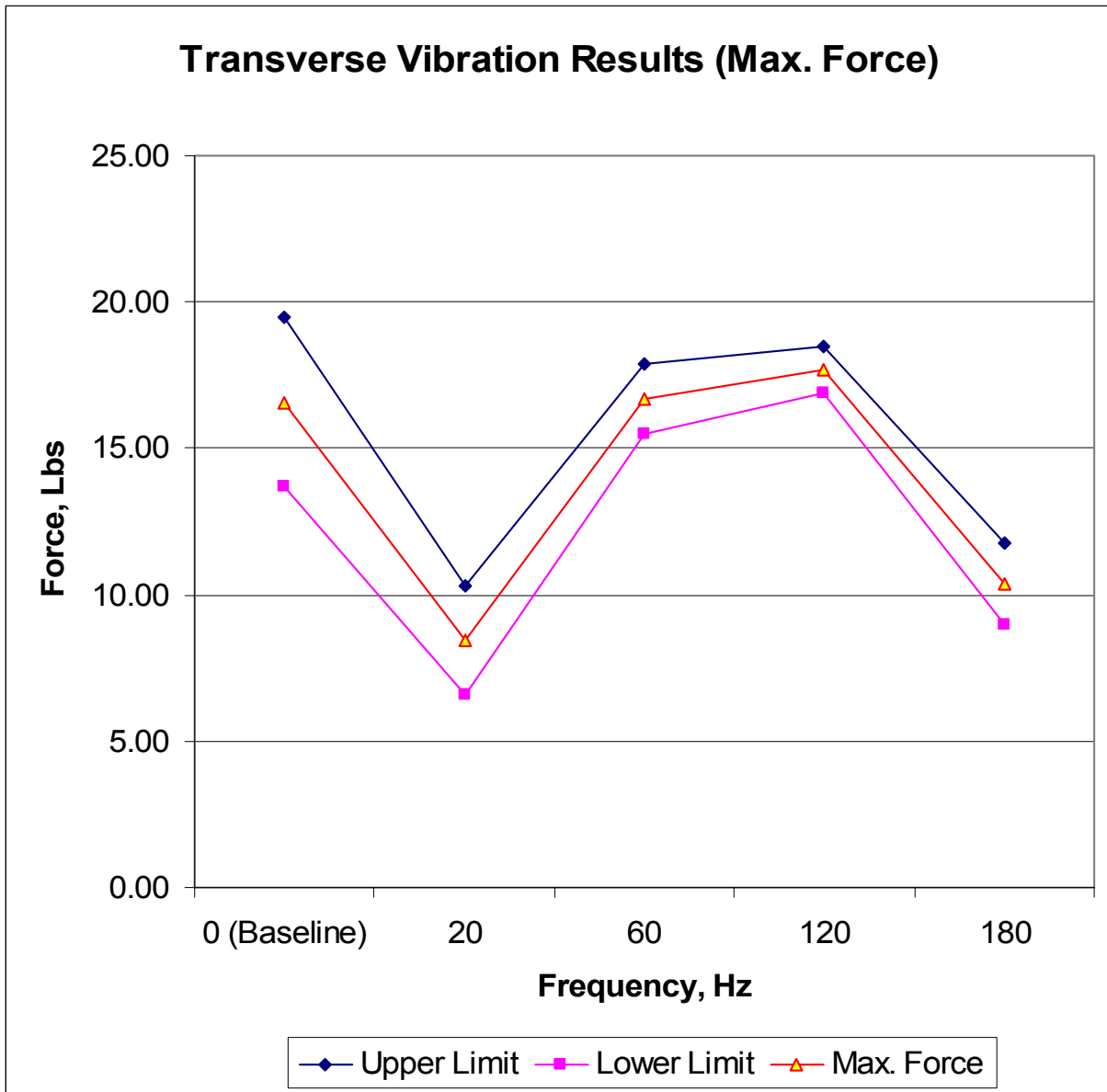
Frequency (Hz)	120		
Trial	Maximum Force (lbs)	Minimum Force (lbs)	Average Force (lbs)
1	17.97	0.13	8.83
2	18.32	0.00	7.10
3	16.76	0.00	8.70
Trial Average	17.68	0.04	8.21
Standard Deviation	0.82	0.08	0.96

Frequency (Hz)	180		
Trial	Maximum Force (lbs)	Minimum Force (lbs)	Average Force (lbs)
1	11.74	0.00	5.07
2	8.96	0.00	4.55
3	10.35	0.00	4.68
Trial Average	10.35	0.00	4.76
Standard Deviation	1.39	0.00	0.27

Frequency (Hz)	0 (Baseline)		
Trial	Maximum Force (lbs)	Minimum Force (lbs)	Average Force (lbs)
1	18.66	0.00	10.61
2	17.80	0.00	7.45
3	13.29	0.82	6.67
Trial Average	16.59	0.27	8.24
Standard Deviation	2.88	0.48	2.09

Appendix F - Transverse Vibration Maximum Force With Biomechanical Test Blocks

Frequency (Hertz)	Average Force (pounds)	Standard Deviation (pounds)	Upper Limit Standard Deviation	Lower Limit Standard Deviation
0 (Baseline)	16.59	2.88	19.47	13.70
20	8.44	1.83	10.28	6.61
60	16.70	1.22	17.92	15.48
120	17.68	0.82	18.50	16.86
180	10.35	1.39	11.74	8.96



Appendix G – Axial Vibration Voltage Data With Biomechanical Test Blocks

Biomechanical Material Vibration Experiments

Axial Vibration of the Rod at Varying Frequencies

Frequency (Hz)	20		
Trial	Maximum Reading (mV)	Minimum Reading (mV)	Average Reading (mV)
1	64	61.6	62.4
2	64	61.2	62.6
3	64	60.8	62.5
Trial Average	64	61.2	62.5
Standard Deviation	0.00	0.40	0.10

Frequency (Hz)	60		
Trial	Maximum Reading (mV)	Minimum Reading (mV)	Average Reading (mV)
1	64	61.2	62.3
2	64.4	60.8	62
3	64	62	62.7
Trial Average	64.13	61.33	62.33
Standard Deviation	0.23	0.61	0.35

Frequency (Hz)	120		
Trial	Maximum Reading (mV)	Minimum Reading (mV)	Average Reading (mV)
1	64	62	62.7
2	63.6	61.2	62.1
3	63.6	61.2	62.1
Trial Average	63.73	61.47	62.3
Standard Deviation	0.23	0.46	0.35

Frequency (Hz)	180		
Trial	Maximum Reading (mV)	Minimum Reading (mV)	Average Reading (mV)
1	64	60.8	62.1
2	64	62	62.6
3	64	62	62.8
Trial Average	64	61.6	62.5
Standard Deviation	0.00	0.69	0.36

Frequency (Hz)	0 (Baseline)		
Trial	Maximum Reading (mV)	Minimum Reading (mV)	Average Reading (mV)
1	63.6	54.8	60.4
2	64	59.6	61.3
3	63.6	59.2	61.8
Trial Average	63.73	57.87	61.17
Standard Deviation	0.23	2.66	0.71

Appendix H - Axial Vibration Force Data With Biomechanical Test Blocks

Frequency (Hz)	20		
Trial	Maximum Force (lbs)	Minimum Force (lbs)	Average Force (lbs)
1	0.95	0.00	0.61
2	1.13	0.00	0.52
3	1.30	0.00	0.56
Trial Average	1.13	0.00	0.56
Standard Deviation	0.17	0.00	0.04

Frequency (Hz)	60		
Trial	Maximum Force (lbs)	Minimum Force (lbs)	Average Force (lbs)
1	1.13	0.00	0.65
2	1.30	0.00	0.78
3	0.78	0.00	0.48
Trial Average	1.07	0.00	0.64
Standard Deviation	0.26	0.00	0.15

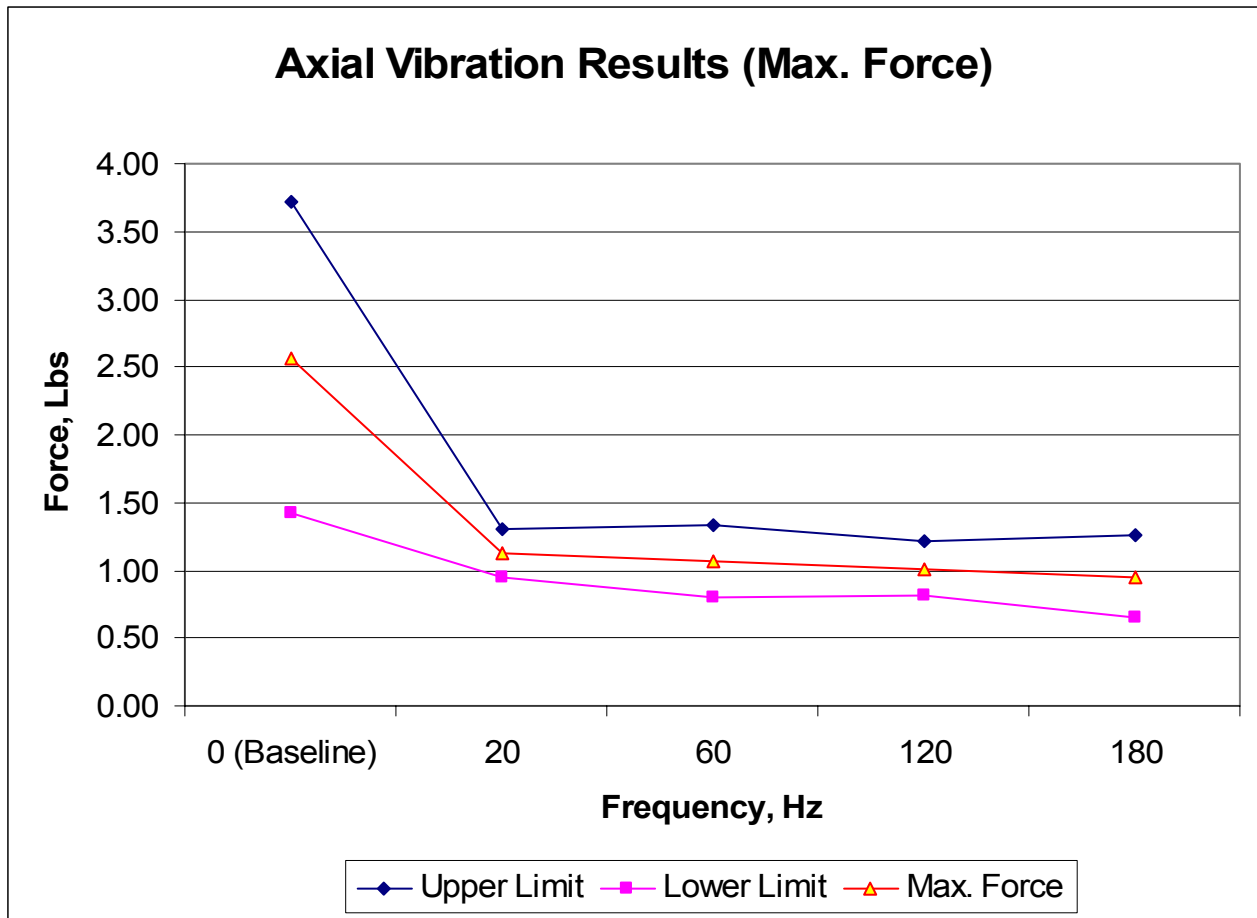
Frequency (Hz)	120		
Trial	Maximum Force (lbs)	Minimum Force (lbs)	Average Force (lbs)
1	0.78	0.00	0.48
2	1.13	0.09	0.74
3	1.13	0.09	0.74
Trial Average	1.01	0.06	0.65
Standard Deviation	0.20	0.05	0.15

Frequency (Hz)	180		
Trial	Maximum Force (lbs)	Minimum Force (lbs)	Average Force (lbs)
1	1.30	0.00	0.74
2	0.78	0.00	0.52
3	0.78	0.00	0.43
Trial Average	0.95	0.00	0.56
Standard Deviation	0.30	0.00	0.16

Frequency (Hz)	0 (Baseline)		
Trial	Maximum Force (lbs)	Minimum Force (lbs)	Average Force (lbs)
1	3.90	0.09	1.47
2	1.82	0.00	1.08
3	1.99	0.09	0.87
Trial Average	2.57	0.06	1.14
Standard Deviation	1.15	0.05	0.31

Appendix I - Axial Vibration Maximum Force With Biomechanical Test Blocks

Frequency (Hertz)	Average Force (pounds)	Standard Deviation (pounds)	Upper Limit Standard Deviation	Lower Limit Standard Deviation
0 (Baseline)	2.57	1.15	3.72	1.42
20	1.13	0.17	1.30	0.95
60	1.07	0.26	1.33	0.80
120	1.01	0.20	1.21	0.81
180	0.95	0.30	1.25	0.65



Appendix J – Transverse Vibration Voltage Data With UHMW-PE

UHMW Polyethylene Vibration Experiments

Transverse Vibration of the Rod at Varying Frequencies

Frequency (Hz)	10		
Trial	Maximum Reading (mV)	Minimum Reading (mV)	Average Reading (mV)
1	60.8	50.8	53.6
2	61.2	48.8	53.0
3	60.8	49.2	53.4
4	61.2	49.2	53.5
5	61.2	49.2	53.7
Trial Average	61.04	49.44	53.44
Standard Deviation	0.22	0.78	0.27

Frequency (Hz)	15		
Trial	Maximum Reading (mV)	Minimum Reading (mV)	Average Reading (mV)
1	61.2	49.2	52.2
2	61.2	50	53.1
3	61.2	50	52.4
4	61.2	49.2	52.3
5	60.8	49.2	52.7
Trial Average	61.12	49.52	52.54
Standard Deviation	0.18	0.44	0.36

Frequency (Hz)	20		
Trial	Maximum Reading (mV)	Minimum Reading (mV)	Average Reading (mV)
1	60.8	52.4	54.9
2	60.8	52	54.8
3	60.8	52	54.8
4	60.4	51.6	55.1
5	60	51.6	54.9
Trial Average	60.56	51.92	54.9
Standard Deviation	0.36	0.33	0.12

Frequency (Hz)	22		
Trial	Maximum Reading (mV)	Minimum Reading (mV)	Average Reading (mV)
1	61.6	51.6	54.8
2	60.8	52.8	55.4
3	61.6	52.4	55.5
4	61.6	52.4	55.6
5	61.6	52.8	54.9
Trial Average	61.44	52.4	55.24
Standard Deviation	0.36	0.49	0.36

Frequency (Hz)	25		
Trial	Maximum Reading (mV)	Minimum Reading (mV)	Average Reading (mV)
1	61.2	44.8	49.9
2	58.4	49.2	52.2
3	61.2	48.4	52.2
4	60.8	47.2	52.2
5	61.2	48.8	52.5
Trial Average	60.56	47.68	51.8
Standard Deviation	1.22	1.78	1.07

Frequency (Hz)	30		
Trial	Maximum Reading (mV)	Minimum Reading (mV)	Average Reading (mV)
1	60	46	50.5
2	61.2	44.8	50.3
3	60.4	45.2	50.8
4	61.2	46.4	51
5	60.4	48.4	51
Trial Average	60.64	46.16	50.72
Standard Deviation	0.54	1.40	0.31

Frequency (Hz)	40		
Trial	Maximum Reading (mV)	Minimum Reading (mV)	Average Reading (mV)
1	58	40	46.3
2	59.2	42	47.1
3	58.8	39.2	49
4	53.2	42.4	48.6
5	60	42.4	49.9
Trial Average	57.84	41.2	48.18
Standard Deviation	2.69	1.50	1.46

Frequency (Hz)	60		
Trial	Maximum Reading (mV)	Minimum Reading (mV)	Average Reading (mV)
1	61.6	48.4	53.1
2	61.6	50	54
3	60	50.8	54.1
4	60.8	51.6	53.9
5	59.6	48.8	53.9
Trial Average	60.72	49.92	53.8
Standard Deviation	0.91	1.34	0.40

Frequency (Hz)	90		
Trial	Maximum Reading (mV)	Minimum Reading (mV)	Average Reading (mV)
1	60.8	44.8	48.7
2	60	46.8	50.9
3	58.4	46.8	50.6
4	60	46.8	50.5
5	60	48	51.3
Trial Average	59.84	46.64	50.4
Standard Deviation	0.88	1.15	1.00

Frequency (Hz)	120		
Trial	Maximum Reading (mV)	Minimum Reading (mV)	Average Reading (mV)
1	60	48	52.4
2	59.6	49.6	53.1
3	60.4	50.4	53
4	60.4	48.8	52.9
5	58.4	51.2	54.4
Trial Average	59.76	49.6	53.16
Standard Deviation	0.83	1.26	0.74

Frequency (Hz)	150		
Trial	Maximum Reading (mV)	Minimum Reading (mV)	Average Reading (mV)
1	60.4	48	51.1
2	59.2	48.8	52
3	59.6	48	51.4
4	59.6	50	52.1
5	59.6	49.2	51.9
Trial Average	59.68	48.8	51.7
Standard Deviation	0.44	0.85	0.43

Frequency (Hz)	180		
Trial	Maximum Reading (mV)	Minimum Reading (mV)	Average Reading (mV)
1	56.8	42.4	50.7
2	56	46.8	51.8
3	59.2	46.4	53.1
4	59.6	50.8	53.9
5	58.8	49.6	53.4
Trial Average	58.08	47.2	52.58
Standard Deviation	1.58	3.26	1.31

Frequency (Hz)	220		
Trial	Maximum Reading (mV)	Minimum Reading (mV)	Average Reading (mV)
1	60	49.6	52.4
2	59.6	48.8	53.2
3	57.2	49.2	51.7
4	61.6	47.6	52.3
5	59.6	50	53.6
Trial Average	59.6	49.04	52.64
Standard Deviation	1.57	0.92	0.76

Frequency (Hz)	260		
Trial	Maximum Reading (mV)	Minimum Reading (mV)	Average Reading (mV)
1	59.6	40.4	47.2
2	58	45.2	50.3
3	57.2	46.4	50.5
4	61.2	43.6	52
5	59.6	40.8	52.6
Trial Average	59.12	43.28	50.52
Standard Deviation	1.56	2.64	2.10

Frequency (Hz)	0 (Baseline)		
Trial	Maximum Reading (mV)	Minimum Reading (mV)	Average Reading (mV)
1	60	26.8	41.3
2	53.6	26	36.4
3	59.6	30.8	41.1
4	52.8	33.6	42.5
5	58.4	36	43.3
6	59.6	33.2	45.5
7	56.4	38.8	44.7
8	60.4	37.6	45.3
9	53.2	39.2	44.7
10	54.8	41.6	47.6
Trial Average	56.88	34.36	43.24
Standard Deviation	3.07	5.27	3.13

Transverse sweep from 10 Hz to 260 Hz in 25 seconds

Frequency (Hz)	10 - 260 (sweep)		
Trial	Maximum Reading (mV)	Minimum Reading (mV)	Average Reading (mV)
1	60	50.4	53.2
2	59.6	51.6	53.3
3	61.2	51.2	54
4	61.2	52	54.4
5	61.2	52.8	54.3
6	61.2	51.2	53.9
7	60.4	51.6	54.3
8	61.2	50.8	54.7
9	61.2	52.4	54.6
10	61.2	52	54.3
Trial Average	60.84	51.6	54.1
Standard Deviation	0.61	0.73	0.51

Appendix K - Transverse Vibration Force Data With UHMW-PE

Frequency (Hz)	10		
Trial	Maximum Force (lbs)	Minimum Force (lbs)	Average Force (lbs)
1	3.81	0.00	2.60
2	4.68	0.00	2.86
3	4.50	0.00	2.68
4	4.50	0.00	2.64
5	4.50	0.00	2.55
Trial Average	4.40	0.00	2.67
Standard Deviation	0.34	0.00	0.12

Frequency (Hz)	15		
Trial	Maximum Force (lbs)	Minimum Force (lbs)	Average Force (lbs)
1	4.50	0.00	3.20
2	4.16	0.00	2.81
3	4.16	0.00	3.12
4	4.50	0.00	3.16
5	4.50	0.00	2.99
Trial Average	4.37	0.00	3.06
Standard Deviation	0.19	0.00	0.16

Frequency (Hz)	20		
Trial	Maximum Force (lbs)	Minimum Force (lbs)	Average Force (lbs)
1	3.12	0.00	2.04
2	3.29	0.00	2.08
3	3.29	0.00	2.08
4	3.46	0.00	1.95
5	3.46	0.00	2.04
Trial Average	3.33	0.00	2.04
Standard Deviation	0.14	0.00	0.05

Frequency (Hz)	22		
Trial	Maximum Force (lbs)	Minimum Force (lbs)	Average Force (lbs)
1	3.46	0.00	2.08
2	2.94	0.00	1.82
3	3.12	0.00	1.78
4	3.12	0.00	1.73
5	2.94	0.00	2.04
Trial Average	3.12	0.00	1.89
Standard Deviation	0.21	0.00	0.16

Frequency (Hz)		25	
Trial	Maximum Force (lbs)	Minimum Force (lbs)	Average Force (lbs)
1	6.41	0.00	4.20
2	4.50	0.52	3.20
3	4.85	0.00	3.20
4	5.37	0.00	3.20
5	4.68	0.00	3.07
Trial Average		5.16	0.10
Standard Deviation		0.77	0.23

Frequency (Hz)		30	
Trial	Maximum Force (lbs)	Minimum Force (lbs)	Average Force (lbs)
1	5.89	0.00	3.94
2	6.41	0.00	4.03
3	6.24	0.00	3.81
4	5.72	0.00	3.72
5	4.85	0.00	3.72
Trial Average		5.82	0.00
Standard Deviation		0.61	0.00

Frequency (Hz)		40	
Trial	Maximum Force (lbs)	Minimum Force (lbs)	Average Force (lbs)
1	8.49	0.69	5.76
2	7.62	0.17	5.41
3	8.83	0.35	4.59
4	7.45	2.77	4.76
5	7.45	0.00	4.20
Trial Average		7.97	0.80
Standard Deviation		0.65	1.13

Frequency (Hz)		60	
Trial	Maximum Force (lbs)	Minimum Force (lbs)	Average Force (lbs)
1	4.85	0.00	2.81
2	4.16	0.00	2.43
3	3.81	0.00	2.38
4	3.46	0.00	2.47
5	4.68	0.00	2.47
Trial Average		4.19	0.00
Standard Deviation		0.58	0.00

Frequency (Hz)	90		
Trial	Maximum Force (lbs)	Minimum Force (lbs)	Average Force (lbs)
1	6.41	0.00	4.72
2	5.54	0.00	3.77
3	5.54	0.52	3.90
4	5.54	0.00	3.94
5	5.02	0.00	3.59
Trial Average	5.61	0.10	3.98
Standard Deviation	0.50	0.23	0.43

Frequency (Hz)	120		
Trial	Maximum Force (lbs)	Minimum Force (lbs)	Average Force (lbs)
1	5.02	0.00	3.12
2	4.33	0.00	2.81
3	3.98	0.00	2.86
4	4.68	0.00	2.90
5	3.64	0.52	2.25
Trial Average	4.33	0.10	2.79
Standard Deviation	0.55	0.23	0.32

Frequency (Hz)	150		
Trial	Maximum Force (lbs)	Minimum Force (lbs)	Average Force (lbs)
1	5.02	0.00	3.68
2	4.68	0.17	3.29
3	5.02	0.00	3.55
4	4.16	0.00	3.25
5	4.50	0.00	3.33
Trial Average	4.68	0.03	3.42
Standard Deviation	0.37	0.08	0.19

Frequency (Hz)	180		
Trial	Maximum Force (lbs)	Minimum Force (lbs)	Average Force (lbs)
1	7.45	1.21	3.85
2	5.54	1.56	3.38
3	5.72	0.17	2.81
4	3.81	0.00	2.47
5	4.33	0.35	2.68
Trial Average	5.37	0.66	3.04
Standard Deviation	1.41	0.69	0.57

Frequency (Hz)	220		
Trial	Maximum Force (lbs)	Minimum Force (lbs)	Average Force (lbs)
1	4.33	0.00	3.12
2	4.68	0.00	2.77
3	4.50	1.04	3.42
4	5.20	0.00	3.16
5	4.16	0.00	2.60
Trial Average	4.57	0.21	3.01
Standard Deviation	0.40	0.46	0.33

Frequency (Hz)	260		
Trial	Maximum Force (lbs)	Minimum Force (lbs)	Average Force (lbs)
1	8.31	0.00	5.37
2	6.24	0.69	4.03
3	5.72	1.04	3.94
4	6.93	0.00	3.29
5	8.14	0.00	3.03
Trial Average	7.07	0.35	3.93
Standard Deviation	1.15	0.49	0.91

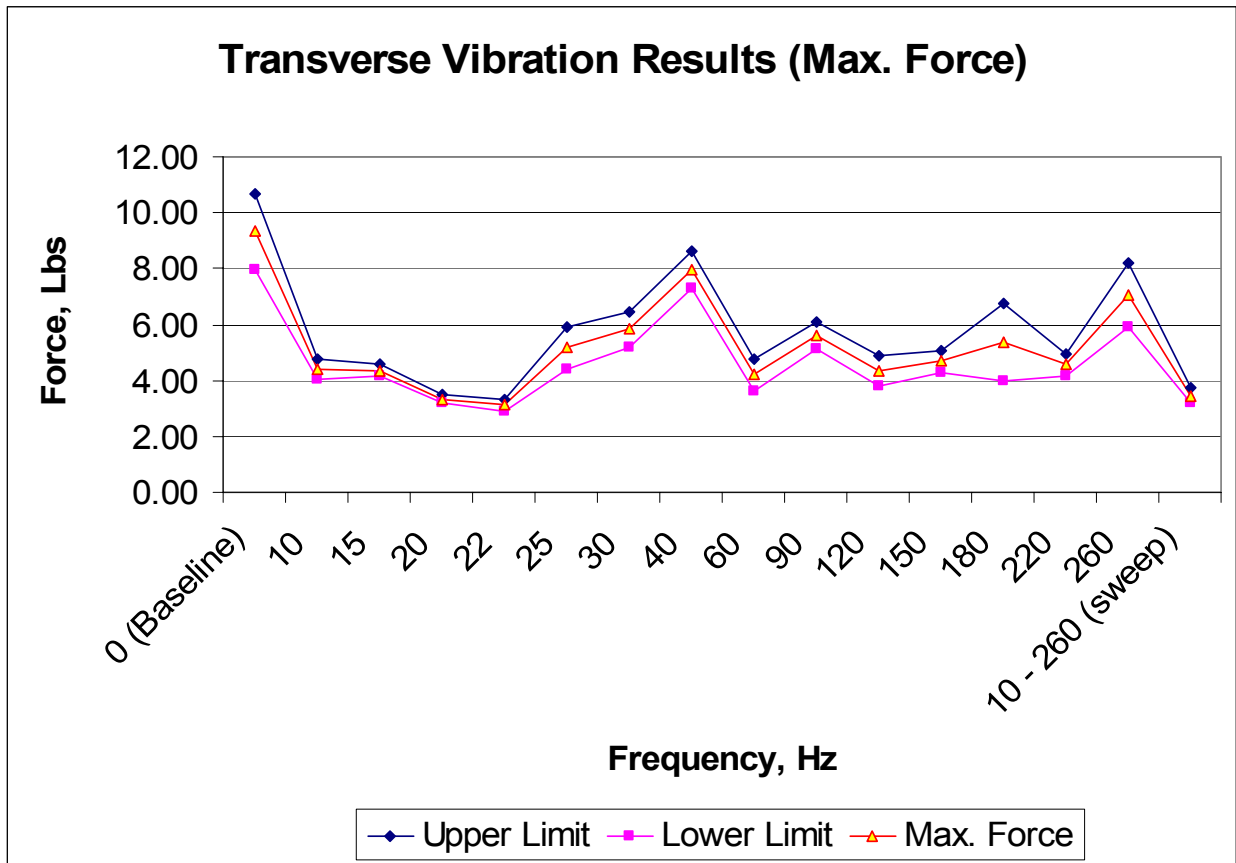
Frequency (Hz)	0 (Baseline)		
Trial	Maximum Force (lbs)	Minimum Force (lbs)	Average Force (lbs)
1	14.20	0.00	7.92
2	14.55	2.60	10.05
3	12.47	0.00	8.01
4	11.26	2.94	7.41
5	10.22	0.52	7.06
6	11.43	0.00	6.11
7	9.01	1.39	6.45
8	9.53	0.00	6.19
9	8.83	2.77	6.45
10	7.79	2.08	5.20
Trial Average	9.32	1.25	6.08
Standard Deviation	1.34	1.24	0.52

Transverse sweep from 10 Hz to 260 Hz in 25 seconds

Frequency (Hz)	10 - 260 (sweep)		
Trial	Maximum Force (lbs)	Minimum Force (lbs)	Average Force (lbs)
1	3.98	0.00	2.77
2	3.46	0.00	2.73
3	3.64	0.00	2.43
4	3.29	0.00	2.25
5	2.94	0.00	2.30
6	3.64	0.00	2.47
7	3.46	0.00	2.30
8	3.81	0.00	2.12
9	3.12	0.00	2.17
10	3.29	0.00	2.30
Trial Average	3.46	0.00	2.27
Standard Deviation	0.27	0.00	0.14

Appendix L- Transverse Vibration Maximum Force With UHMW-PE

Frequency (Hz)	Maximum Force (lbs)	Standard Deviation	Upper Limit Standard Deviation	Lower Limit Standard Deviation
0 (Baseline)	9.32	1.34	10.66	7.98
10	4.40	0.34	4.74	4.06
15	4.37	0.19	4.55	4.18
20	3.33	0.14	3.47	3.18
22	3.12	0.21	3.33	2.91
25	5.16	0.77	5.93	4.39
30	5.82	0.61	6.43	5.21
40	7.97	0.65	8.62	7.32
60	4.19	0.58	4.77	3.61
90	5.61	0.50	6.11	5.11
120	4.33	0.55	4.88	3.78
150	4.68	0.37	5.04	4.31
180	5.37	1.41	6.78	3.96
220	4.57	0.40	4.97	4.17
260	7.07	1.15	8.21	5.92
10 - 260 (sweep)	3.46	0.27	3.74	3.19



Appendix M – Axial Vibration Voltage Data With UHMW-PE

UHMW Polyethylene Vibration Experiments

Axial Vibration of the Rod at Varying Frequencies

Frequency (Hz)	10		
Trial	Maximum Reading (mV)	Minimum Reading (mV)	Average Reading (mV)
1	60.8	51.2	56.8
2	60.8	54.4	57.3
3	60.8	48	56.3
4	60.8	50.4	56.6
5	60.8	52.8	57.3
Trial Average	60.8	51.36	56.86
Standard Deviation	0	2.43	0.44

Frequency (Hz)	15		
Trial	Maximum Reading (mV)	Minimum Reading (mV)	Average Reading (mV)
1	60	54.8	56.8
2	60	53.6	56.6
3	60.4	54	56.2
4	59.2	55.2	56.8
5	60	53.6	57.1
Trial Average	59.92	54.24	56.7
Standard Deviation	0.44	0.73	0.33

Frequency (Hz)	20		
Trial	Maximum Reading (mV)	Minimum Reading (mV)	Average Reading (mV)
1	59.6	55.2	56.9
2	58.8	52.8	56.5
3	59.2	53.6	56.7
4	59.6	54	57.2
5	58.8	54	56.7
Trial Average	59.2	53.92	56.8
Standard Deviation	0.40	0.87	0.26

Frequency (Hz)	22		
Trial	Maximum Reading (mV)	Minimum Reading (mV)	Average Reading (mV)
1	60.4	55.2	57
2	60	54.8	56.6
3	60	53.2	56.5
4	60.4	53.6	56.4
5	60.4	53.6	56.4
Trial Average	60.24	54.08	56.58
Standard Deviation	0.22	0.87	0.25

Frequency (Hz)		25	
Trial	Maximum Reading (mV)	Minimum Reading (mV)	Average Reading (mV)
1	60	53.6	56
2	59.6	54.8	56.3
3	58.8	52.8	55.7
4	58.8	51.6	56.1
5	58.4	52.8	56.4
Trial Average		59.12	53.12
Standard Deviation		0.66	1.18

Frequency (Hz)		30	
Trial	Maximum Reading (mV)	Minimum Reading (mV)	Average Reading (mV)
1	58.4	53.6	55.4
2	58	52.8	55.8
3	60	52	55.8
4	59.2	53.2	55.7
5	59.6	50	55.6
Trial Average		59.04	52.32
Standard Deviation		0.83	1.43

Frequency (Hz)		40	
Trial	Maximum Reading (mV)	Minimum Reading (mV)	Average Reading (mV)
1	58.4	52.8	55
2	59.2	52	54.7
3	60	53.2	55.4
4	60.4	52.8	55.8
5	60	54.4	55.9
Trial Average		59.6	53.04
Standard Deviation		0.80	0.88

Frequency (Hz)		60	
Trial	Maximum Reading (mV)	Minimum Reading (mV)	Average Reading (mV)
1	56.8	51.2	54.5
2	58.4	52.4	54.7
3	58.8	51.2	55
4	58.4	50.4	54.8
5	57.6	51.2	55.2
Trial Average		58	51.28
Standard Deviation		0.80	0.72

Frequency (Hz)		90		
Trial	Maximum Reading (mV)	Minimum Reading (mV)	Average Reading (mV)	
1	57.2	50.4	54.1	
2	57.6	50	54.4	
3	57.6	48.4	54.1	
4	57.6	52	54.8	
5	58.4	52	54.5	
Trial Average		57.68	50.56	54.38
Standard Deviation		0.44	1.51	0.29

Frequency (Hz)		120		
Trial	Maximum Reading (mV)	Minimum Reading (mV)	Average Reading (mV)	
1	59.2	50.8	54.7	
2	59.2	52.4	54.7	
3	58.8	51.6	54.7	
4	57.6	49.2	54.6	
5	58	51.2	54.3	
Trial Average		58.56	51.04	54.6
Standard Deviation		0.73	1.19	0.17

Frequency (Hz)		150		
Trial	Maximum Reading (mV)	Minimum Reading (mV)	Average Reading (mV)	
1	59.6	49.2	54.1	
2	59.2	50.8	54.4	
3	57.2	49.2	54	
4	58	50.4	54.1	
5	59.6	50.8	54.5	
Trial Average		58.72	50.08	54.22
Standard Deviation		1.07	0.82	0.22

Frequency (Hz)		180		
Trial	Maximum Reading (mV)	Minimum Reading (mV)	Average Reading (mV)	
1	59.2	49.6	53.5	
2	58.8	49.2	53.7	
3	58.4	48.4	53.9	
4	58.8	50.8	53.8	
5	58.8	51.2	54.3	
Trial Average		58.8	49.84	53.84
Standard Deviation		0.28	1.15	0.30

Frequency (Hz)	220		
Trial	Maximum Reading (mV)	Minimum Reading (mV)	Average Reading (mV)
1	59.2	51.2	53.7
2	59.6	50.8	54
3	58.8	51.2	53.9
4	59.6	51.2	54.4
5	60	50.8	53.9
Trial Average	59.44	51.04	53.98
Standard Deviation	0.46	0.22	0.26

Frequency (Hz)	260		
Trial	Maximum Reading (mV)	Minimum Reading (mV)	Average Reading (mV)
1	60	47.6	51.4
2	60.4	48.4	52.3
3	59.6	48	52.7
4	60.4	48.8	52.9
5	60.4	48.8	53.7
Trial Average	60.16	48.32	52.6
Standard Deviation	0.36	0.52	0.84

Frequency (Hz)	0 (Baseline)		
Trial	Maximum Reading (mV)	Minimum Reading (mV)	Average Reading (mV)
1	59.2	33.6	40
2	60	37.2	42.5
3	60	38.8	44.8
4	60	41.6	45.7
5	56	38.8	44.1
6	60	42.4	46
7	58	41.6	46.5
8	59.2	42	46.9
9	58.8	44	47.4
10	58.8	44	47.5
Trial Average	59	40.4	45.14
Standard Deviation	1.25	3.28	2.39

Transverse sweep from 10 Hz to 260 Hz in 25 seconds

Frequency (Hz)	10 - 260 (sweep)		
Trial	Maximum Reading (mV)	Minimum Reading (mV)	Average Reading (mV)
1	64	54.8	59.6
2	63.6	54.8	60
3	63.6	56.4	59
4	64	56.8	60.4
5	62	54.8	58.8
6	64	56.8	59.9
7	64	56	59.5
8	63.4	54	59.3
9	64	56	60.9
10	64	56	59.7
Trial Average	63.66	55.64	59.71
Standard Deviation	0.63	0.97	0.63

Appendix N - Axial Vibration Force Data With UHMW-PE

Frequency (Hz)		10	
Trial	Maximum Force (lbs)	Minimum Force (lbs)	Average Force (lbs)
1	4.05	0.00	1.62
2	2.66	0.00	1.41
3	5.43	0.00	1.84
4	4.40	0.00	1.71
5	3.36	0.00	1.41
Trial Average		3.98	0.00
Standard Deviation		1.05	0.00

Frequency (Hz)		15	
Trial	Maximum Force (lbs)	Minimum Force (lbs)	Average Force (lbs)
1	2.49	0.24	1.62
2	3.01	0.24	1.71
3	2.84	0.06	1.88
4	2.32	0.58	1.62
5	3.01	0.24	1.49
Trial Average		2.73	0.27
Standard Deviation		0.31	0.19

Frequency (Hz)		20	
Trial	Maximum Force (lbs)	Minimum Force (lbs)	Average Force (lbs)
1	2.32	0.41	1.58
2	3.36	0.76	1.75
3	3.01	0.58	1.67
4	2.84	0.41	1.45
5	2.84	0.76	1.67
Trial Average		2.87	0.58
Standard Deviation		0.38	0.17

Frequency (Hz)		22	
Trial	Maximum Force (lbs)	Minimum Force (lbs)	Average Force (lbs)
1	2.32	0.06	1.54
2	2.49	0.24	1.71
3	3.18	0.24	1.75
4	3.01	0.06	1.80
5	3.01	0.06	1.80
Trial Average		2.80	0.13
Standard Deviation		0.38	0.09

Frequency (Hz)		25	
Trial	Maximum Force (lbs)	Minimum Force (lbs)	Average Force (lbs)
1	3.01	0.24	1.97
2	2.49	0.41	1.84
3	3.36	0.76	2.10
4	3.88	0.76	1.93
5	3.36	0.93	1.80
Trial Average	3.22	0.62	1.93
Standard Deviation	0.51	0.28	0.12

Frequency (Hz)		30	
Trial	Maximum Force (lbs)	Minimum Force (lbs)	Average Force (lbs)
1	3.01	0.93	2.23
2	3.36	1.10	2.06
3	3.70	0.24	2.06
4	3.18	0.58	2.10
5	4.57	0.41	2.14
Trial Average	3.56	0.65	2.12
Standard Deviation	0.62	0.36	0.07

Frequency (Hz)		40	
Trial	Maximum Force (lbs)	Minimum Force (lbs)	Average Force (lbs)
1	3.36	0.93	2.40
2	3.70	0.58	2.53
3	3.18	0.24	2.23
4	3.36	0.06	2.06
5	2.66	0.24	2.01
Trial Average	3.25	0.41	2.25
Standard Deviation	0.38	0.35	0.22

Frequency (Hz)		60	
Trial	Maximum Force (lbs)	Minimum Force (lbs)	Average Force (lbs)
1	4.05	1.62	2.62
2	3.53	0.93	2.53
3	4.05	0.76	2.40
4	4.40	0.93	2.49
5	4.05	1.28	2.32
Trial Average	4.01	1.10	2.47
Standard Deviation	0.31	0.35	0.12

Frequency (Hz)		90		
Trial	Maximum Force (lbs)	Minimum Force (lbs)	Average Force (lbs)	
1	4.40	1.45	2.79	
2	4.57	1.28	2.66	
3	5.26	1.28	2.79	
4	3.70	1.28	2.49	
5	3.70	0.93	2.62	
Trial Average		4.33	1.24	2.67
Standard Deviation		0.66	0.19	0.13

Frequency (Hz)		120		
Trial	Maximum Force (lbs)	Minimum Force (lbs)	Average Force (lbs)	
1	4.22	0.58	2.53	
2	3.53	0.58	2.53	
3	3.88	0.76	2.53	
4	4.92	1.28	2.58	
5	4.05	1.10	2.71	
Trial Average		4.12	0.86	2.58
Standard Deviation		0.51	0.31	0.08

Frequency (Hz)		150		
Trial	Maximum Force (lbs)	Minimum Force (lbs)	Average Force (lbs)	
1	4.92	0.41	2.79	
2	4.22	0.58	2.66	
3	4.92	1.45	2.84	
4	4.40	1.10	2.79	
5	4.22	0.41	2.62	
Trial Average		4.53	0.79	2.74
Standard Deviation		0.35	0.46	0.09

Frequency (Hz)		180		
Trial	Maximum Force (lbs)	Minimum Force (lbs)	Average Force (lbs)	
1	4.74	0.58	3.05	
2	4.92	0.76	2.97	
3	5.26	0.93	2.88	
4	4.22	0.76	2.92	
5	4.05	0.76	2.71	
Trial Average		4.64	0.76	2.91
Standard Deviation		0.50	0.12	0.13

Frequency (Hz)	220		
Trial	Maximum Force (lbs)	Minimum Force (lbs)	Average Force (lbs)
1	4.05	0.58	2.97
2	4.22	0.41	2.84
3	4.05	0.76	2.88
4	4.05	0.41	2.66
5	4.22	0.24	2.88
Trial Average	4.12	0.48	2.85
Standard Deviation	0.09	0.20	0.11

Frequency (Hz)	260		
Trial	Maximum Force (lbs)	Minimum Force (lbs)	Average Force (lbs)
1	5.61	0.24	3.96
2	5.26	0.06	3.57
3	5.43	0.41	3.40
4	5.09	0.06	3.31
5	5.09	0.06	2.97
Trial Average	5.30	0.17	3.44
Standard Deviation	0.23	0.15	0.36

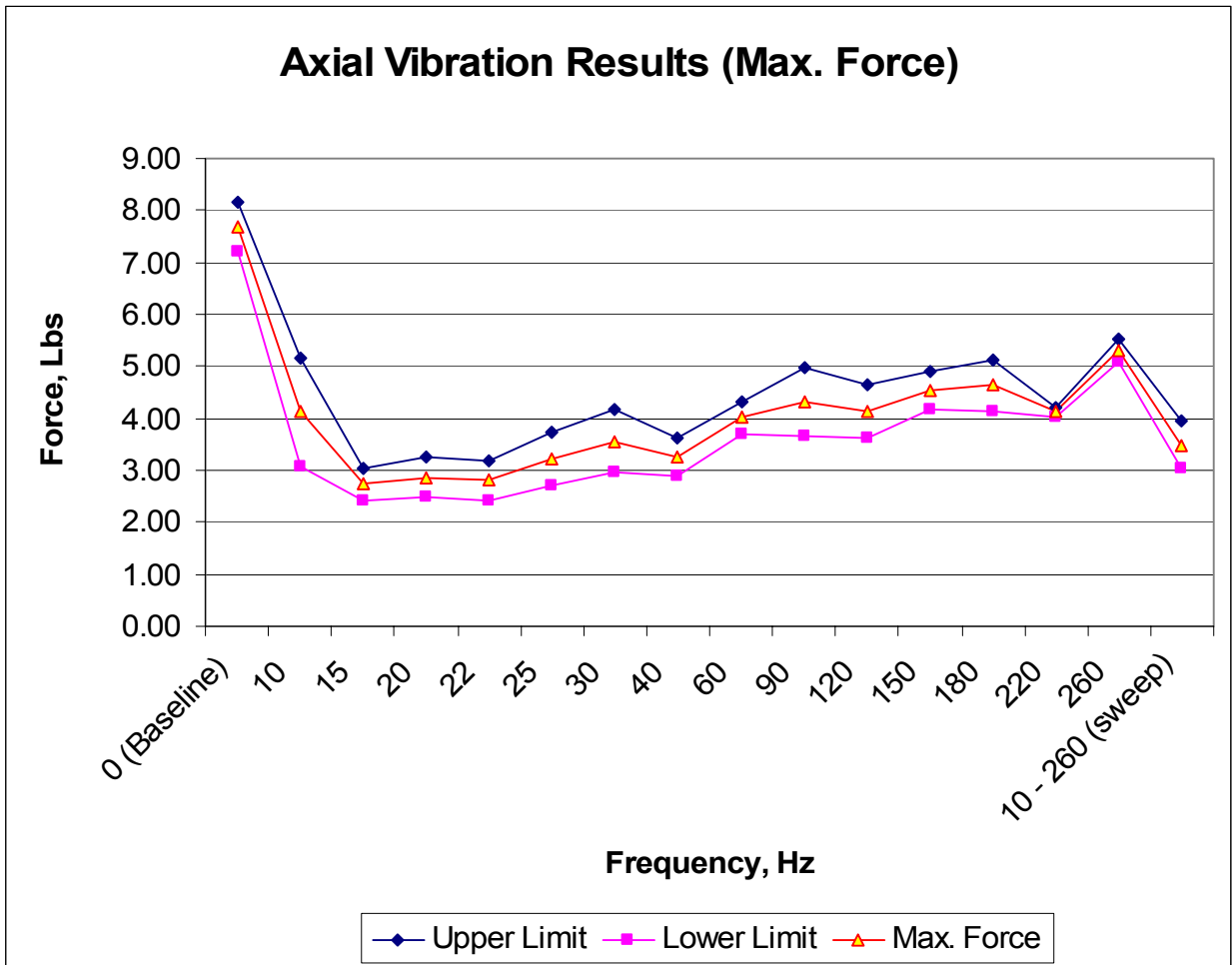
Frequency (Hz)	0 (Baseline)		
Trial	Maximum Force (lbs)	Minimum Force (lbs)	Average Force (lbs)
1	11.67	0.58	8.90
2	10.11	0.24	7.82
3	9.42	0.24	6.82
4	8.21	0.24	6.43
5	9.42	1.97	7.12
6	7.86	0.24	6.30
7	8.21	1.10	6.08
8	8.03	0.58	5.91
9	7.17	0.76	5.69
10	7.17	0.76	5.65
Trial Average	7.69	0.69	5.93
Standard Deviation	0.49	0.31	0.27

Transverse sweep from 10 Hz to 260 Hz in 25 seconds

Frequency (Hz)	10 - 260 (sweep)		
Trial	Maximum Force (lbs)	Minimum Force (lbs)	Average Force (lbs)
1	3.90	0.00	1.82
2	3.90	0.09	1.65
3	3.20	0.09	2.08
4	3.03	0.00	1.47
5	3.90	0.78	2.17
6	3.03	0.00	1.69
7	3.38	0.00	1.86
8	4.24	0.17	1.95
9	3.38	0.00	1.26
10	3.38	0.00	1.78
Trial Average	3.48	0.03	1.71
Standard Deviation	0.45	0.08	0.27

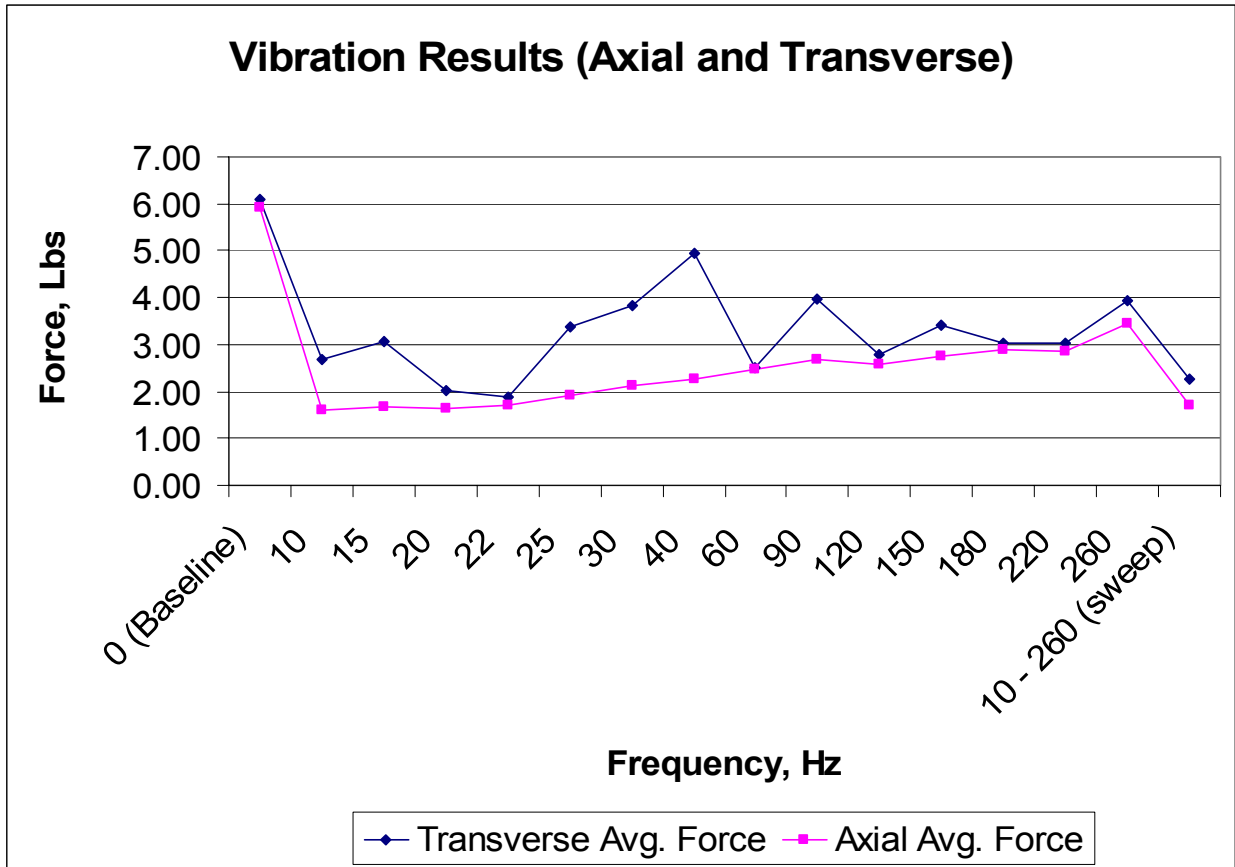
Appendix O- Axial Vibration Maximum Force With UHMW-PE

Frequency (Hz)	Average Force (lbs)	Standard Deviation	Upper Limit Standard Deviation	Lower Limit Standard Deviation
0 (Baseline)	7.69	0.49	8.18	7.20
10	4.12	1.05	5.17	3.07
15	2.73	0.31	3.05	2.42
20	2.87	0.38	3.25	2.50
22	2.80	0.38	3.18	2.43
25	3.22	0.51	3.73	2.71
30	3.56	0.62	4.18	2.95
40	3.25	0.38	3.63	2.87
60	4.01	0.31	4.32	3.70
90	4.33	0.66	4.98	3.67
120	4.12	0.51	4.63	3.60
150	4.53	0.35	4.89	4.18
180	4.64	0.50	5.14	4.14
220	4.12	0.09	4.21	4.02
260	5.30	0.23	5.52	5.07
10 - 260 (sweep)	3.48	0.45	3.93	3.03



Appendix P- UHMW-PE Transverse and Axial Vibration Results Comparison

Frequency (Hz)	Transverse Average Force (lbs)	Axial Average Force (lbs)
0 (Baseline)	6.08	5.93
10	2.67	1.60
15	3.06	1.67
20	2.04	1.62
22	1.89	1.72
25	3.38	1.93
30	3.85	2.12
40	4.95	2.25
60	2.51	2.47
90	3.98	2.67
120	2.79	2.58
150	3.42	2.74
180	3.04	2.91
220	3.01	2.85
260	3.93	3.44
10 - 260 (sweep)	2.27	1.71



Appendix Q - Material Properties Used in ALGOR Analyses

T-Handle and Nail Properties

[Customer Defined] (Part1) -Brick

Material Model	Standard
Material Source	Not Applicable
Material Source File	
Date Last Updated	2006/09/07-21:49:10
Material Description	Customer defined material properties
Mass Density	0.000729814 lbf*s ² /in/in ³
Modulus of Elasticity	28500000 lbf/in ²
Poisson's Ratio	.272
Shear Modulus of Elasticity	11202830 lbf/in ²
Thermal Coefficient of Expansion	.000006 1/°F

End Mass Properties

[Customer Defined] (Part2) -Brick

Material Model	Standard
Material Source	Not Applicable
Material Source File	
Date Last Updated	2006/09/07-21:50:30
Material Description	Customer defined material properties
Mass Density	.000086365 lbf*s ² /in/in ³
Modulus of Elasticity	2393122.68 lbf/in ²
Poisson's Ratio	.365
Shear Modulus of Elasticity	876601.71 lbf/in ²
Thermal Coefficient of Expansion	.000006 1/°F

Appendix R – MathCAD Natural Frequency Analysis

Free Longitudinal Vibration of a Prismatic Bar

Length of prismatic bar: $l := 13 \cdot \text{in}$

Modulus of elasticity: $E := 28500000 \text{psi}$

Density of prismatic bar: $\rho := 0.282 \frac{\text{lb}}{\text{in}^3}$

Velocity of vibration waves: $a := \sqrt{\frac{E}{\rho}} \quad a = 16461.15 \frac{\text{ft}}{\text{s}}$

Range of i to determine frequencies: $i := 1, 3, \dots, 9$

Natural frequency equation for axial vibration: $\omega(i) := \frac{i \cdot \pi \cdot a}{2 \cdot l}$

Fundamental natural frequency: $\omega(1) = 23868.1 \text{Hz}$

$$f_1 := \frac{\omega(1)}{2 \cdot \pi} \quad f_1 = 3798.73 \text{Hz}$$

Second natural frequency: $\omega(3) = 71604.3 \text{Hz}$

$$f_2 := \frac{\omega(3)}{2 \cdot \pi} \quad f_2 = 11396.18 \text{Hz}$$

Third natural frequency: $\omega(5) = 119340.5 \text{Hz}$

$$f_3 := \frac{\omega(5)}{2 \cdot \pi} \quad f_3 = 18993.63 \text{Hz}$$

Free Transverse Vibration of a Prismatic Bar

Length of prismatic bar:	$l := 13 \cdot \text{in}$	
Modulus of elasticity:	$E := 28500000 \frac{\text{lbf}}{\text{in}^2}$	
Density of prismatic bar:	$\rho := 0.282 \frac{\text{lb}}{\text{in}^3}$	
Radius of the prismatic bar:	$r := 0.156 \text{ in}$	
Area of the prismatic bar:	$A := \pi \cdot r^2$ $A = 0.076 \text{ in}^2$	
Moment of inertia of the bar:	$I := \frac{\pi \cdot r^4}{4}$ $I = 0.00047 \text{ in}^4$	
Velocity of vibration waves:	$a := \sqrt{\left(\frac{E \cdot I}{\rho \cdot A}\right)}$ $a = 107 \frac{\text{ft}}{\text{s}}$	
Fundamental natural frequency:	$f_1 := \frac{a}{2 \cdot \pi} \cdot \left(\frac{1.875}{l}\right)^2$	$f_1 = 51.01 \text{ Hz}$
Second natural frequency:	$f_2 := \frac{a}{2 \cdot \pi} \cdot \left(\frac{4.694}{l}\right)^2$	$f_2 = 319.71 \text{ Hz}$
Third natural frequency:	$f_3 := \frac{a}{2 \cdot \pi} \cdot \left(\frac{7.855}{l}\right)^2$	$f_3 = 895.29 \text{ Hz}$
Fourth natural frequency:	$f_4 := \frac{a}{2 \cdot \pi} \cdot \left(\frac{10.996}{l}\right)^2$	$f_4 = 1754.44 \text{ Hz}$